

PL-TR-97-2140

MSD-FR-97-15919

## **Seismic Discrimination with Regional Phase Spectral Ratios: Investigation of Transportability**

**Theron J. Bennett  
Ronald W. Cook  
Jerry A. Carter**

**Maxwell Technologies, Inc.  
8888 Balboa Ave.  
San Diego, CA 92123-1506**

**October, 1997**

**Final Report**

**31 July 1995 – 31 July 1997**

19980413 025

**Approved for public release; distribution unlimited**



**PHILLIPS LABORATORY  
Directorate of Geophysics  
AIR FORCE MATERIEL COMMAND  
HANSCOM AIR FORCE BASE, MA 01731-3010**

**DTIC QUALITY INSPECTED 3**

SPONSORED BY  
Air Force Technical Applications Center  
Directorate of Nuclear Treaty Monitoring  
Project Authorization T/5101


MONITORED BY  
Phillips Laboratory  
CONTRACT No. F19628-95-C-0108

The views and conclusions contained in this document are those of the authors and should not be interpreted as representing the official policies, either express or implied, of the Air Force or U.S. Government.

This technical report has been reviewed and is approved for publication.



JAMES C. BATTIS  
Contract Manager



CHARLES P. PIKE, Deputy Director  
Integration and Operations Division

This report has been reviewed by the ESD Public Affairs Office (PA) and is releasable to the National Technical Information Service (NTIS).

Qualified requestors may obtain copies from the Defense Technical Information Center. All others should apply to the National Technical Information Service.

If your address has changed, or you wish to be removed from the mailing list, or if the addressee is no longer employed by your organization, please notify PL/IM, 29 Randolph Road, Hanscom AFB, MA 01731-3010. This will assist us in maintaining a current mailing list.

Do not return copies of the report unless contractual obligations or notices on a specific document requires that it be returned.

REPORT DOCUMENTATION PAGE			Form Approved OMB No. 0704-0188	
Public reporting burden for this collection of information is estimated to average 1 hour per response, including the time for reviewing instructions, searching existing data sources, gathering and maintaining the data needed, and completing and reviewing the collection of information. Send comments regarding this burden estimate or any other aspect of this collection of information, including suggestions for reducing this burden, to Washington Headquarters Services, Directorate for Information Operations and Reports, 1215 Jefferson Davis Highway, Suite 1204, Arlington, VA 22202-4302, and to the Office of Management and Budget, Paperwork Reduction Project (0704-0188), Washington, DC 20503.				
1. AGENCY USE ONLY (Leave blank)		2. REPORT DATE October, 1997	3. REPORT TYPE AND DATES COVERED Final Report 7/31/95 - 7/31/97	
4. TITLE AND SUBTITLE Seismic Discrimination with Regional Phase Spectral Ratios: Investigation of Transportability			5. FUNDING NUMBERS Contract No. F19628-95-C-0108  PE 35999F  PR 5101 TA GM WU AD	
6. AUTHOR(S)  Theron J. Bennett, Ronald W. Cook, and Jerry A. Carter				
7. PERFORMING ORGANIZATION NAME(S) AND ADDRESS(ES)  Maxwell Technologies, Inc. 8888 Balboa Avenue San Diego, CA 9212301509			8. PERFORMING ORGANIZATION REPORT NUMBER  MSD-FR-97-15919	
9. SPONSORING/MONITORING AGENCY NAME(S) AND ADDRESS(ES)  Phillips Laboratory 29 Randolph Road Hanscom AFB, MA 01731-3010  Contract Manager: James Battis/GPI			10. SPONSORING/MONITORING AGENCY REPORT NUMBER  PL-TR-97-2140	
11. SUPPLEMENTARY NOTES				
12a. DISTRIBUTION/AVAILABILITY STATEMENT  Approved for public release; distribution unlimited			12b. DISTRIBUTION CODE	
13. ABSTRACT (Maximum 200 words) The Comprehensive Test Ban Treaty (CTBT) requires the location and identification of seismic events which might be associated with small potential underground nuclear explosion tests. For monitoring the CTBT at low magnitude thresholds, reliance must be placed on regional seismic measurements. Various regional discrimination techniques have been shown to be effective for identifying events in some areas, but the transportability of such methods into uncalibrated source areas remains a problem. This research developed procedures which could be useful for transporting regional phase spectral ratio discriminant measures by accounting for propagation path effects using prior knowledge of attenuation. We have found that by correcting for attenuation the scatter in Lg spectral ratio observations between stations could be reduced. However, these measurements still show considerable overlap between different source types which weakens the reliability of the discriminant. It might be possible to improve the reliability of regional phase spectral ratios by limiting effects of noise on the measurements by focusing on nearer stations, limiting the frequency band over which the ratios are formed, and refining the attenuation (over)				
14. SUBJECT TERMS  Seismic                      Regional                      Europe                      Spectra Discrimination              North America              Asia                      Transportability			15. NUMBER OF PAGES 78	
			16. PRICE CODE	
17. SECURITY CLASSIFICATION OF REPORT UNCLASSIFIED	18. SECURITY CLASSIFICATION OF THIS PAGE UNCLASSIFIED	19. SECURITY CLASSIFICATION OF ABSTRACT UNCLASSIFIED	20. LIMITATION OF ABSTRACT UNLIMITED	

# Table of Contents

	<u>Page</u>
1. Introduction.....	1
1.1 Objectives.....	1
1.2 Accomplishments.....	2
1.3 Report Organization.....	4
2. Regional Phase Spectral Ratios: Measurement Procedures and Corrections. ....	5
2.1 Background.....	5
2.2 Spectral Analysis Methods for Regional Signals.....	7
2.3 Correction for Station Instrument Response.....	11
2.4 Attenuation Corrections.....	14
2.4.1 Theory.....	14
2.4.2 Attenuation Models.....	15
3. Database for Spectral Ratio Studies.....	22
3.1 Limitations of the Regional Database.....	22
3.2 Data Sources.....	23
4. Application and Event Analyses.....	29
4.1 Some Tests of Attenuation Models.....	29
4.1.1 Western U.S.....	29
4.1.2 Eurasia.....	36
4.2 Comparison of the Larger Data Samples.....	41
4.3 Discrimination Analyses of Selected Events.....	52
5. Conclusions and Recommendations.....	63
5.1 Summary of Main Findings.....	63
5.2 Recommendations.....	65
6. References.....	67

## List of Illustrations

	<u>Page</u>
1 Comparison of peak amplitude (top) and RMS (bottom) spectral ratio estimates using broad band-pass filters for $L_g$ from NTS explosions recorded at LLNL station KNB.....	9
2 Comparison of spectral ratio estimates using narrow band-pass Gaussian filters (top) and Fourier analysis (bottom) for $L_g$ from NTS explosions recorded at LLNL station KNB.....	10
3 Comparison of $L_g$ spectral ratio estimates before (top) and after (bottom) correction for the shape of the station instrument response at nine regional stations for the NTS explosion JUNCTION.....	13
4 Attenuation at 1 Hz ( $Q_0$ ) from $L_g$ coda adapted from work by Mitchell et al. (cf. Xie and Mitchell, 1990; Mitchell et al., 1996).....	17
5 Frequency dependence of attenuation ( $\eta$ ) from $L_g$ coda adapted from work by Mitchell et al. (cf. Xie and Mitchell, 1990; Mitchell et al., 1996).....	18
6 Predicted attenuation correction factors for $L_g$ spectral ratios for specific station paths from NTS nuclear explosion JUNCTION.....	19
7 Predicted attenuation correction factors for $L_g$ spectral ratios for specific station paths from an earthquake in northwestern China near Lop Nor.....	21
8 Locations of selected explosions, earthquakes, and stations used in analyzing regional phase spectral ratios from western U.S. events.....	24
9 Locations of selected explosions, earthquakes, and stations used in analyzing regional phase spectral ratios from Eurasian events.....	25
10 Comparison of the instrument-corrected $L_g$ spectral ratio estimates for NTS explosion JUNCTION (top) and the same spectral ratios after correction for path-specific attenuation (bottom) developed from the attenuation model...	30
11 Comparison of standard deviations for $L_g$ spectral ratios based on measurements at five of the better stations (viz. ISA, PAS, PFO, SBC, and ANMO) for NTS explosion JUNCTION before and after attenuation corrections.....	32

12	Comparison of standard deviations for $L_g$ spectral ratios based on measurements at the four LLNL stations for the 1979/12/25 earthquake near NTS before and after attenuation corrections.....	33
13	Comparison of standard deviations for $L_g$ spectral ratios based on measurements at the four LLNL stations for the 1980/10/25 earthquake near NTS before and after attenuation corrections.....	34
14	Comparison of standard deviations for $L_g$ spectral ratios based on measurements at the four LLNL stations for the 1982/05/12 earthquake near NTS before and after attenuation corrections.....	35
15	Comparison of the instrument-corrected $L_g$ spectral ratio estimates for the 1996/01/09 earthquake in northwestern China near Lop Nor (top) and the same spectral ratios after correction for path-specific attenuation (bottom) developed from the attenuation model.....	37
16	Comparison of standard deviations for $L_g$ spectral ratios based on measurements at the regional stations for the 1996/01/09 earthquake in northwestern China near Lop Nor before and after attenuation corrections...	39
17	Comparison of standard deviations for $L_g$ spectral ratios based on measurements at the regional stations for the 1996/03/26 earthquake in East Kazakhstan before and after attenuation corrections.....	40
18	Comparison of standard deviations for $L_g$ spectral ratios based on measurements at the regional stations for the 1996/06/08 explosion in China at Lop Nor before and after attenuation corrections.....	42
19	$L_g$ spectral ratios determined from Gaussian bandpass filters applied to 79 explosion signals (solid lines) and 60 earthquake signals (dashed lines) before any corrections.....	43
20	$L_g$ spectral ratios from Figure 19 after corrections for instrument responses applied to 74 explosion signals (solid lines) and 60 earthquake signals (dashed lines).....	44
21	$L_g$ spectral ratios from Figure 20 after corrections for path attenuation applied to 74 explosion signals (solid lines) and 60 earthquake signals (dashed lines).....	46
22	$L_g$ spectral ratios after instrument and attenuation corrections for 35 explosion signals (solid lines) and 18 earthquake signals (dashed lines) at station distances less than 5 degrees.....	47

23	$L_g$ spectral ratios after instrument and attenuation corrections for 41 explosion signals (solid lines) and 31 earthquake signals (dashed lines) at station distances less than 10 degrees.....	48
24	$L_g$ spectral ratios after instrument and attenuation corrections for 52 explosion signals (solid lines) and 35 earthquakes signals (dashed lines) for all distances with outliers removed.....	50
25	Comparison of $L_g$ spectral ratios after instrument and attenuation corrections for explosion and earthquake signals in the western hemisphere (top) and eastern hemisphere (bottom) for events at all regional distances.....	51
26	Comparison of $L_g$ spectral ratios after instrument and attenuation corrections for explosion and earthquake signals in the western hemisphere (top) and eastern hemisphere (bottom) for events recorded at distances less than 10 degrees.....	53
27	$L_g$ spectral ratios after corrections at five stations (top) and discrimination analysis based on average $L_g$ spectral ratios (bottom) for East Kazakhstan event of 1996/03/26.....	55
28	$L_g$ spectral ratios after corrections at three stations (top) and discrimination analysis based on average $L_g$ spectral ratios (bottom) for Jordan-Syria event of 1997/03/26.....	56
29	$L_g$ spectral ratios after corrections at three stations (top) and discrimination analysis based on average $L_g$ spectral ratios (bottom) for North Korea event of 1996/09/14.....	58
30	$L_g$ spectral ratios after corrections at single station (top) and discrimination analysis based on the $L_g$ spectral ratios (bottom) for Pakistan event of 1996/12/22.....	59
31	$L_g$ spectral ratios after corrections at three stations (top) and discrimination analysis based on average $L_g$ spectral ratios (bottom) for Balapan, East Kazakhstan explosion of 1988/09/14.....	61

## List of Tables

	<u>Page</u>
1 List of Events and their Respective Stations Used in this Study.....	27

# 1. Introduction

## 1.1 Objectives

The Comprehensive Test Ban Treaty (CTBT) requires the location and identification of seismic events which might be associated with small potential underground nuclear explosion tests. Pushing the threshold down to the low magnitude levels specified by the treaty requires improved monitoring capability which must rely on regional seismic stations. While some distant seismic stations may sometimes be helpful in locating events to fairly low levels, local and regional stations are critically important to identification and discrimination of such small events. Unfortunately, regional seismic discrimination techniques have been slow to evolve and have not been thoroughly tested. In particular, various regional discrimination methods have been found effective for identifying nuclear explosions in specific source areas. However, because nuclear explosion tests have been conducted at only a very limited number of sites and co-located earthquakes or other source types are often not available for comparison, many regions of the world remain uncalibrated for regional discrimination.

For several years, regional phase spectral ratios have been recognized as potential seismic discriminants for distinguishing underground nuclear explosions from other source types. Comparison of seismic events near NTS showed that  $L_g$  signals for earthquakes were enriched at high frequencies, compared to underground nuclear explosions with similar propagation paths; and other regional phases also indicated some potential for differentiating seismic events with respect to source type. However, attempts to apply this potential discrimination technique in other geographic regions were less successful or ambiguous, due in part to uncertainties associated with seismic station response and propagation path variations between the events available for comparison. It has been the goal of this research program to analyze how station response and attenuation differences between regions might affect regional phase spectral ratios. Understanding the effects of these factors on regional phase spectral ratios is critical to evaluating the transportability of regional phase spectral ratio discriminant measures and assessing their usefulness for CTBT monitoring in uncalibrated areas.



## 1.2 Accomplishments

This investigation combined an empirical element and a theoretical element. For the empirical element we collected and analyzed the behavior of regional phase signals from representative samples of underground nuclear explosions, earthquakes, rockbursts, and mine explosions in several different tectonic regions. These signals were used to develop regional phase spectral ratio discriminant measures as a function of frequency. Although we have considered several different regional phases in our analyses, we have focused mainly on  $L_g$  spectral ratios for two reasons: First, they have a stronger historical background as discriminant measures; and, second, there exists a more reliable and consistent database for  $L_g$  propagation worldwide than for other regional phases, and this can be used to adjust for propagation effects. This prior knowledge of  $L_g$  propagation serves as the basis for the theoretical element of the investigation which attempts to remove effects of attenuation and normalize the spectral ratios at a common distance range.

The regional phase ratios measured in these studies were determined using a band-pass filter procedure which produces spectral estimates which closely match Fourier spectral amplitudes over the regional phase group velocity windows. The spectral values were normalized to the average amplitudes in the frequency band near 1 Hz to produce spectral ratios as a function of frequency (i.e. the ratio of the spectral amplitude at that frequency to the spectral level near 1 Hz). The measured spectral ratios were corrected for instrument response, and then adjusted for propagation using a scheme, developed as part of this study, which utilizes prior knowledge of  $Q$  and its frequency dependence along the propagation path between the source and seismic station.

We applied the corrections to selected regional signals from different source types in several different regions. We focused initially on processing several events, including explosions and earthquakes, from the well-calibrated region near NTS, and subsequently analyzed events from other nuclear test sites at Balapan (in eastern Kazakhstan) and Lop Nor (in China). In addition to these nuclear test sites, we have also analyzed propagation effects on regional signals from events in other areas of interest, including North Korea, Jordan-Syria, and Pakistan. For events in each of these areas, we retrieved the available

signals from IDC, IRIS, and other regional stations; we performed spectral analyses on the regional signals; we removed the instrument response, developed the corrections for propagation utilizing a known  $Q$  model, and compared the corrected regional phase spectral ratios between different source types, regions, and stations. For several events and regions, we also performed tests to verify the attenuation model by comparing inter-station variations in the spectral ratio measurements.

In general, these studies have defined a systematic approach to provide measurements of regional phase spectral ratios which can be determined routinely and which should be independent of the propagation path and instrument response at the recording station. Application of the attenuation corrections developed from the  $Q$  model usually was found to reduce the scatter in the  $L_g$  spectral ratio measurements between stations for common events. However, there appear to be some observations where the path corrections do not work properly; and in those cases some revision of the attenuation model may be useful. When the model-derived attenuation corrections were applied to a larger sample of explosions and earthquakes, we found that the  $L_g$  spectral ratios for the two source types separated on average; but there was considerable overlap between the measurements. If  $L_g$  spectral ratios are ever to provide a reliable discriminant, more definite separation of measurements for different source types will be required. One of the main factors contributing to the scatter in the observations appeared to be noise. The  $L_g$  signals for small events tend to fall into the background noise at high frequencies; this was particularly the case for observations from stations at larger regional distances. Corrections to the  $L_g$  spectral ratios at farther regional stations tend to blow-up the noise at high frequencies and produce anomalous measurements. These observations point out the need for care in eliminating noisy signals from  $L_g$  spectral ratio measurements. They also suggest that nearer regional stations and regional phase spectral ratio measurements based on a more limited, lower range of frequencies are likely to provide more reliable discriminant measures which are less susceptible to vagaries of the model. On a more positive note, we found that discrimination analyses using the attenuation- and instrument-corrected  $L_g$  spectral ratios were successful in identifying several Eurasian events from selected areas of interest in CTBT monitoring.

### **1.3 Report Organization**

This report is divided into five sections including these introductory remarks. Section 2 discusses the band-pass filtering procedures used to determine spectral ratios for the regional signals and the attenuation model used to develop the corrections to the spectral ratios. Section 3 describes the event database which we have been working with. Section 4 describes application of the corrections to test the model and discrimination analyses for selected regional events. Section 5 summarizes the results of this research program and offers some suggestions for improving the reliability and transportability of regional phase spectral ratio discriminants.

## **2. Regional Phase Spectral Ratios: Measurement Procedures and Corrections**

### **2.1 Background**

Regional seismic signals have been recognized for more than 20 years as providing an important tool for identifying seismic events (cf. Pomeroy et al., 1982; Blandford, 1981). In particular, for small events seismic recordings at regional stations are likely to provide the only data with signals above background noise to use for location and discrimination. Therefore, implementation of a CTBT and the need to identify small events which could be potential underground nuclear explosion tests have raised the significance of local and regional seismic stations for treaty monitoring. Installation of a worldwide network of high-quality digital seismic stations has enabled acquisition of regional waveform data from smaller events in many areas. However, the value of these regional data for event identification has only been partly realized for several reasons. First, potential regional discrimination methods have not been thoroughly tested and implemented in the monitoring environment. Second, the capacity to test and calibrate regional discrimination methods is restricted by limitations on the availability of data associated with historical nuclear testing practice, limited geographic areas of historical testing, and the experience with historical seismicity or other source types used for comparison. Finally, the physical behavior of regional signals and their relationship to the seismic source mechanism has only been partially worked out, so that we cannot analytically compensate or adequately predict variations in regional phase behavior between different sources. Therefore, analysis of the performance of regional discriminants in different tectonic regions (viz. transportability) is an important, outstanding issue which must be addressed to assess the effectiveness of regional discriminants for CTBT monitoring. In the research reported here, we have investigated issues associated with transportability of a particular class of regional seismic discriminants: regional phase spectral ratios.

In general, spectral ratio discriminants involve the exploitation and parameterization of differences in the relative spectral shape, or frequency content, of

regional phase seismic signals observed from different source types. Over the years, several authors have reported spectral differences in regional phase signals for explosions and earthquakes. Ryall (1970) found differences in the spectra of P and S waves over a frequency band from 0.5 to 5 Hz for a small sample of NTS explosions and earthquakes recorded at near-regional distances in Nevada. Murphy and Bennett (cf. Murphy and Bennett, 1982; Bennett and Murphy, 1986) found that  $L_g$  spectra at regional VELA array stations in the western U.S. were significantly richer in high-frequency energy for earthquakes near NTS than for the corresponding NTS nuclear explosion tests at recording distances from 430 km to 900 km. In the latter studies,  $P_g$  spectra also showed some differences, but not  $P_n$ . Using a larger sample of NTS explosions and western U.S. earthquakes recorded at the regional LLNL station network surrounding NTS, Taylor et al. (1988, 1989) confirmed the findings of Murphy and Bennett and concluded that regional phase spectral comparisons had good potential for discrimination; but they suggested a need to account for attenuation differences and to select optimal frequency bands for event comparisons in different regions.

In a prior report under this contract (cf. Bennett et al., 1996), we summarized the characteristics of a large waveform database available for regional discrimination analyses of underground nuclear explosions and other seismic source types. We also presented in that report observations of  $L_g$  spectral ratios for nuclear explosion and earthquake sources in the western U.S. and Asia, and we described the effects of source magnitude differences on the regional phase spectral ratio measurements. In particular, we found that uncorrected  $L_g$  spectral ratios discriminated earthquakes and nuclear explosions in the western U.S. but provided little distinction between event types in Eurasia. Furthermore, theoretical scaling of the western U.S. observed signals, to make the source sizes more similar, appeared to reduce some of the  $L_g$  spectral differences between earthquakes and explosions.

The goal of the studies reported here has been to refine regional phase spectral ratio measurements by including corrections for station instrument response and knowledge of attenuation. We have sought to determine whether correcting the  $L_g$  spectral ratios for path attenuation based on regional models has an effect in reducing the

scatter between stations for individual events and whether the corrections enhance or diminish regional phase spectral differences between different source types. We have also incorporated in our analysis a spectral estimation procedure based on band-pass filtering which has certain operational advantages over other spectral analysis methods.

## **2.2 Spectral Analysis Methods for Regional Signals**

The original work to develop regional phase spectral ratios as discriminants was based on Fourier analyses of the signals to determine their relative level in a low frequency band compared to a high frequency band (cf. Murphy and Bennett, 1982). In several subsequent studies (e.g. Bennett et al., 1992, 1995), we used band-pass filter analyses to examine regional phase spectral ratios, as well as  $L_g/P$  ratios, as a function of frequency. The latter approach has some advantages in that it can be applied to determine the regional signal spectrum in the course of normal, routine processing without special knowledge of the event origin or travel time information, which would require off-line processing. The traditional band-pass filter analyses from several of our earlier studies (cf. Bennett et al., 1992) utilized a suite of fairly broad overlapping filters to extract the spectral estimates, and spectral ratios were formed by dividing by the amplitude from the filter output for a band near 1 Hz. In our prior report under this contract (cf. Bennett et al., 1996), we briefly noted a band-pass filtering scheme which uses much narrower Gaussian filters to extract the spectral information from the regional signals.

During the recent phase of this research, we have compared several of these alternative spectral estimation methods by applying the different procedures to the same regional phase signals for several events. The first two methods involved variations on the overlapping broad band-pass filters. In both of these methods we used eight filter passbands: 0.5 - 1.0 Hz, 0.75 - 1.5 Hz, 1 - 2 Hz, 1.5 - 3 Hz, 2 - 4 Hz, 3 - 6 Hz, 4.5 - 9 Hz, and 6 - 12 Hz; beyond the indicated passbands the filter responses fell off at a rate of 60 dB per octave. The difference between the two methods was that in one case we simply picked the maximum amplitude of the filter output in the regional phase window (approximately in the group velocity window 3.6 - 3.0 km/sec for  $L_g$  and 6.0 - 5.1 km/sec

for  $P_g$ ), while in the alternative method we computed an RMS average of the amplitudes over the same group velocity window. In both cases, we normalized the spectral amplitude estimates by dividing by the amplitude for the filter passband 0.75 - 1.5 Hz. Thus, the resulting normalized spectra effectively represent a regional phase spectral ratio (i.e. the ratio of the regional phase amplitude in the selected passband to the regional phase amplitude in the 0.75 - 1.5 Hz passband). Figure 1 shows a comparison of the  $L_g$  spectral ratio estimates using the peak (top) and RMS (bottom) amplitude measures for five NTS explosions recorded at station KNB ( $R \approx 290$  km). The  $L_g$  spectral ratios for the explosions generally have their maximum values in the vicinity of 1 Hz and drop off gradually by two orders of magnitude over the interval from 1 to 9 Hz. Although the two methods show some differences, they are basically quite consistent; and we found similar consistency between these methods for other regional phases, other events, and other stations.

In addition to these spectral estimates with the broad filters, we have continued to investigate the use of processing techniques developed previously under this contract (cf. Bennett et al., 1996) and in related studies (cf. Murphy et al., 1996), which use Gaussian filters to determine the spectral measurements. The Gaussian filters are much narrower than the broad-band filters described above, with filter quality factors equal to six times the center frequency. In our processing we used a suite of filters with center frequencies uniformly spaced at intervals of 0.25 Hz over the band from 0.25 Hz to 10 Hz. The spectral estimates are obtained from a RMS average of the amplitudes with the selected regional phase window; for  $L_g$  we used a consistent group velocity window from 3.6 km/sec to 3.0 km/sec. We found that this window included most of the  $L_g$  energy for most stations and distances.

Figure 2 (top) shows the  $L_g$  spectral ratio estimates for the same NTS explosions as in Figure 1 recorded at station KNB. Comparing the two data sets (i.e. the top of Figure 2 with Figure 1), the Gaussian filter results tend to show a similar behavior, with the  $L_g$  spectral ratios for the NTS explosions falling off toward higher frequencies. The Gaussian filter spectral ratios tend to show more detail and fall off more rapidly with increasing frequency. We believe that both of these differences can be attributed to the

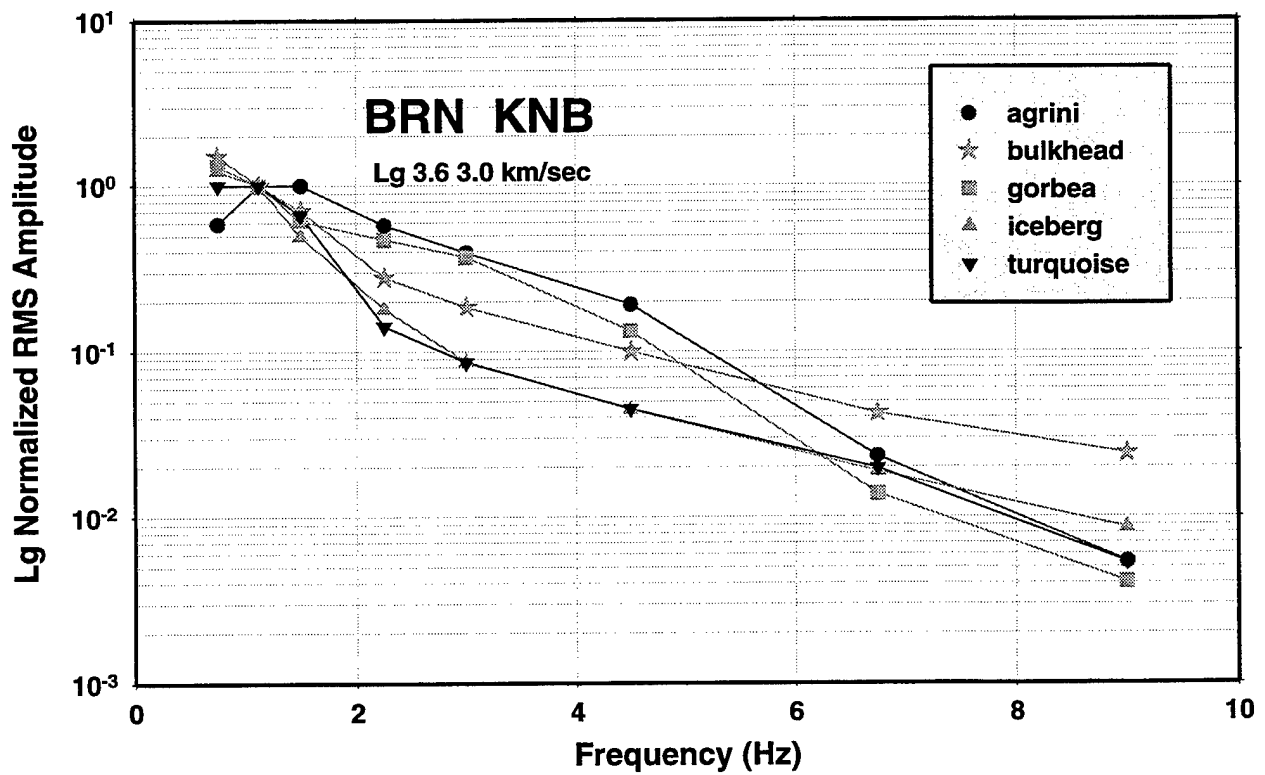
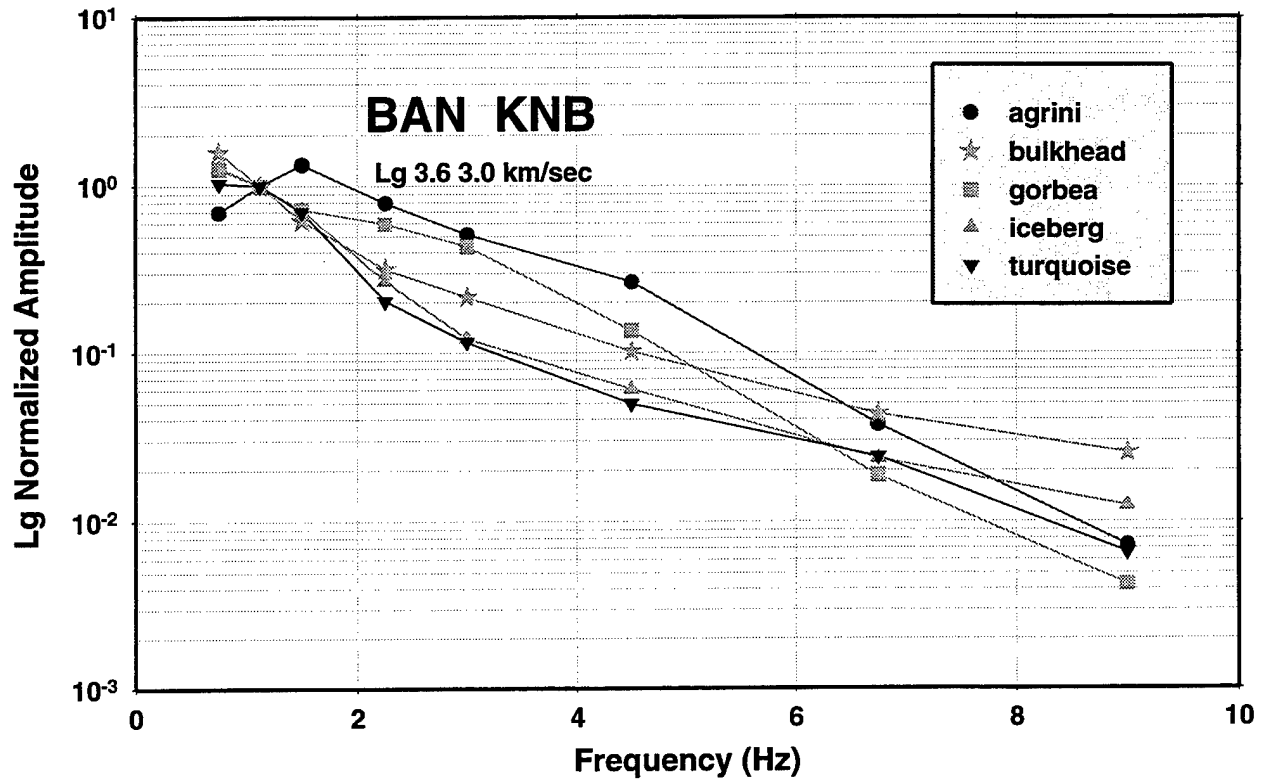


Figure 1. Comparison of peak amplitude (top) and RMS (bottom) spectral ratio estimates using broad band-pass filters for  $L_g$  from NTS explosions recorded at LLNL station KNB.



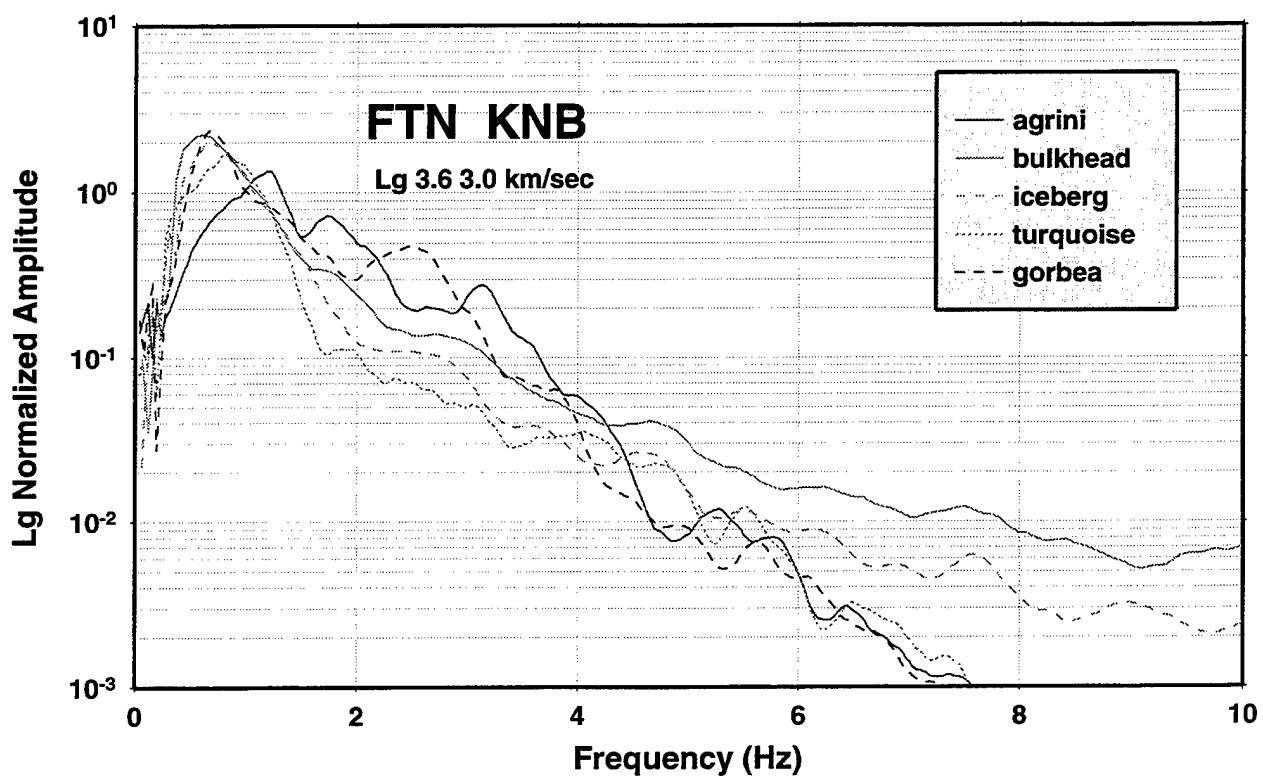
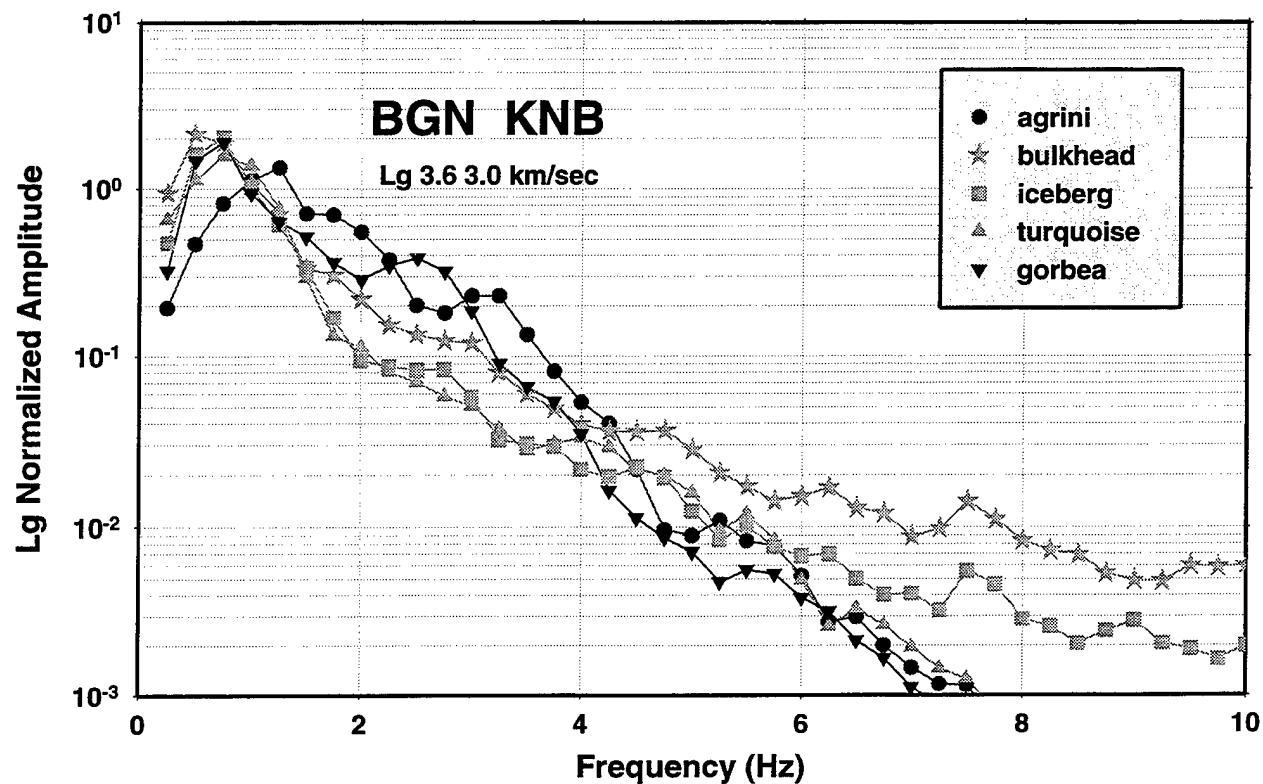


Figure 2. Comparison of spectral estimates using narrow band-pass Gaussian filters (top) and Fourier analysis (bottom) for  $L_g$  from NTS explosions recorded at LLNL station KNB.

narrower frequency band for the Gaussian filters. The broader passbands of the original filters tend to smooth the spectra by including energy from the wide frequency range. This also appears to be the cause of inflation of the spectrum at higher frequencies (in Figure 1), as the broad band actually samples signal energy from well below the center frequency at which the results are plotted.

For comparison, we have plotted at the bottom of Figure 2 the  $L_g$  spectral ratios obtained from Fourier analyses of the same  $L_g$  signals for the group velocity window 3.6 km/sec to 3.0 km/sec. The Fourier spectra were smoothed using a running average to obtain similar resolution to the Gaussian filter results. The comparisons indicate that the  $L_g$  spectral ratios using the Gaussian filters closely match the spectral ratios developed from Fourier spectra. We have tested this observation on other data samples and other regional phases and found similar results. Even though the Fourier spectral measurements tend to be faster, we believe that the Gaussian filters may offer some operational advantages for real-time processing, because they do not necessarily require prior knowledge to window the record segments for use in the spectral estimates, as noted above. Therefore, we have used the Gaussian filter measurements of the  $L_g$  spectral ratios throughout our investigations of regional phase spectral ratio transportability.

### **2.3 Correction for Station Instrument Response**

The shape of the regional phase spectrum can be affected by many factors. Traditionally, these factors have been represented as linear processes in which the seismic source spectrum is modified by 1) the source site response, 2) propagation path between the source and receiver, 3) receiver site response, and 4) instrument response at the recording station. In analyzing the transportability of regional phase spectral ratios as discriminants, we have attempted to account in these studies for knowledge of the station instrument response and source-to-receiver propagation. Clearly, instrument response could have a significant effect on regional phase spectral ratio measurements if the response varied with frequency between the bands in which the measurements were made. Many older seismic recording systems had fairly sharp response peaks in limited

frequency bands. However, most modern stations have fairly broad-band recording systems, so that station response may not be a strong factor in altering regional phase spectral ratio measurements, at least over the band of fairly flat response.

We illustrate the effects of correcting the  $L_g$  spectral ratio measurements for station instrument response in Figure 3. The top of Figure 3 shows the  $L_g$  spectral ratios for NTS explosion JUNCTION measured for nine stations at distances between  $2.3^\circ$  and  $19.9^\circ$ ; at the bottom of the figure are shown the same spectral ratios after correcting for the shape of the instrument responses. The recording systems for these stations are clearly rather broad-band; the corrections appear to produce no drastic changes in the overall spectral shapes. The main effect appears to be a slight increase in the  $L_g$  spectral ratio decay toward higher frequencies. This seems to be true for all stations except LON where the spectral level increases slightly at higher frequencies; this might indicate incorrect response information for LON, but we have not been able to verify that. More important from the standpoint of consistency of the measurements is that the instrument corrections appear to produce no noticeable improvement in the scatter of the measurements between stations. At some frequencies the variations between stations are reduced, but at others they are increased; and in all cases the changes in the scatter are only slight.

We have developed procedures to adjust regional phase spectral ratio measurements for station instrument responses, and we have used the available instrument response information to correct the spectral ratio measurements at the various stations used in this study. As described above, because of the fairly broad response characteristics of most stations used, this correction does not strongly affect the spectral ratio measurements in most cases. However, it should be noted that, for some small events and at some larger distances, signals may fall into the background noise; and in those cases instrument corrections beyond the normal passband of the recording system could artificially inflate the noise measurements.

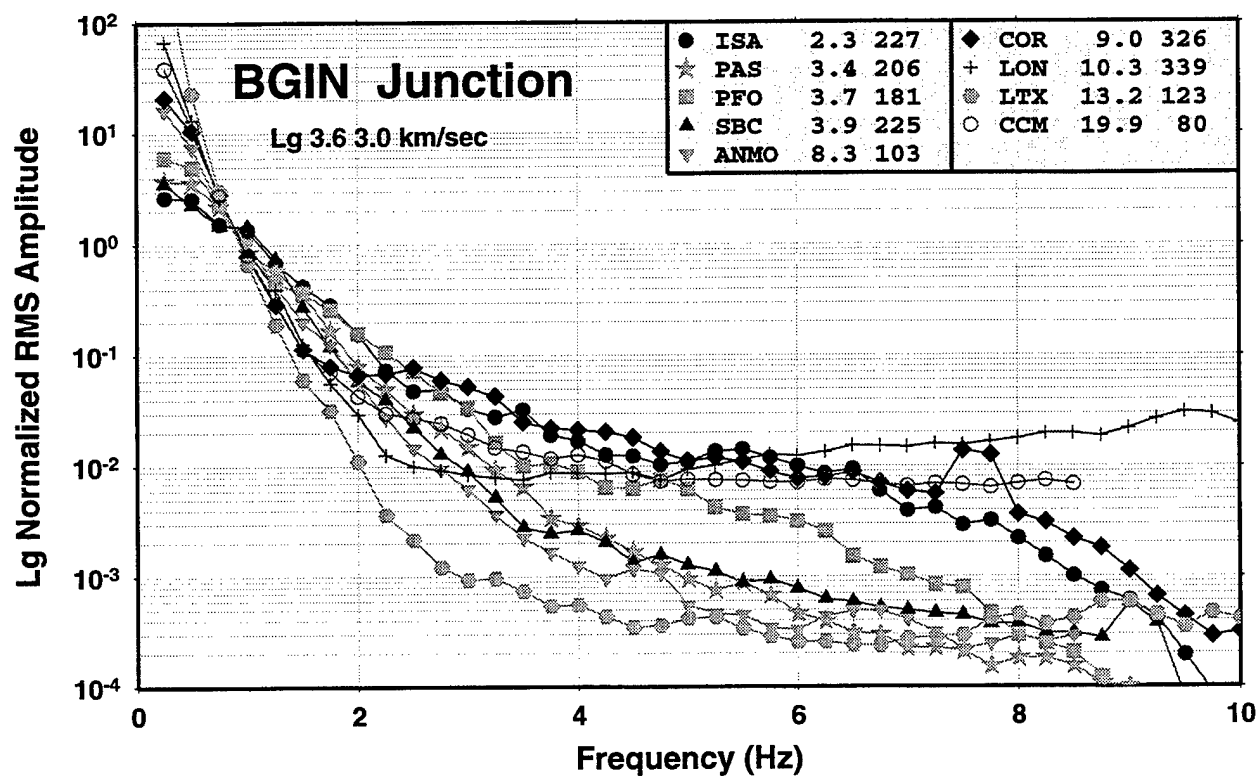
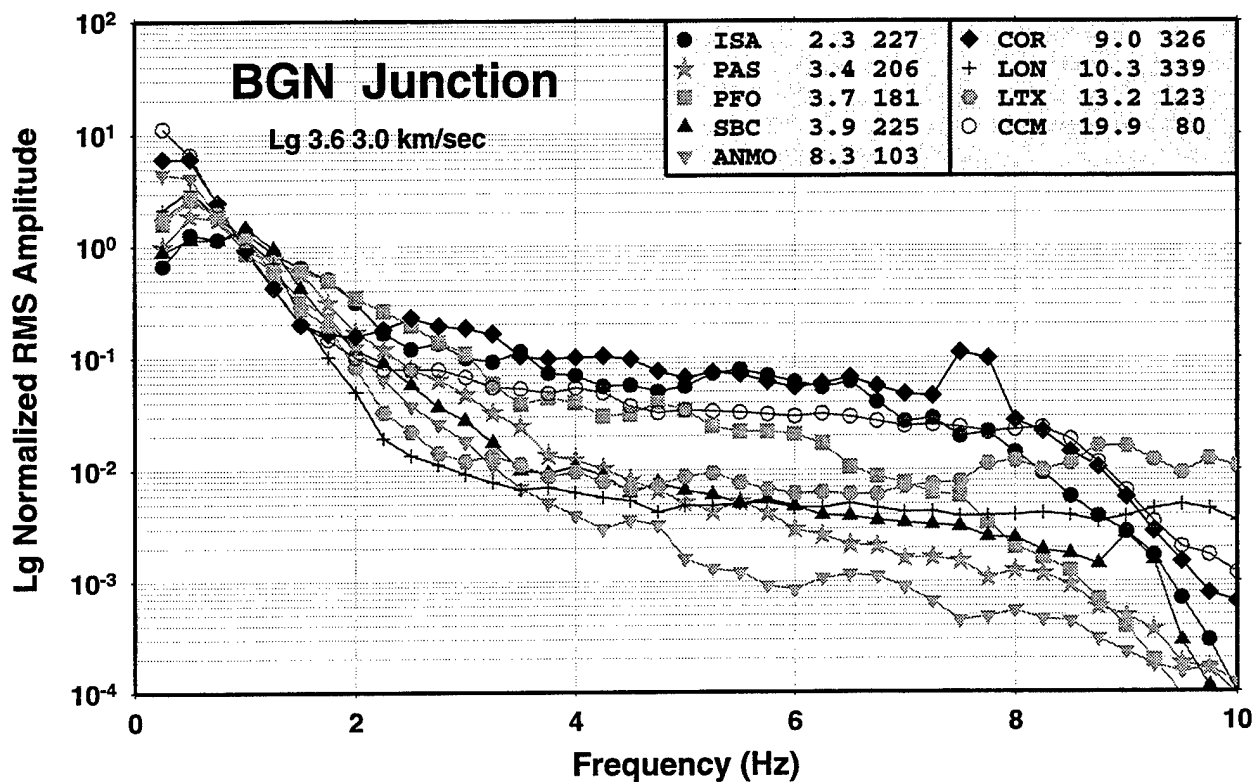


Figure 3. Comparison of  $L_g$  spectral ratio estimates before (top) and after (bottom) correction for the shape of the station instrument response at nine regional stations for the NTS Explosion JUNCTION.

## 2.4 Attenuation Corrections

### 2.4.1 Theory

Given the lack of calibration information for use in global CTBT monitoring, transportability of the regional phase spectral ratio discriminant is critically dependent on proper correction of the measurements for attenuation between source and receiver. In this section, we discuss the theory used in developing these kinds of corrections. The corrections are based on pre-existing models of attenuation covering the U.S. and Eurasia, which have been developed from prior research on regional phase propagation. The characteristics of these models and their general effects on regional signals are also described. We focus in particular on corrections to  $L_g$  spectral ratios because the attenuation models for  $L_g$  are more complete and better understood; however, similar corrections may be reasonably applied to other crustal phases, like  $P_g$ , or to other guided regional phases, after developing further attenuation models or possibly with some simplifying assumptions.

As alluded to above, the observed spectrum  $A(f,r)$  from a seismic source can be represented as

$$A(f,r) = S(f) \cdot G(r,r_0) \cdot e^{-\pi\eta/Q(f)} \quad (1)$$

where  $S(f)$  = the spectrum of the seismic source

$f$  = frequency

$r$  = distance

$r_0$  = a reference distance

$t$  = travel time from source to receiver

$G(r,r_0)$  = a geometric spreading term

$Q(f)$  = a frequency dependent quality factor describing attenuation.

The frequency-dependent  $Q(f)$  is represented by

$$Q(f) = Q_0 \cdot f^\eta \quad (2)$$

where  $Q_0$  = attenuation at 1 Hz

$\eta$  = the frequency dependence of  $Q$ .

As the earth is not homogeneous,  $Q_0$  and  $\eta$  vary with location and depth. Because the  $L_g$  phase is confined to a waveguide and samples the earth's crust, we make the simplifying assumption that the average  $Q_0$  and  $\eta$  in the crust are representative of the effective attenuation and ignore the depth dependence. Thus, we assume that the  $Q$  model consists of point samples (a grid) of  $Q_0$  and  $\eta$  varying over the earth's crust.

The method we have used to correct the spectral ratios is to determine the source-to-receiver path through the grid of  $Q$  values in the model and to sum the attenuation contributions from each cell. The attenuation factor thus becomes:

$$\Gamma(f) = e^{-\pi f \sum_{i=1}^n t_i^*} \quad (3)$$

where

$$\sum_{i=1}^n t_i^* = \frac{t_1}{Q_1} + \frac{t_2}{Q_2} + \dots + \frac{t_n}{Q_n} \quad (4)$$

The  $t_i$  are the travel times spent by the phase in the individual grid cells along the path, and the  $Q$  values are calculated from the prior model using equation (2). The  $L_g$  attenuation corrections as a function of frequency along any path can be estimated using the method described above, and these can then be used as corrections to the  $L_g$  spectral ratios.

#### 2.4.2 Attenuation Models

When applying path corrections to the observations from events that might be at any location, an attenuation model is required that includes all possible paths. For  $L_g$  this would include all continental crustal areas to be modeled. Although models are not complete for all areas and are subject to revision as more abundant observations become available, much work has been done to understand  $L_g$  attenuation in many different parts of the world.  $L_g$  coda  $Q$  models have been developed for Africa (cf. Xie and Mitchell, 1990), Eurasia (cf. Mitchell et al., 1996), and the U.S. (cf. Mitchell, 1997). These model were derived through inversion of  $L_g$  coda in a back projection algorithm that produces a tomographic image of  $Q(L_g)$ . Thus, the models represent attenuation from both intrinsic and scattering mechanisms. The original models from Mitchell et al. were presented as

3-by-3 degree grid cells for  $Q_0$  and  $\eta$ . The U.S. model is presented with smaller spacing in a 2-by-2 degree grid.

We have merged the different model results from Mitchell et al. into global maps for  $Q_0$  and  $\eta$ , as shown in Figures 4 and 5. The maps are generally consistent with experience indicating low  $L_g$  attenuation (i.e. relatively high  $Q$ ) in shield and relatively stable platform regions and high attenuation (i.e. low  $Q$ ) in tectonically complex and active regions. This is in particular true for the  $Q_0$  map, while the variations on the  $\eta$  map are more complex; it should be noted that the  $\eta$  map for Eurasia has been altered somewhat from that originally described by Mitchell et al. (1996). It should also be emphasized that these maps represent an effective  $Q$ ; so that, in regions which are more tectonically complex, the model may not be adequate. Thus, regions of complex crustal structure, corresponding to rapid changes in crustal thickness or sudden changes in layer properties, may not be properly accounted for by this model and will require more detailed consideration if they are to be used in regional monitoring.

To illustrate the effect of attenuation on the  $L_g$  spectra and on  $L_g$  spectral ratio measurements, we have used the models to calculate the correction factors (as described in Section 2.4.2 above) for several specific source-station paths. Figure 6 shows the  $L_g$  spectra correction factors for nine stations surrounding the NTS nuclear explosion JUNCTION. The station distance ranges vary from  $2.3^\circ$  to  $19.9^\circ$ , and the paths cover a broad range in azimuth around NTS (cf. Figure 8 below). The correction factors are plotted as adjustments to the  $L_g$  spectral ratio, so they are normalized to one in the band near 1.0 Hz. The factors are plotted at frequency intervals of 0.25 Hz over the range from 0.25 Hz to 10 Hz. The plot indicates that the  $L_g$  correction factors are large at large distances and high frequencies, in general; but azimuth is also a factor, as paths crossing low- $Q$  zones are in some cases more highly attenuative (i.e. larger correction factors) than are longer paths through high- $Q$  zones. For the western U.S. the greatest attenuation appears to be for paths to the north and northwest (viz. to stations COR and LON), while paths to the east and out of the Basin and Range region (viz. to stations LTX and CCM) predict less severe  $L_g$  attenuation. At lower frequencies, the  $L_g$  correction factors are not too large, staying in a range from 1 to 10 at 2 Hz and from 2 to 100 at 4 Hz. However, at

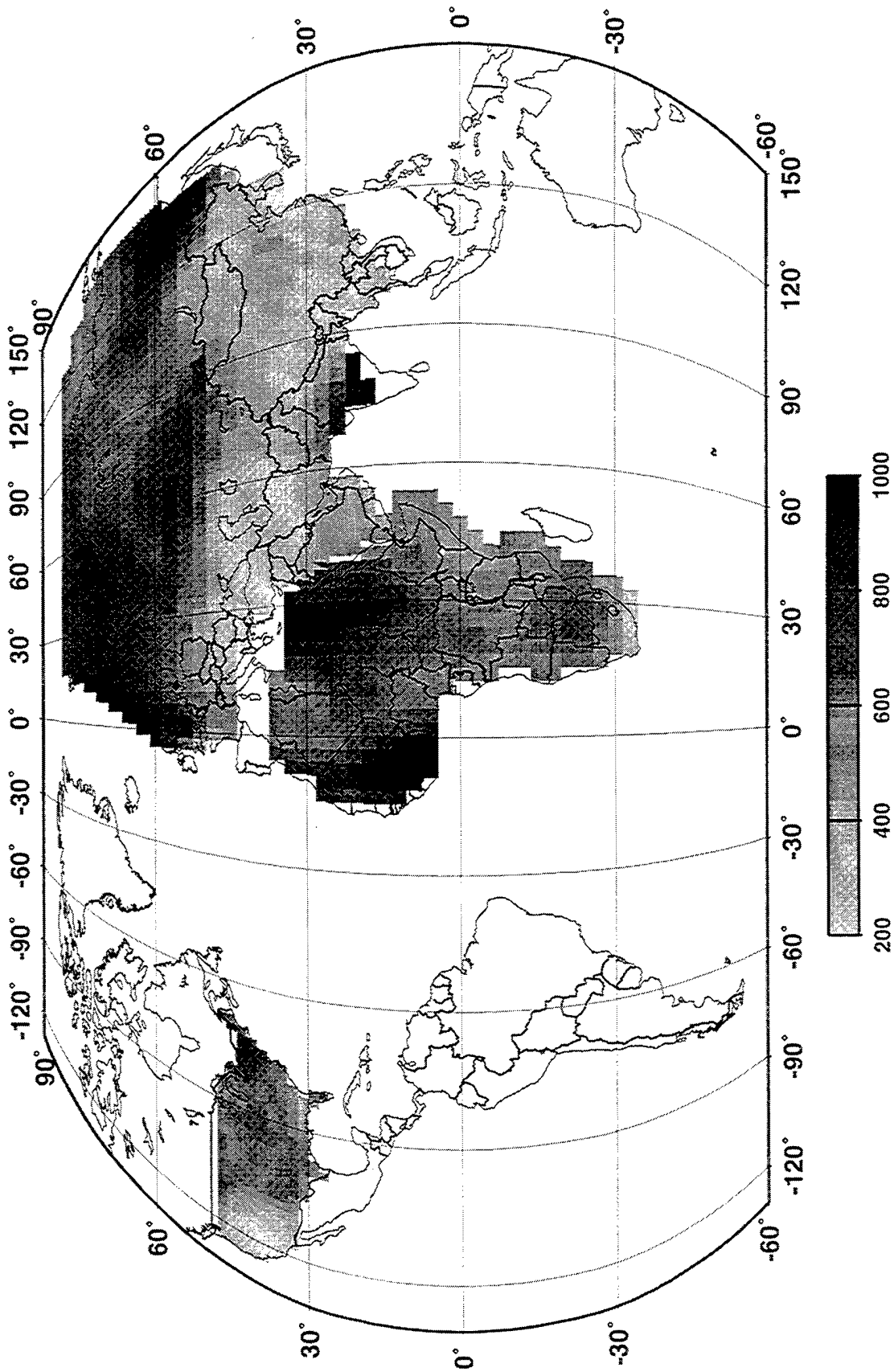


Figure 4. Attenuation at 1Hz ( $Q_0$ ) from Lg Coda adapted from work by Mitchell et al. (cf. Xie and Mitchell, 1990, Mitchell et al., 1996)



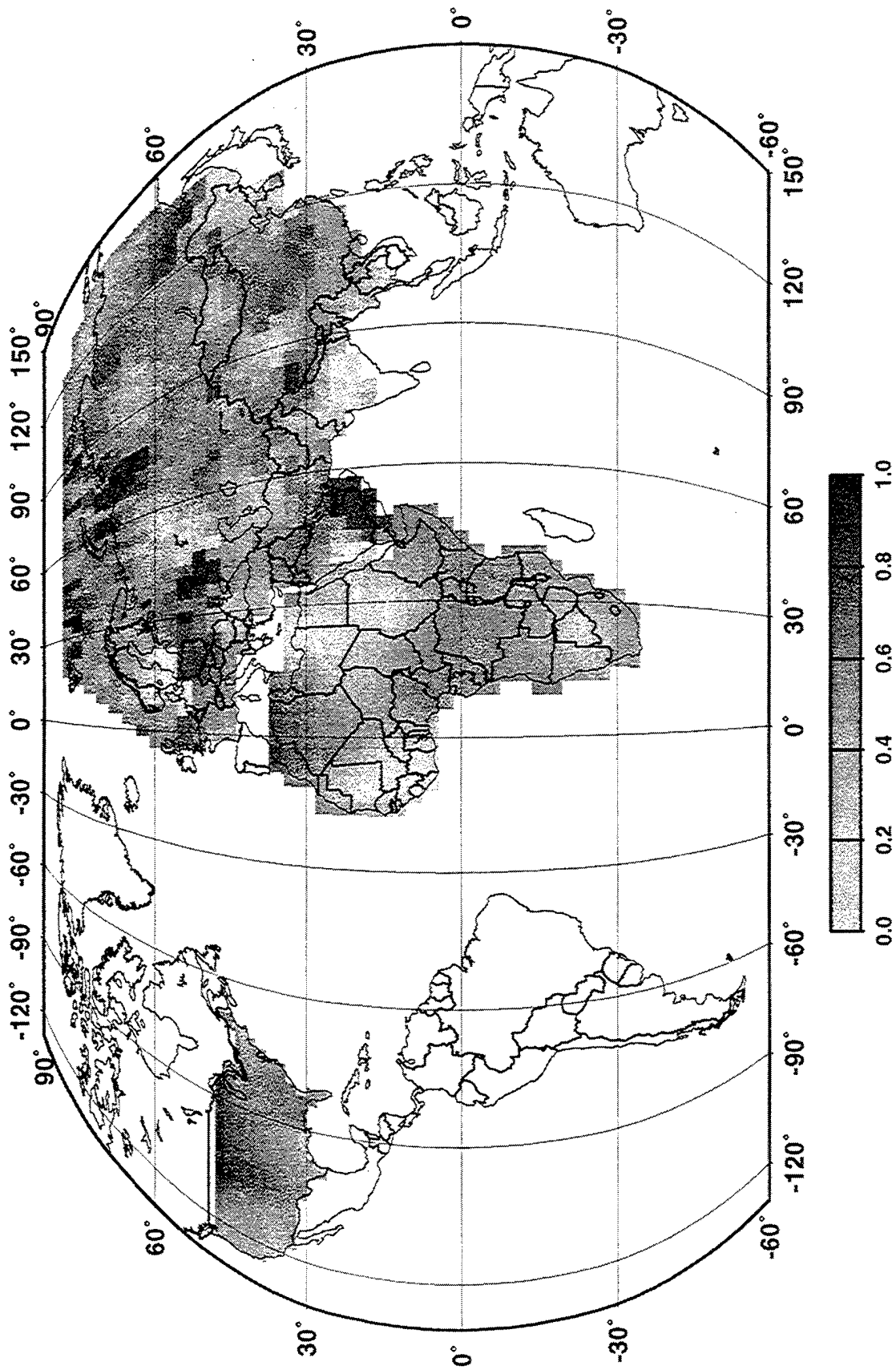


Figure 5. Frequency dependence of attenuation ( $\eta$ ) from  $L_g$  coda adapted from work by Mitchell et al. (cf. Xie and Mitchell, 1990, Mitchell et al., 1996)

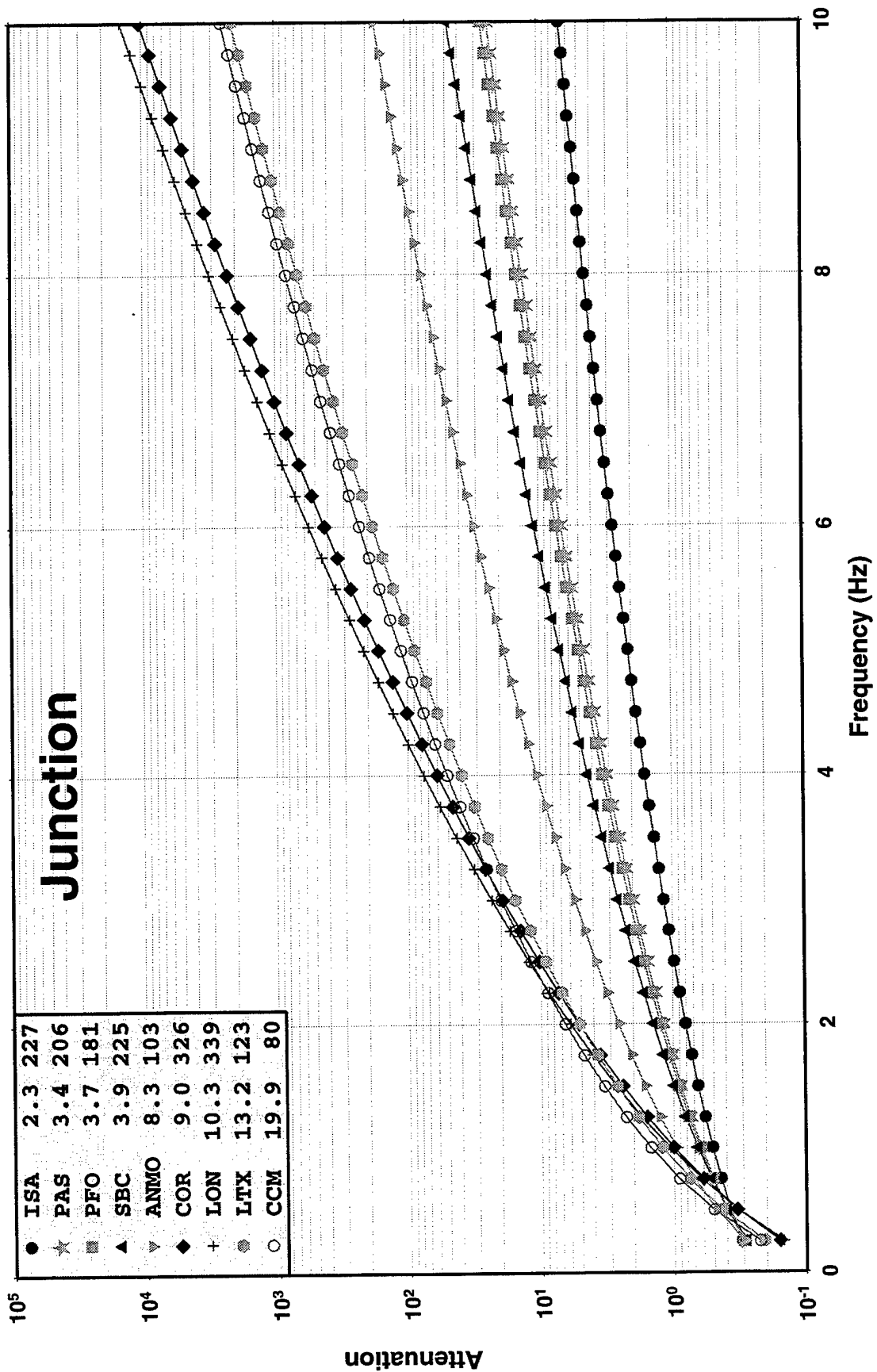


Figure 6. Predicted attenuation correction factors for  $L_g$  spectral ratios for specific station paths from NTS nuclear explosion JUNCTION.

high frequencies the correction factors predicted by the model can become quite large: 5 to 600 at 6 Hz, 8 to 3000 at 8 Hz, and 12 to 15,000 at 10 Hz. It should be noted that these large correction factors also imply very weak signals, so that actual  $L_g$  signals are likely to fall below the noise level at higher frequencies for many of the more-distant stations.

Figure 7 shows the same kind of  $L_g$  spectral correction factors for eight stations surrounding an earthquake in northwestern China near Lop Nor. The stations in this case are at distances from  $1.4^\circ$  to  $14.6^\circ$  and cover a broad range in azimuths. The  $L_g$  spectral ratio correction factor at the nearest station, WMQ, varies only from about 1 to 2 over the frequency range from 1 Hz to 10 Hz. However, at the most-distant station the correction factor exceeds  $10^5$  at 8 Hz. There is also apparent a fairly strong azimuthal dependence. Looking just at the more-distant stations, which are all at similar distances between  $13.9^\circ$  and  $14.6^\circ$ , the  $L_g$  correction factors differ by almost a factor of 1000 at 6 Hz and by about a factor of 50,000 at 10 Hz. For sources in northwestern China the most severe  $L_g$  attenuation occurs at azimuths to the south (e.g. to station LSA) and southwest (e.g. to station NIL). The paths to these stations are known to cross very complex tectonic zones. Again, it should be noted that we would not expect to be able to observe the weak signals implied by such large attenuation. This will be discussed more below when we show how the correction factors affect actual measurements.

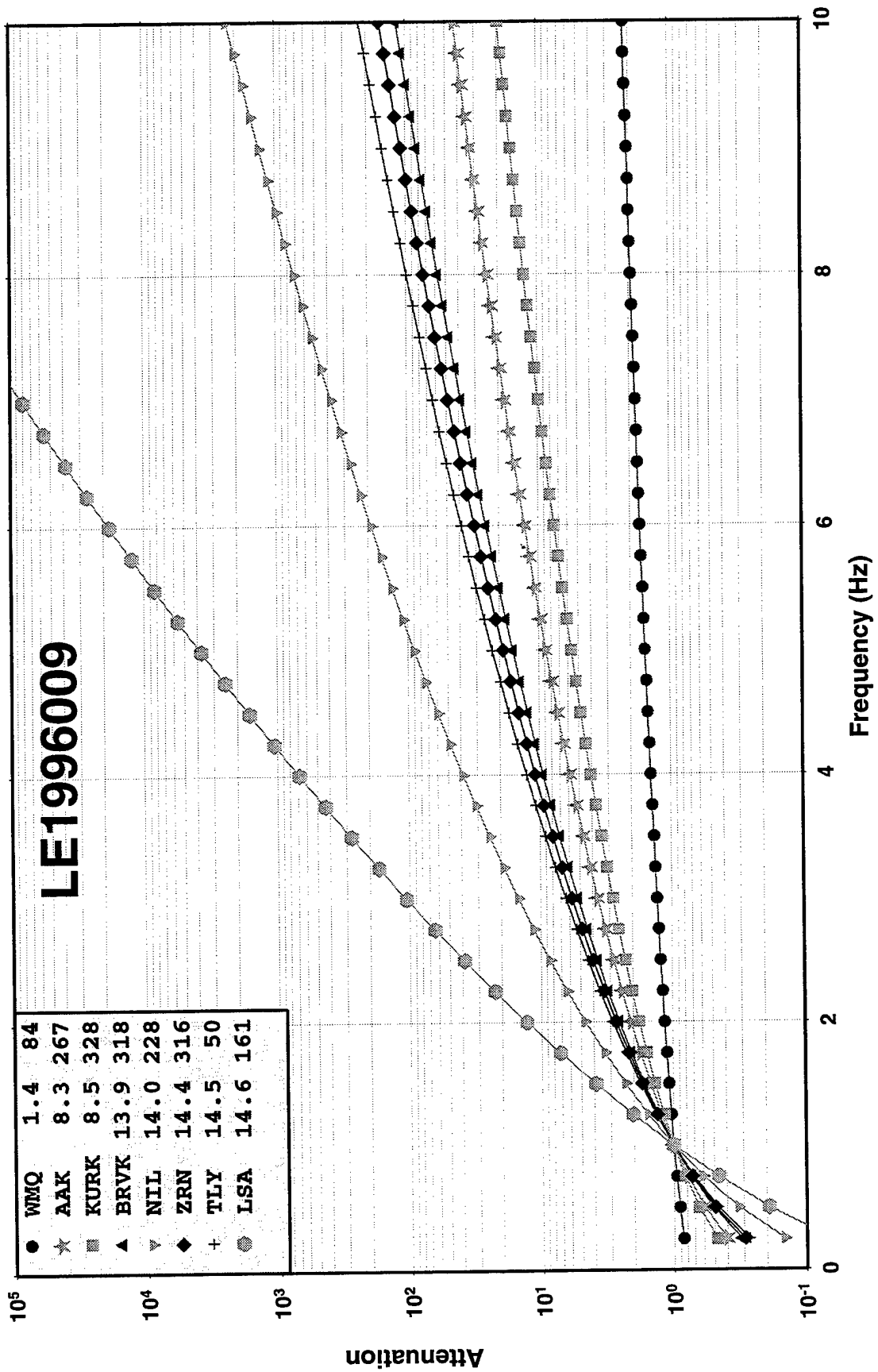


Figure 7. Predicted attenuation correction factors for  $L_g$  spectral ratios for specific station paths from an earthquake in northwestern China near Lop Nor.

### **3. Database for Spectral Ratio Studies**

#### **3.1 Limitations of the Regional Database**

Some of the most useful seismic data for investigating regional discrimination based on spectral characteristics of regional phases comes from nuclear explosion tests in the western U.S., in eastern Kazakhstan in the Former Soviet Union, at Lop Nor in western China, from numerous PNE explosions in the Former Soviet Union, and from earthquakes or other sources in similar tectonic environments and at comparable propagation distances. In several prior investigations (cf. Bennett et al., 1989, 1992), we have collected and compared the spectral characteristics of regional phase signals from nuclear explosions at specific test sites and other nearby source types (e.g. earthquakes) recorded at common seismic stations, so that propagation differences and station effects would be minimized. In our previous report under this contract (cf. Bennett et al., 1996), we reviewed the characteristics and limitations of a large regional database which was compiled as part of these prior investigations to develop regional discrimination techniques. However, as noted above, in monitoring a CTBT we need to extend regional discrimination capability into areas with little or no prior calibration experience. Calibration is lacking because of geographic limitations in the locations of prior events and because many high-quality regional stations have only recently begun operation. In these uncalibrated areas propagation effects can be expected to significantly modify the spectral content of regional phases, as was noted in the discussion presented in Section 2. Therefore, if regional phase spectral ratios are to be generally applicable and transportable into uncalibrated regions, they should be adjusted for both instrument response and propagation path effects.

It has been the goal of this project to investigate how regional phase spectral ratio measurements might be affected by both recording instrument response and attenuation along the propagation path between the source and station. To accomplish this objective we have sought to apply corrections to the regional phase spectral ratio measurements for selected, representative samples of events from several distinct tectonic regions. These

samples have included events from well-calibrated regions (e.g. western U.S.) as well as single events from uncalibrated regions which would be of interest in CTBT monitoring.

### 3.2 Data Sources

Figures 8 and 9 show the locations of stations and events in the U.S. and Eurasia respectively for which the regional phase signals were collected and reviewed for use in these analyses. For the western U.S. our database tends to be dominated by recordings from the Lawrence Livermore National Laboratory (LLNL) seismic network surrounding NTS for which we have significant samples of underground nuclear explosions and nearby earthquakes. As noted above, these observations provide some of the best regional signals from known underground nuclear explosions and earthquakes from a common source area and were (along with VELA station measurements) important to the early development of  $L_g$  spectral ratios as discriminants. However, to prevent these data from having too strong an influence on our results, we have limited the number of events recorded at LLNL stations used in these analyses and have supplemented the database with additional recordings of nuclear explosions, earthquakes, and chemical explosions recorded at several other regional stations. In many instances these additional stations are located at somewhat larger distances, and the signal-to-noise level at these more-distant stations is diminished, particularly at high frequencies.

For Eurasia we selected events from several areas of interest, including representative nuclear explosion tests from the test sites at Balapan in the Former Soviet Union and Lop Nor in China. We also reviewed data for explosions and other events from the vicinity of the Russian test site at Novaya Zemlya; but the regional records there showed little evidence of  $L_g$  signals, presumably because of  $L_g$  propagation path blockage surrounding the island. Also, in the interest of assessing capabilities for a realistic CTBT monitoring environment, we focused primarily on high-quality stations, including those which are routinely used by the IDC. However, because of the scarcity of high-quality stations in Eurasia, events are often recorded by only one or two favorably located regional stations. Even for fairly large events, the stations at large regional distances may only record regional phases with signal-to-noise ratios greater than one in a fairly

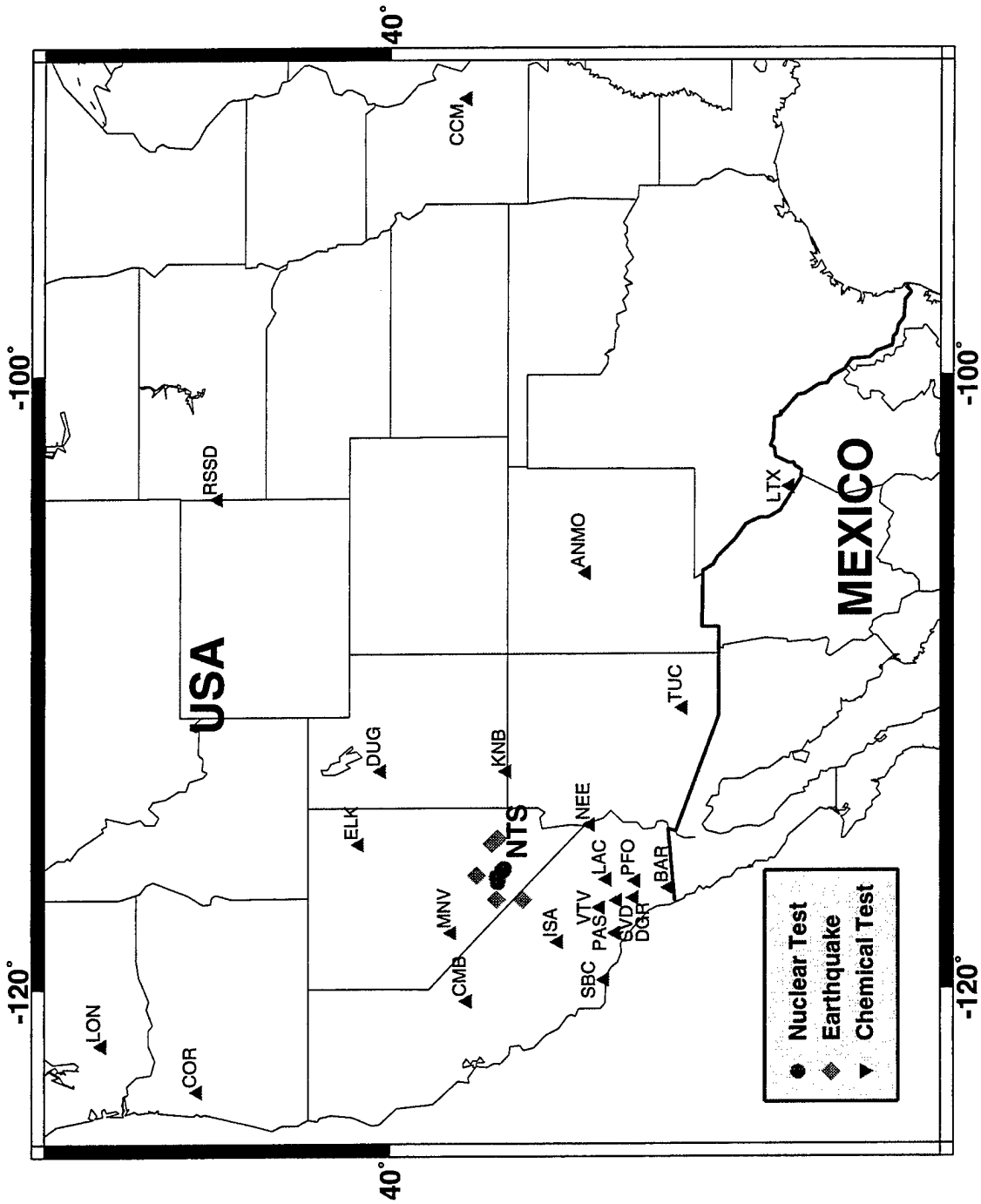
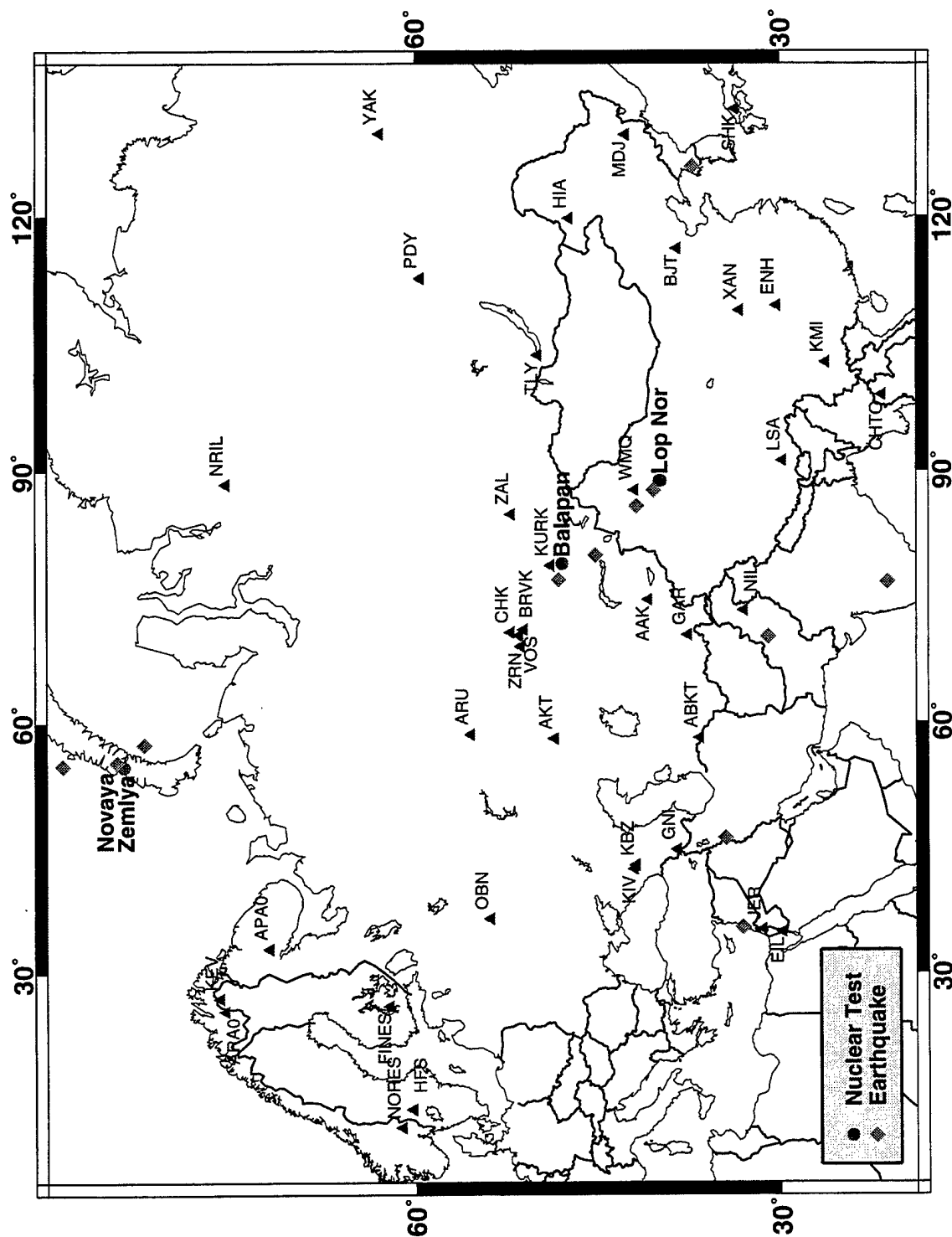


Figure 8. Locations of selected explosions, earthquakes, and stations used in analyzing regional phase spectral ratios from western U. S. events.





limited frequency band. Therefore, these records aren't always useful for determining  $L_g$  spectral ratios which require comparisons of the relative signal energy in contrasting frequency bands.

Table 1 summarizes the events and recording stations used in analyzing the regional phase spectral ratios. The events used range in magnitude from 3.77 to 6.2 and include 17 explosions and 14 earthquakes. We collected the records from 57 different stations in the regional distance range for these events. Many of these records turned out not to be useful because of low signal-to-noise level and were excluded from the final analyses.

**Table 1. List of Events and their Respective Stations Used in this Study.**

**Nuclear Explosions at Balapan, former Soviet Test Site (Joint Verification Experiment):**

Date	Time	Lat	Lon	Depth	Mag	Locale
1988 Sep 14	03:59:59.6	49.86	78.82	0.00	6.10	EASTERN KAZAKH SSR

Stations: WMQ GAR ARU KIV TUP OBN HIA

**Nuclear Explosions at the Lop Nor, China Test Site:**

Date	Time	Lat	Lon	Depth	Mag	Locale
1990 Aug 16	04:59:57.6	41.56	88.77	0.00	6.20	SO. SINKIANG PROV CHINA

Stations: GAR ARU KIV OBN

1996 Jun 08	02:55:59.4	41.64	88.76	0.00	5.69	SO.SINKIANG PROV CHINA
-------------	------------	-------	-------	------	------	------------------------

Stations: AAK KURK NIL BRVK PDY ABKT CHTO ARU NRIL YAK KBZ OBN

**Nuclear Explosions at the Nevada, USA Test Site:**

Date	Time	Lat	Lon	Depth	Mag	Locale
1977 Apr 05	15:00:00.1	37.12	-116.06	0.00	5.60	SOUTHERN NEVADA-marsilly

Stations: ELK KNB LAC MNV

1977 Apr 27	15:00:00.0	37.09	-116.02	0.00	5.40	SOUTHERN NEVADA-bulkhead
-------------	------------	-------	---------	------	------	--------------------------

Stations: ELK KNB LAC MNV

1978 Mar 23	16:30:00.2	37.10	-116.05	0.00	5.60	SOUTHERN NEVADA-iceberg
-------------	------------	-------	---------	------	------	-------------------------

Stations: ELK KNB LAC MNV

1983 Apr 14	19:05:00.1	37.07	-116.04	0.00	5.70	SOUTHERN NEVADA-turquoise
-------------	------------	-------	---------	------	------	---------------------------

Stations: ELK KNB LAC MNV

1984 Jan 31	15:30:00.0	37.11	-116.12	0.00	4.10	SOUTHERN NEVADA-gorbea
-------------	------------	-------	---------	------	------	------------------------

Stations: ELK KNB LAC MNV

1984 Mar 31	14:30:00.0	37.14	-116.08	0.00	4.10	SOUTHERN NEVADA-agrini
-------------	------------	-------	---------	------	------	------------------------

Stations: KNB

1985 Jun 12	15:15:00.0	37.24	-116.48	0.00	5.50	SOUTHERN NEVADA-salut
1986 Jun 25	20:27:45.1	37.26	-116.49	0.00	5.50	SOUTHERN NEVADA-darwin
1986 Sep 30	22:30:00.1	37.30	-116.30	0.00	5.50	SOUTHERN NEVADA-labquark
1986 Dec 13	17:50:05.0	37.26	-116.41	0.00	5.50	SOUTHERN NEVADA-bodie
1987 Apr 18	13:40:00.6	37.24	-116.50	0.00	5.50	SOUTHERN NEVADA-delamar
1987 Apr 30	13:30:00.0	37.23	-116.42	0.00	5.50	SOUTHERN NEVADA-hardin

Stations: RSSD

1992/086 Mar 26	16:30:00.0	37.27	-116.35	0.00	5.50	SOUTHERN NEVADA-junction
-----------------	------------	-------	---------	------	------	--------------------------

Stations: ISA PAS PFO SBC ANMO COR LON LTX COM

**Chemical Explosions at the Nevada Test Site (Non-proliferation Experiment):**

Date	Time	Lat	Lon	Depth	Mag	Locale
1993 Sep 22	07:01:00.0	37.20	-116.20	0.39	4.10	SOUTHERN NEVADA-npe

Stations: ISA NEE VTV SVD CMB PAS PFO DGR SBC DUG BAR TUC ANMO COR RSSD LTX

### Earthquakes in Eurasia:

Date	Time	Lat	Lon	Depth	Mag	Locale
1996 Jan 09	06:27:55.7	43.68	85.72	33.90	5.20	NO. SINKIANG, CHINA
Stations: WMQ AAK KURK BRVK NIL ZRN TLY LSA AKT ARU ABKT BJT ENH KMI HIA						
1996 Mar 20	02:11:23.4	42.15	87.63	22.50	4.80	NO. SINKIANG, CHINA
Stations: WMQ AAK KURK LSA NIL TLY VOS CHK ZRN XAN BJT ABKT HIA ARU NRIL						
1996 Mar 26	13:58:17.4	50.08	76.97	47.34	3.77	EASTERN KAZAKH SSR
Stations: KURK BRVK ZAL AAK WMQ ARU						
1996 Sep 04	20:39:50.5	35.43	46.08	0.00	4.06	IRAN-IRAQ BORDER REGION
Stations: KIV ABKT						
1996 Sep 14	13:38:54.0	38.58	125.82	0.00	3.94	NORTH KOREA
Stations: MDJ SHK BJT HIA						
1996 Dec 22	20:45:56.1	31.21	70.09	17.21	4.28	PAKISTAN
Stations: NIL AAK						
1997 Mar 26	04:22:54.1	33.75	35.46	0.00	4.58	JORDAN-SYRIA REGION
Stations: JER EIL GNI KIV						

### Earthquakes in the US

Date	Time	Lat	Lon	Depth	Mag	Locale
1979 Aug 12	11:31:19.7	37.26	-115.08	5.00	3.6L	SOUTHERN NEVADA
Stations: KNB						
1979 Aug 16	03:37:44.9	37.25	-115.06	5.00	3.7L	SOUTHERN NEVADA
Stations: KNB						
1979 Dec 25	14:17:10.8	37.27	-117.06	8.00	3.9L	CAL.-NEV. BORDER REG.
Stations: ELK KNB LAC MNV						
1980 Oct 25	00:30:59.0	37.79	-116.28	8.00	3.8L	SOUTHERN NEVADA
Stations: ELK KNB LAC MNV						
1982 Mar 16	07:08:13.1	36.60	-117.07	7.00	3.5L	CAL.-NEV. BORDER REG.
Stations: KNB						
1982 May 12	19:29:24.5	37.27	-115.08	7.00	4.0L	SOUTHERN NEVADA
Stations: ELK KNB LAC MNV KNB						
1983 Jun 04	11:37:40.9	37.39	-115.21	5.00	3.6L	SOUTHERN NEVADA
Stations: KNB						

## 4. Application and Event Analyses

### 4.1 Some Tests of the Attenuation Models

#### 4.1.1 Western U.S.

Data from several events in the western U.S. and Eurasia were used to test the attenuation models and correction procedures. For the western U.S. we used the observations from a well-recorded NTS nuclear explosion, JUNCTION, and three smaller southern Nevada earthquakes (viz. earthquake of 1979/12/25, earthquake of 1980/10/25, and earthquake of 1982/05/12) to analyze the effectiveness of the signal corrections. Source parameters for these events and the regional stations from which observations were available are described in Table 1 above. If the  $L_g$  spectral ratio corrections are to be useful, they should reduce the scatter between stations, particularly for an explosion source. Figure 10 shows a comparison of the  $L_g$  spectral ratios observed at nine regional stations for the 5.5 m<sub>b</sub> JUNCTION nuclear explosion after correction for station instrument response (top) and after correction for attenuation as well as instrument response (bottom). In Figure 3 above we noted for this same data set that the instrument response correction appeared to have little effect on improving the scatter in the  $L_g$  spectral ratio observations between stations. At first appearance the comparison in Figure 10 suggests that the attenuation corrections actually may be acting to increase the scatter between stations. However, closer inspection reveals that this is not the case. In particular, we note that the attenuation-corrected amplitude curves at a few stations (viz. COR, LON, and CCM) depart from a general trend of decreasing amplitude with increasing frequency at about 2 Hz. Furthermore, the spectral ratio at station LTX also appears anomalous, showing a steeper slope than other curves up to about 3 Hz and a shallower slope above 3 Hz. These four stations are the most distant from the JUNCTION explosion and the deviations can be explained by noise. At COR, LON, and CCM, the spectra indicate that the signals are contaminated by background noise above about 2 Hz, and at LTX the spectra suggest contamination above about 3 Hz. There appears to be no useful  $L_g$  energy at higher frequencies in the records at any of these stations for the JUNCTION explosion.

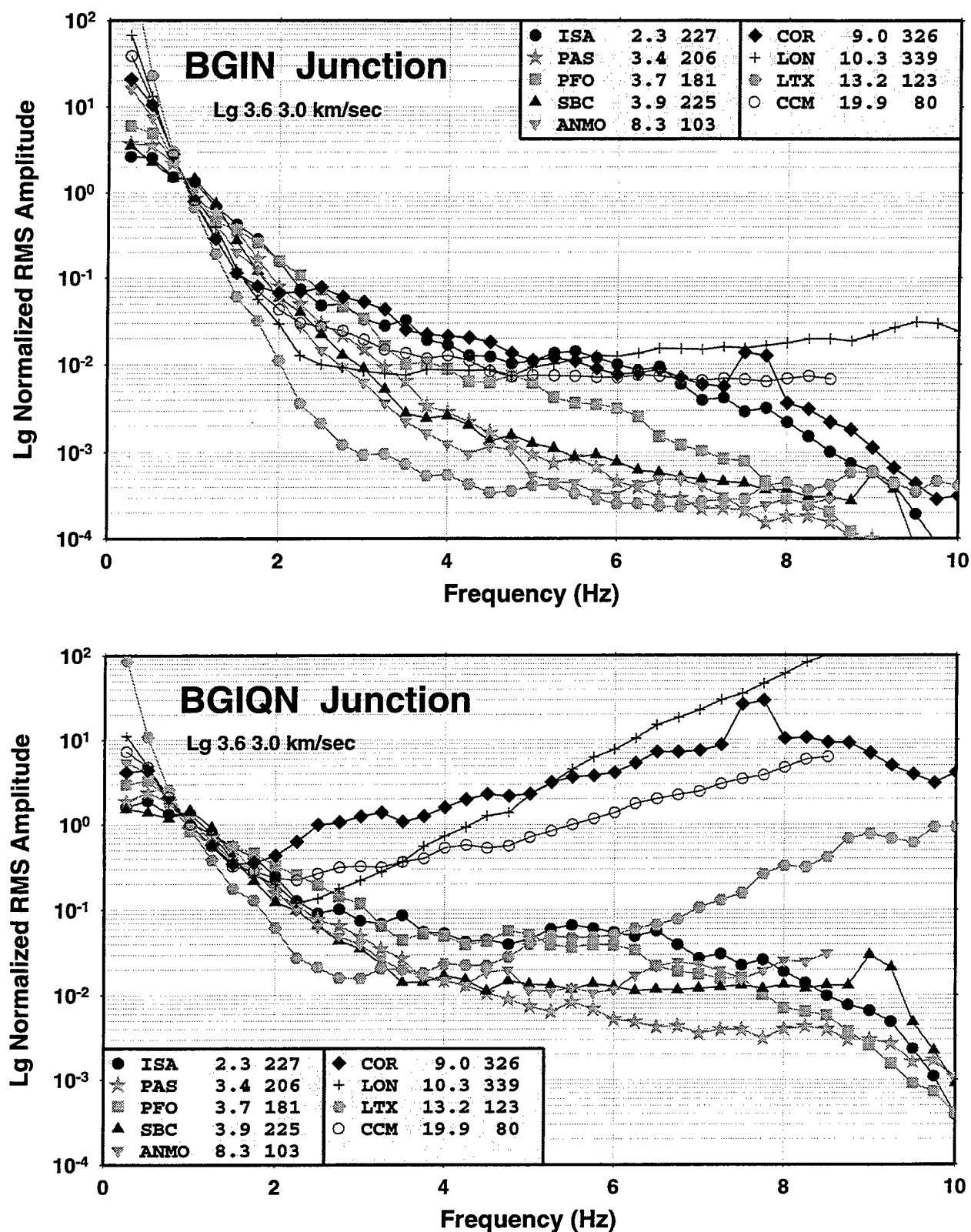


Figure 10. Comparison of the instrument-corrected  $L_g$  spectral ratio estimates for NTS explosion Junction (top) and the same spectral ratios after correction for path-specific attenuation (bottom) developed from the attenuation model.

Ignoring the measurements from stations COR, LON, CCM, and LTX because of the apparent noise contamination, we proceeded with analyses of the remaining five stations which were all at distances less than 1000 km. Focusing on the  $L_g$  spectral ratios in Figure 10 for just stations ISA, PAS, PFO, SBC, and ANMO, it is evident that the scatter between events has effectively been reduced at all frequencies. For example, the variation in the ratios between stations at 4 Hz goes from a factor of 15 or so before the attenuation correction to a factor of about 4 after. At 6 Hz the scatter is reduced from a factor of 30 to a factor of 10, and at 8 Hz from a factor of 10 to a factor of 7. In Figure 11 we show a comparison of the standard deviations based on the spectral ratio measurements at the five stations. The standard deviations as a function of frequency are plotted for both the instrument-corrected spectral ratios and for the attenuation- and instrument-corrected spectral ratios. For reference we also have plotted the variation in the model-predicted corrections between the five stations. It should be noted that the relative drop in the latter curve just above 8 Hz is associated with lack of data at ANMO above that frequency, and we have consequently dropped ANMO from the averages at the highest frequencies. In theory, if the model worked perfectly and there were no site effects or non-uniform source effects, the predicted values would match the instrument-corrected curve and the attenuation- and instrument-corrected curve would have zero standard deviation. As can be seen in Figure 11, the scatter in the instrument-corrected curve does not exactly match the scatter in the model prediction; although the two curves show similar trends with frequency. The standard deviation of the attenuation- and instrument-corrected spectral ratios does not go to zero, but it is lower than the standard deviation for just the instrument-corrected ratios, as we suggested above in Figure 10. The remaining differences can possibly be attributed to errors in the attenuation model or differences in station site response or a combination of these factors.

We performed similar analyses on the observations for the three earthquakes with sources near NTS. Observations for these events were limited to the records from the LLNL network stations, all at distances less than  $5^\circ$ ; and, even though the events were small, they were well-recorded at all four stations. These comparisons are shown in Figures 12 - 14. Again, the scatter in the instrument-corrected curves and the scatter in

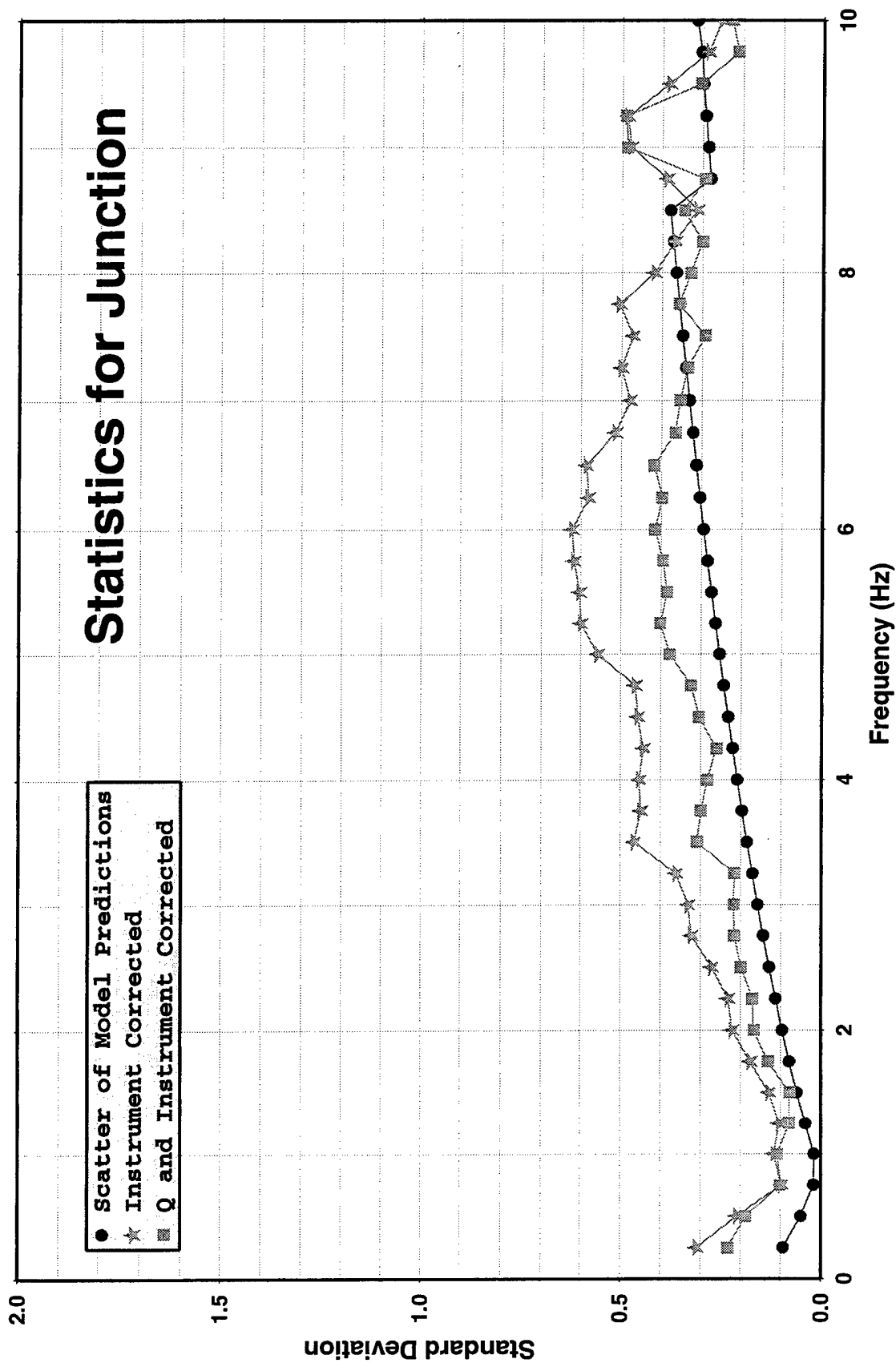


Figure 11. Comparison of standard deviations for  $L_g$  spectral ratios based on measurements at five of the better stations (viz. ISA, PAS, PFO, SBC, and ANMO) for NTS explosion JUNCTION before and after attenuation corrections.

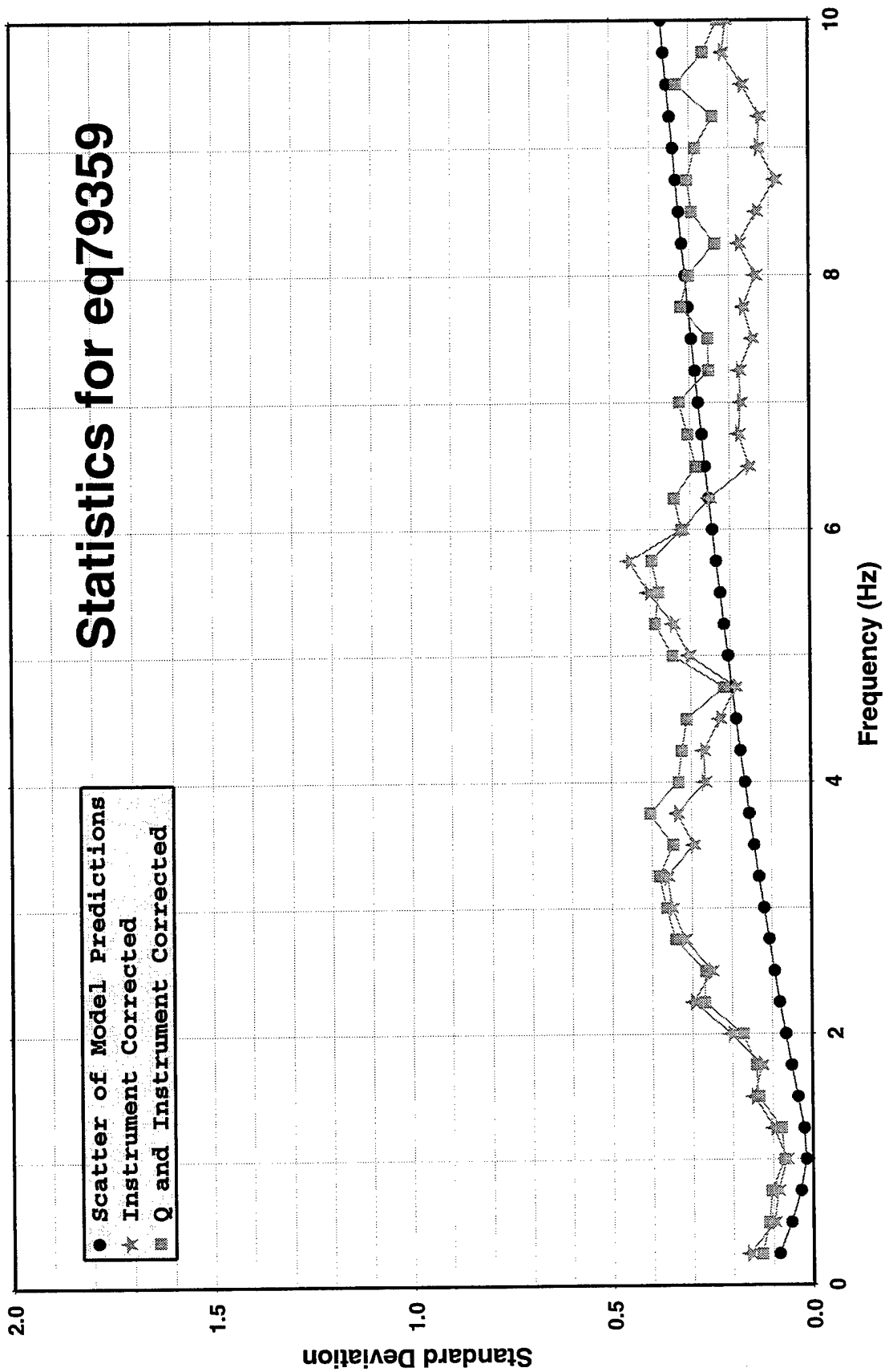


Figure 12. Comparison of standard deviations for  $L_g$  spectral ratios based on measurements at the four LLNL stations for the 1979/12/25 earthquake near NTS before and after attenuation corrections.



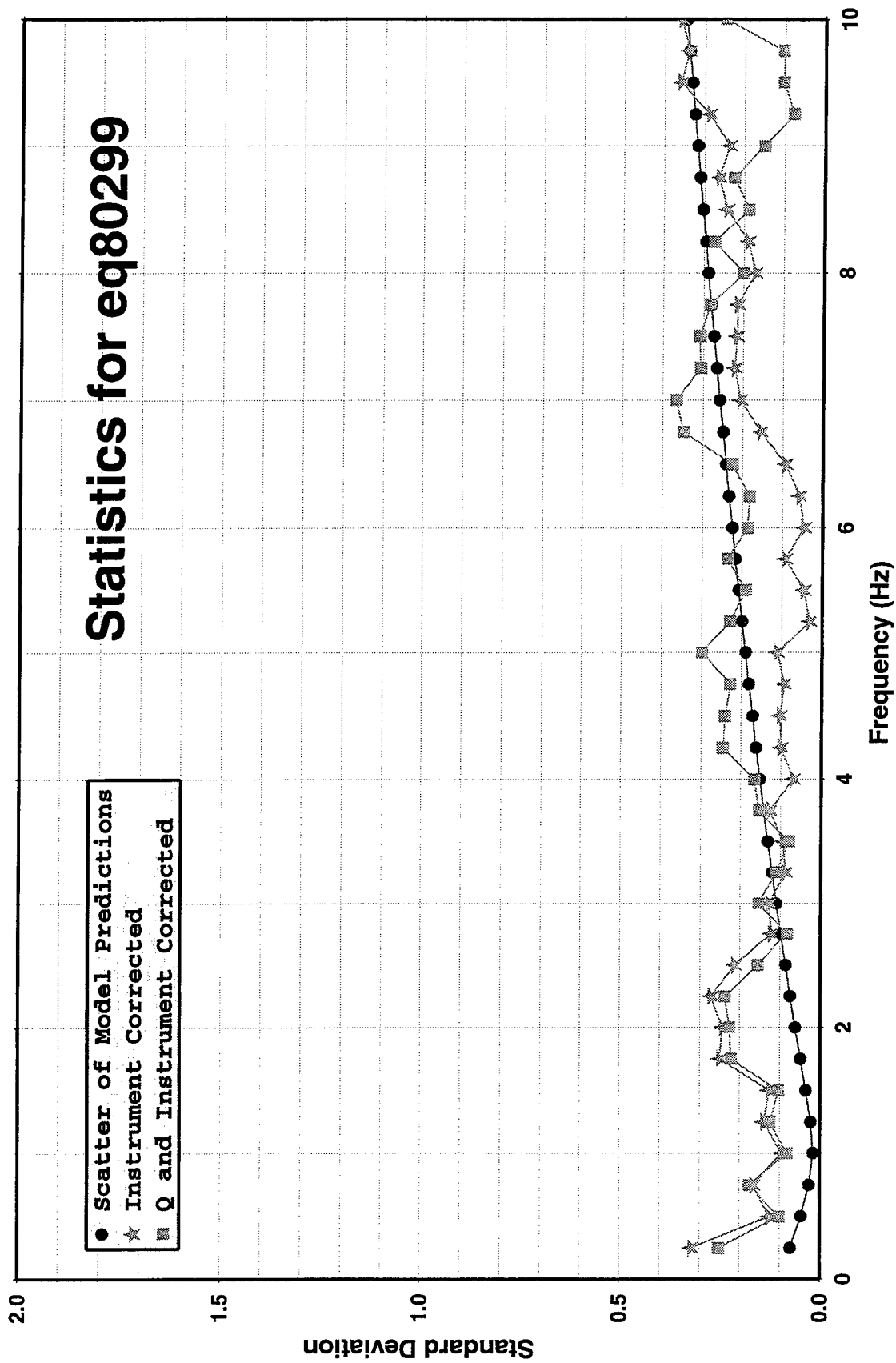


Figure 13. Comparison of standard deviations for  $L_g$  spectral ratios based on measurements at the four LLNL stations for the 1980/10/25 earthquake near NTS before and after attenuation corrections.

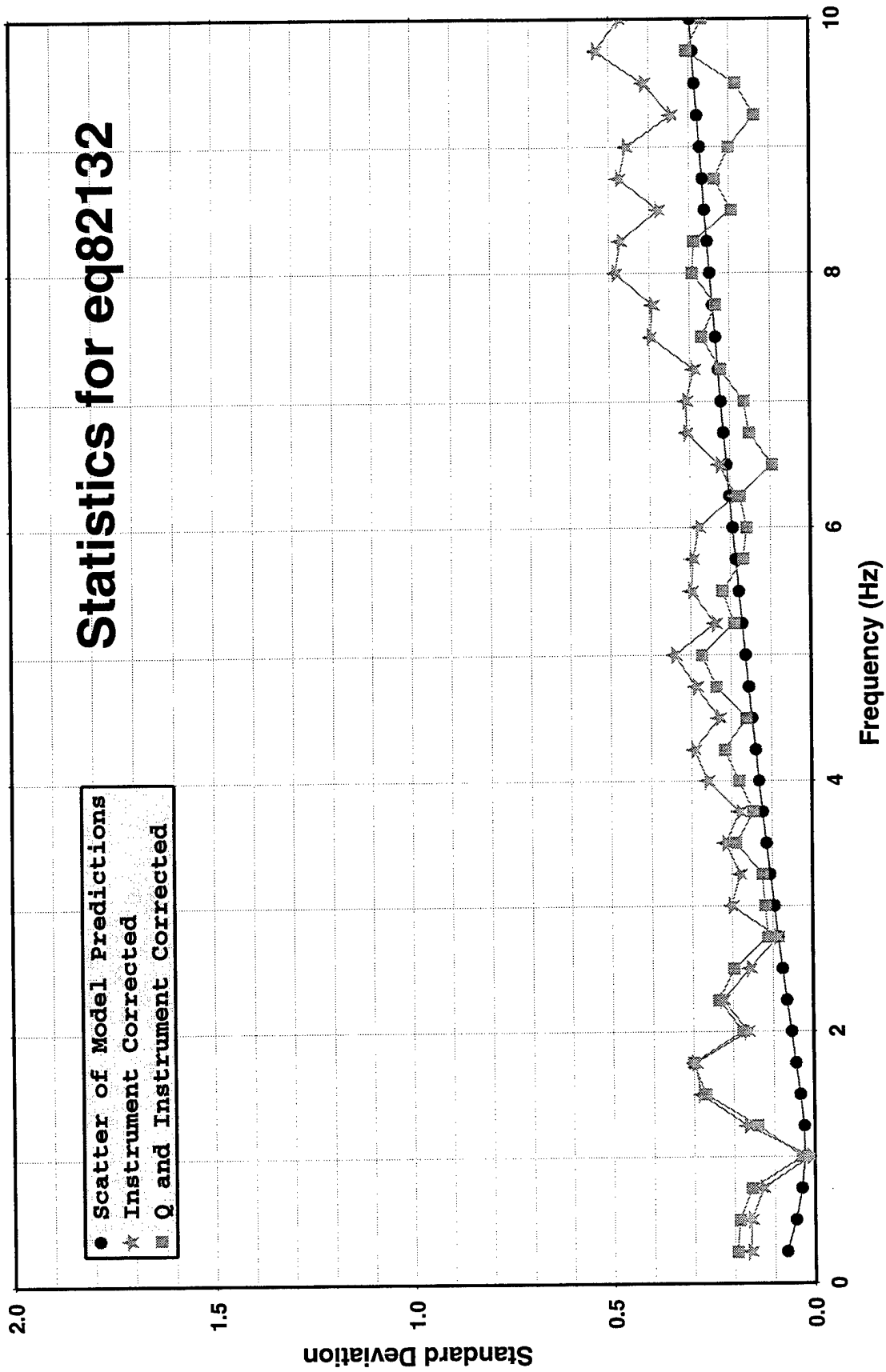


Figure 14. Comparison of standard deviations for  $L_g$  spectral ratios based on measurements at the four LLNL stations for the 1982/05/12 earthquake near NTS before and after attenuation corrections.

the model predictions show similar trends overall, although they do not match. The scatter in all cases is lower than that in Figure 11, which to some extent may reflect superiority of nearer regional stations for these kinds of measurements. One somewhat disturbing result in Figures 12 and 13 is that the standard deviation of the ratios after corrections for both instrument response and attenuation are larger over most of the frequency band than the standard deviations for just the instrument-corrected spectra. This might be interpreted to mean that the attenuation corrections are not working properly to reduce the scatter between stations. However, for the 1982/05/12 earthquake in Figure 14, the attenuation corrections clearly reduce the standard deviation across the entire frequency band; so, the model seems to be working there.

The improvement in the spectral ratio standard deviations for explosion JUNCTION and the 1982/05/12 earthquake after applying the instrument and attenuation corrections suggest that the model may have some validity. However, the lack of improvement in the same corrected measurements for the observations from the other two earthquakes may be interpreted as meaning that the model is not valid; but the latter is open to an alternative interpretation. It is quite reasonable that the scatter in the station spectral ratio measurements for the earthquakes after all the corrections have been applied could be associated with source radiation pattern differences from the earthquakes. In fact, differences in the  $L_g$  spectral ratios and in their station variations between earthquakes suggest that this latter interpretation could be the case. We conclude that the western U.S. attenuation model and the corresponding corrections to the  $L_g$  spectral ratio measurements may be valid.

#### **4.1.2 Eurasia**

We also tested the attenuation correction procedures on the  $L_g$  spectral ratios for three well-recorded Eurasian events. These events were a northwestern China earthquake (viz. earthquake of 1996/01/09), an earthquake in eastern Kazakhstan (viz. earthquake of 1996/03/26), and a nuclear explosion at the Chinese Lop Nor test site (viz. event of 1996/06/08). Source parameters and the available recording stations for these events are described in Table 1 above. Figure 15 shows a comparison of  $L_g$  spectral ratios observed

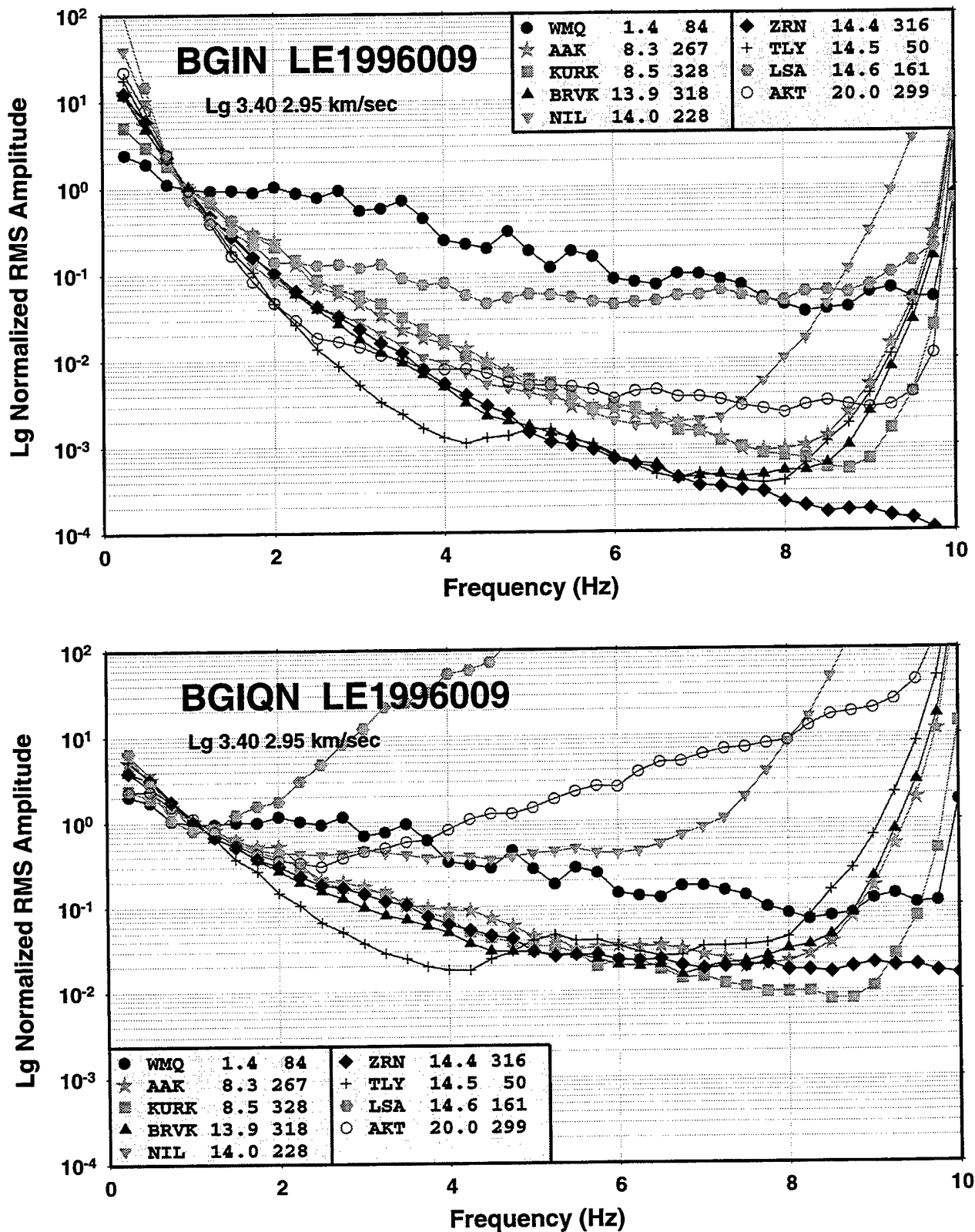


Figure 15. Comparison of the instrument-corrected  $L_g$  spectral ratio estimates for the 1996/01/09 earthquake in northwestern China near Lop Nor (top) and the same spectral ratios after correction for path-specific attenuation (bottom) developed from the attenuation model.

at nine regional stations for the 5.2  $m_b$  northwestern China earthquake of 1996/01/09 after correction for station instrument response (top) and after corrections for attenuation as well as instrument response (bottom). As was noted for the similar plot of the spectral ratios for the NTS explosion JUNCTION, the initial impression is that the corrections for attenuation have brought about an increase in the scatter. However, we can again note that a few stations appear to be anomalous with respect to the remaining spectral ratios. Two of the anomalous stations are the farthest stations (viz. AKT and LSA). They diverge from the other corrected spectral ratio curves above 1 Hz for LSA and above 2 Hz for AKT. The corrected NIL spectral ratios also appear to be anomalous. The problem with the LSA spectral ratios appears to be noise contamination, and this may also be the case for the AKT ratios. However, the NIL instrument-corrected spectral ratios behave reasonably out to almost 7 Hz, and an error in the predicted attenuation correction for that path segment may be the cause of the divergence in the bottom plot. If we eliminate the three anomalous stations and focus on comparing the scatter between the top and bottom plots for the remaining six stations, we again find that the scatter between the stations is reduced. At 4 Hz the variation in the ratios between stations goes from a factor of 200 to a factor of 20; at 6 Hz from a factor of 150 to 8; and at 8 Hz from a factor of 200 to a factor of 10. Furthermore, we see a particularly strong reduction in the variability between stations in the band around 6 Hz. In fact, if we were to assume a somewhat higher-Q path for station WMQ, we could produce a very tight clustering of the  $L_g$  spectral ratio measurements for all six stations.

In Figure 16 we show a comparison of the standard deviations based on the  $L_g$  spectral ratio measurements at the six good stations for the 1996/01/09 earthquake. The scatter in the model-predicted corrections is lower than the standard deviation of the instrument-corrected  $L_g$  spectral ratios, so the standard deviations of the attenuation- and instrument-corrected  $L_g$  spectral ratios do not go to zero. However, the plot indicates that the standard deviations of the attenuation- and instrument-corrected spectral ratios are reduced by about a factor of two over much of the frequency band from the similar standard deviations for the spectra corrected only for the instrument response. Figure 17 shows a similar comparison for six observations from the 1996/03/26 eastern Kazakhstan

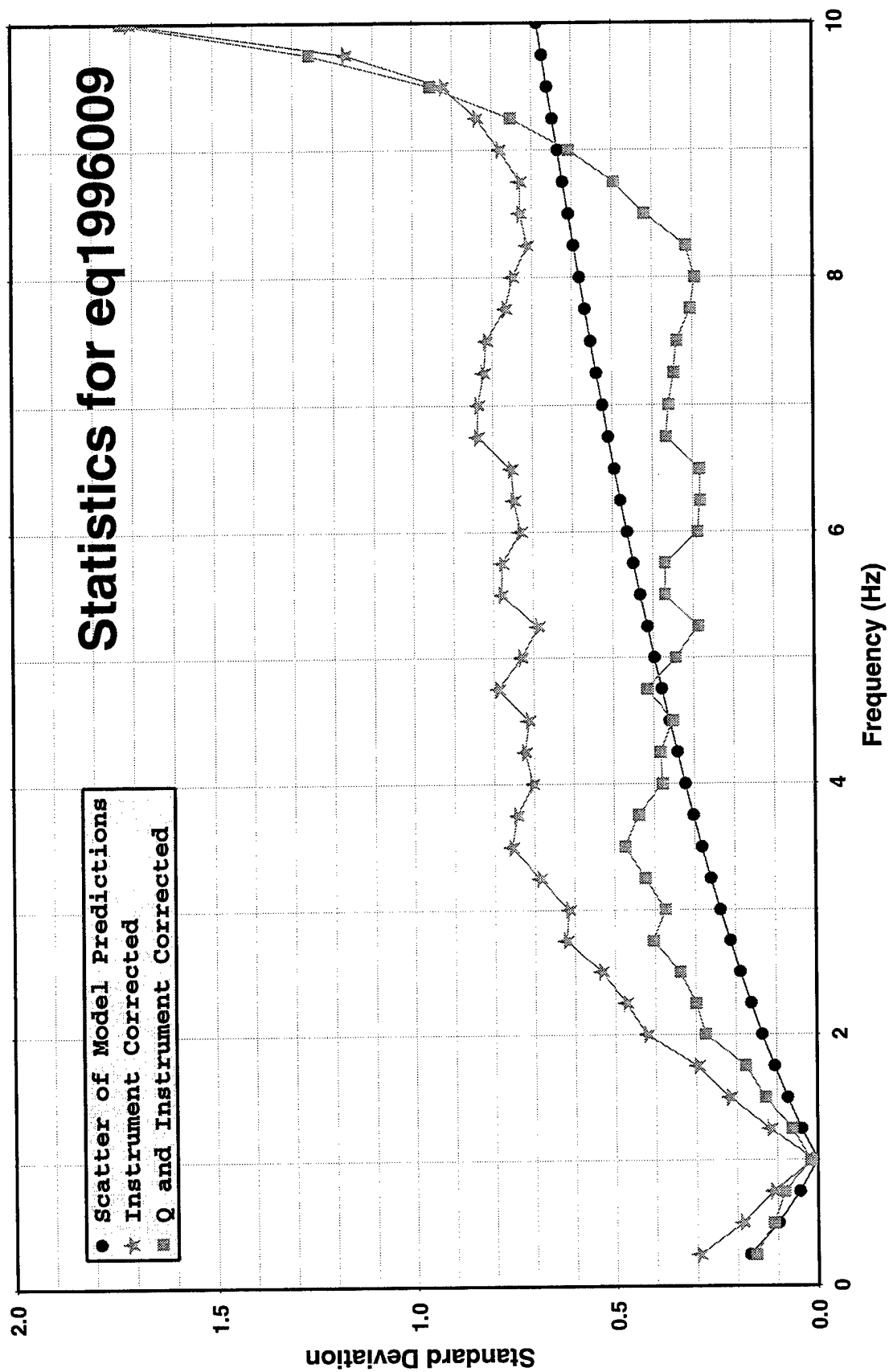


Figure 16. Comparison of standard deviations for  $L_g$  spectral ratios based on measurements at the regional stations for the 1996/01/09 earthquake in northwestern China near Lop Nor before and after attenuation corrections.

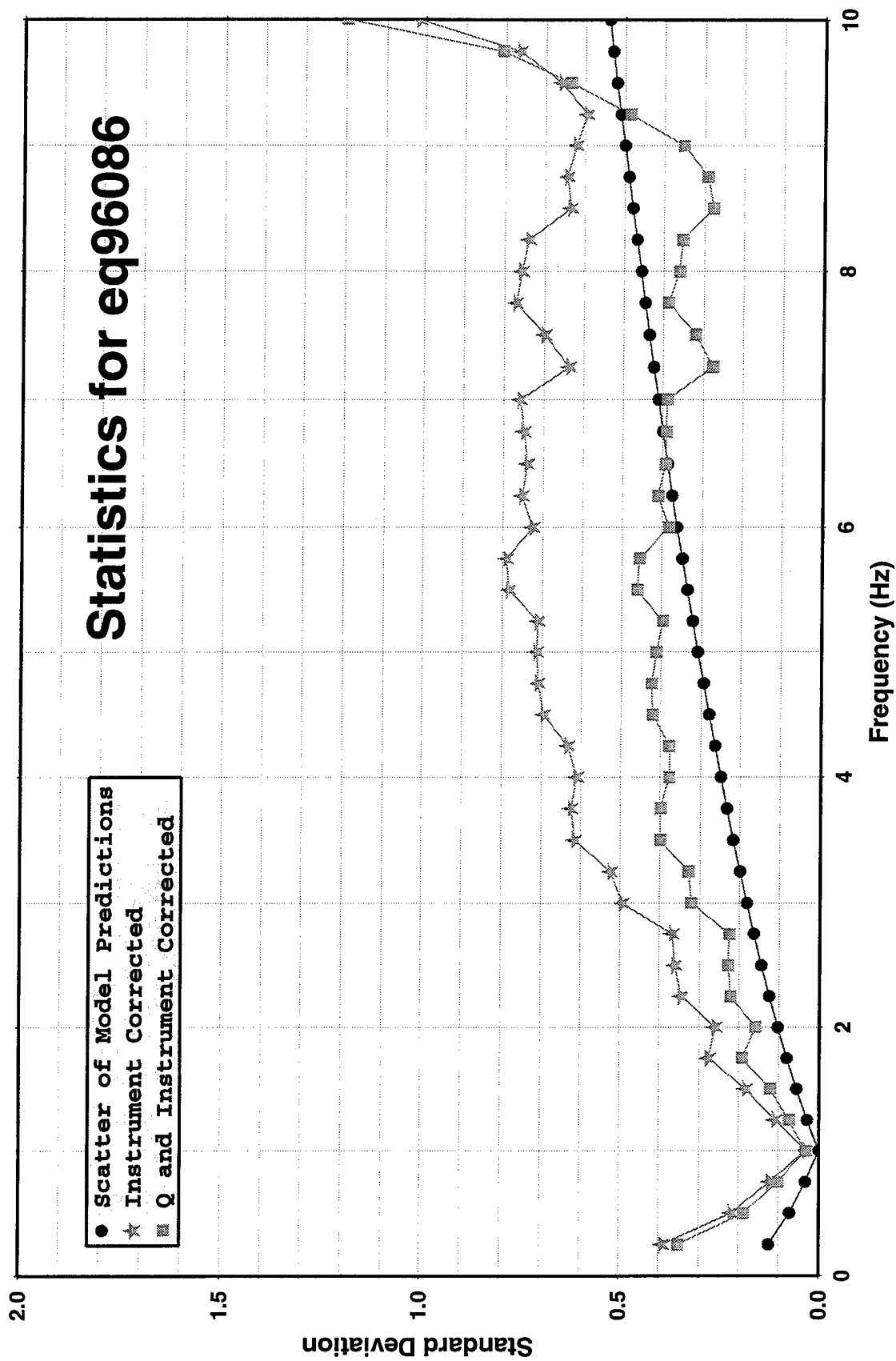


Figure 17. Comparison of standard deviations for  $L_g$  spectral ratios based on measurements at the regional stations for the 1996/03/26 earthquake in East Kazakhstan before and after attenuation corrections.

earthquake. The scatter in the  $L_g$  spectral ratios is again reduced by a factor of two over much of the frequency band as a result of the attenuation correction. Finally, Figure 18 shows the standard deviation comparisons for six observations from the 1996/06/08 explosion at the Lop Nor test site in China. In this last case, the standard deviation of the instrument-corrected  $L_g$  spectral ratios is smaller than the scatter of the model-predicted corrections, and the corresponding attenuation- and instrument-corrected  $L_g$  spectral ratios show larger scatter than the  $L_g$  spectral ratios corrected only for instrument response.

So, for the Eurasian observations the model-predicted attenuation corrections are effective in reducing the scatter in the observations between stations for the two earthquakes but not for the Lop Nor explosion source. The results could be interpreted as indicating that the path corrections for the explosion are not accurate. In particular, some adjustment to the attenuation model for the region around Lop Nor seems to be indicated.

## 4.2 Comparison of the Larger Data Samples

To develop a better understanding of the  $L_g$  spectral ratio corrections and their implications for regional discrimination, we have applied the instrument corrections and the model-predicted attenuation corrections to a larger sample of events and records. Figure 19 shows the  $L_g$  spectral ratio estimates determined from the Gaussian band-pass filters for 79 explosion records and 60 earthquake records without any corrections. The top plot shows the overall data variability and the bottom plot show the means and standard deviations for the two different source types. Although the top plot appears to be thoroughly mixed with little distinction between source types, the bottom plot indicates that on average the earthquake  $L_g$  spectra are enriched in high frequencies when compared to the corresponding explosion spectra. However, the separation between source types is not great and the mean for one source type falls within one standard deviation of the mean for the other source type. The same pattern holds true for the instrument-corrected  $L_g$  spectral ratios which are shown in Figure 20 for 74 explosion records and 60 earthquake records. The instrument-corrected spectra show just about the



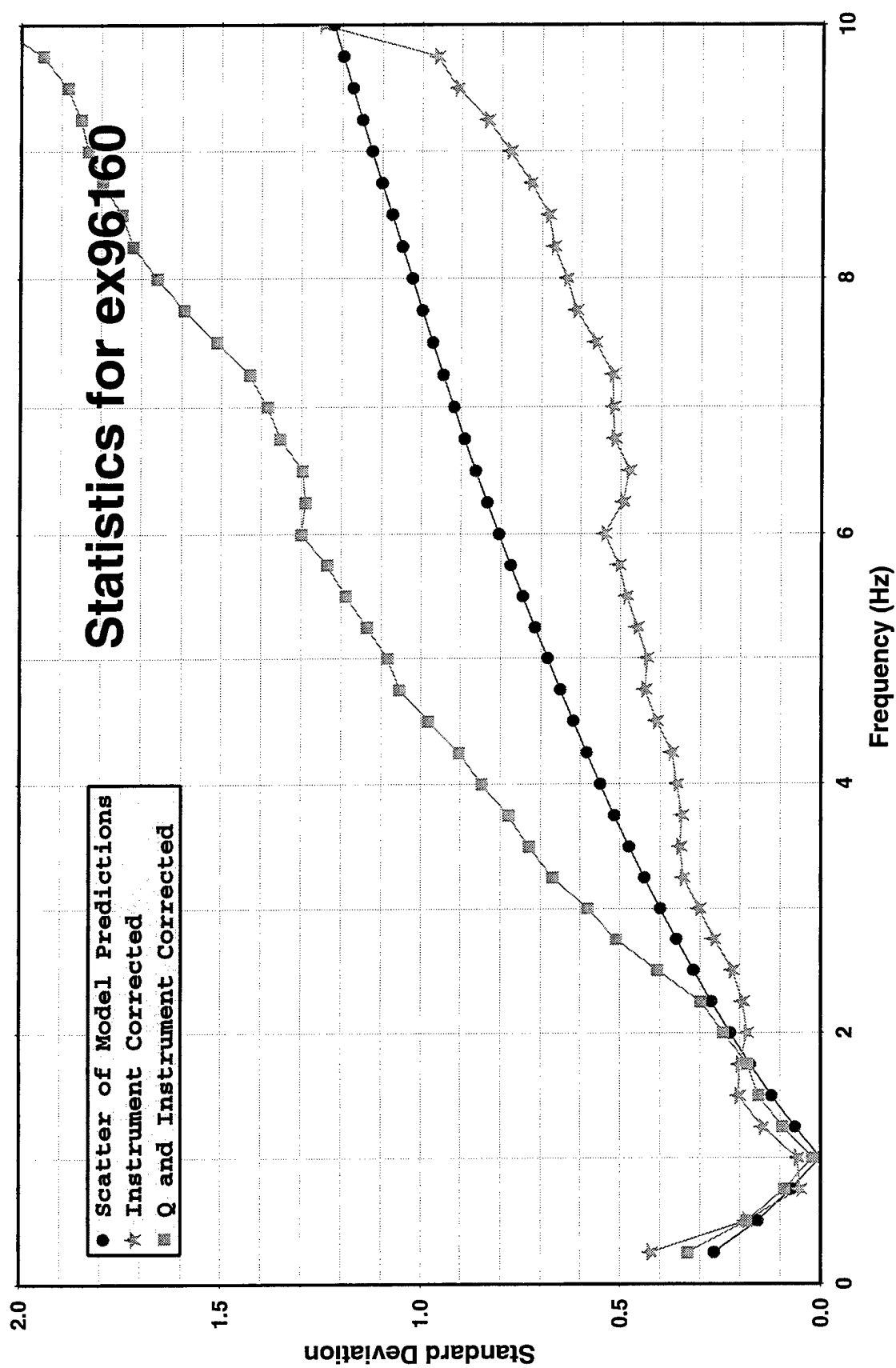


Figure 18. Comparison of standard deviations for  $L_g$  spectral ratios based on measurements at the regional stations for the 1996/06/08 explosion in China at Lop Nor before and after attenuation corrections.

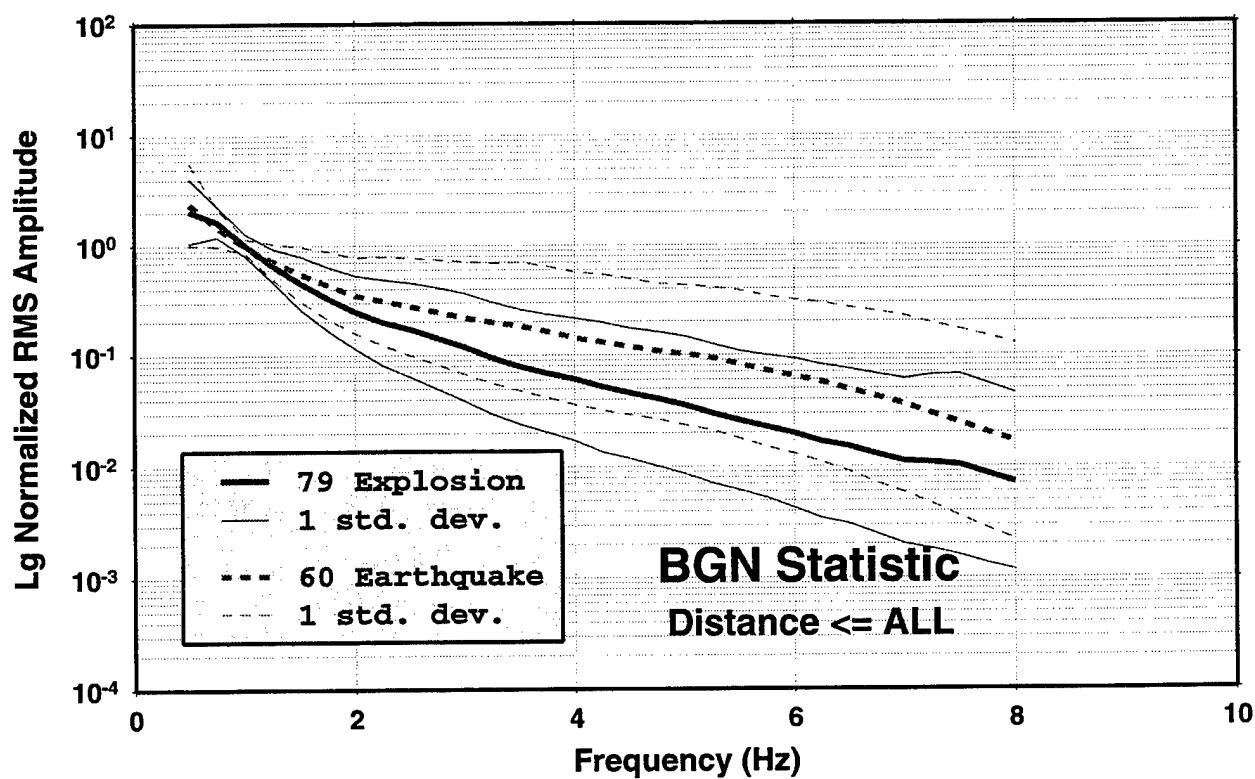
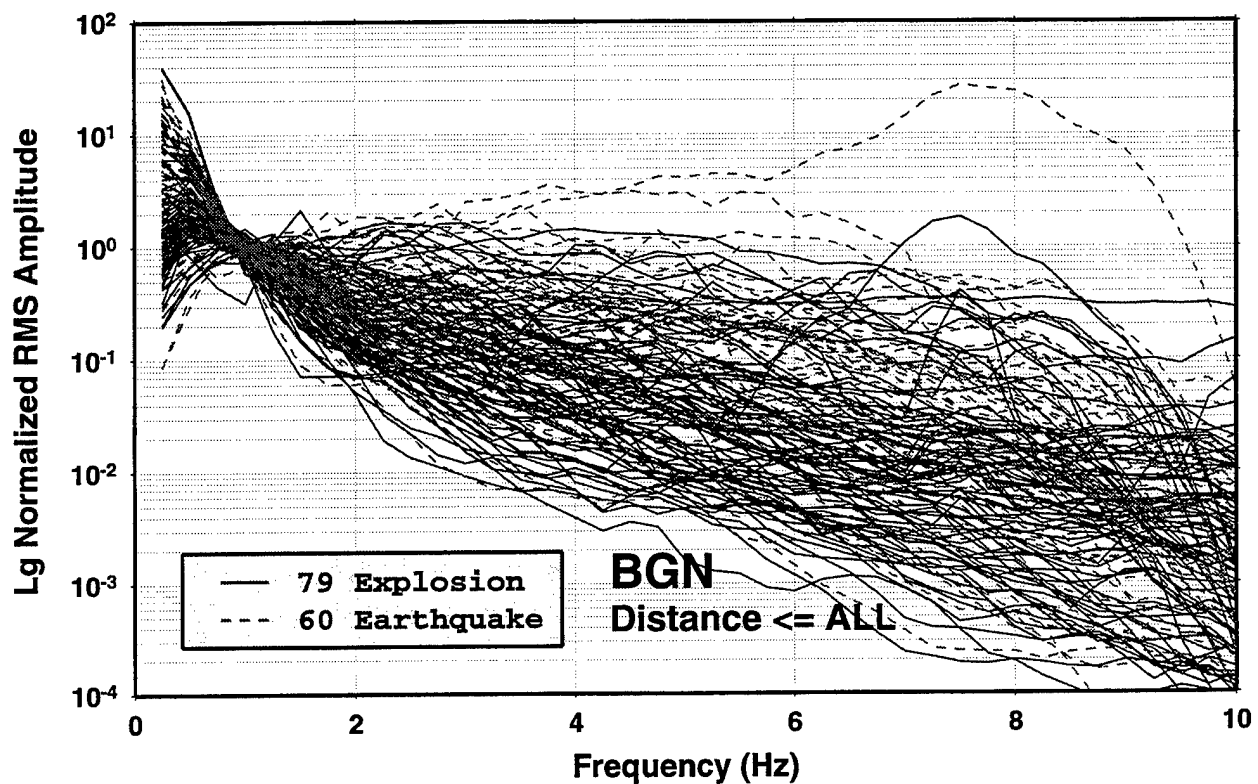


Figure 19.  $L_g$  spectral ratios determined from Gaussian bandpass filters applied to 79 explosion signals (solid lines) and 60 earthquake signals (dashed lines) before any corrections.

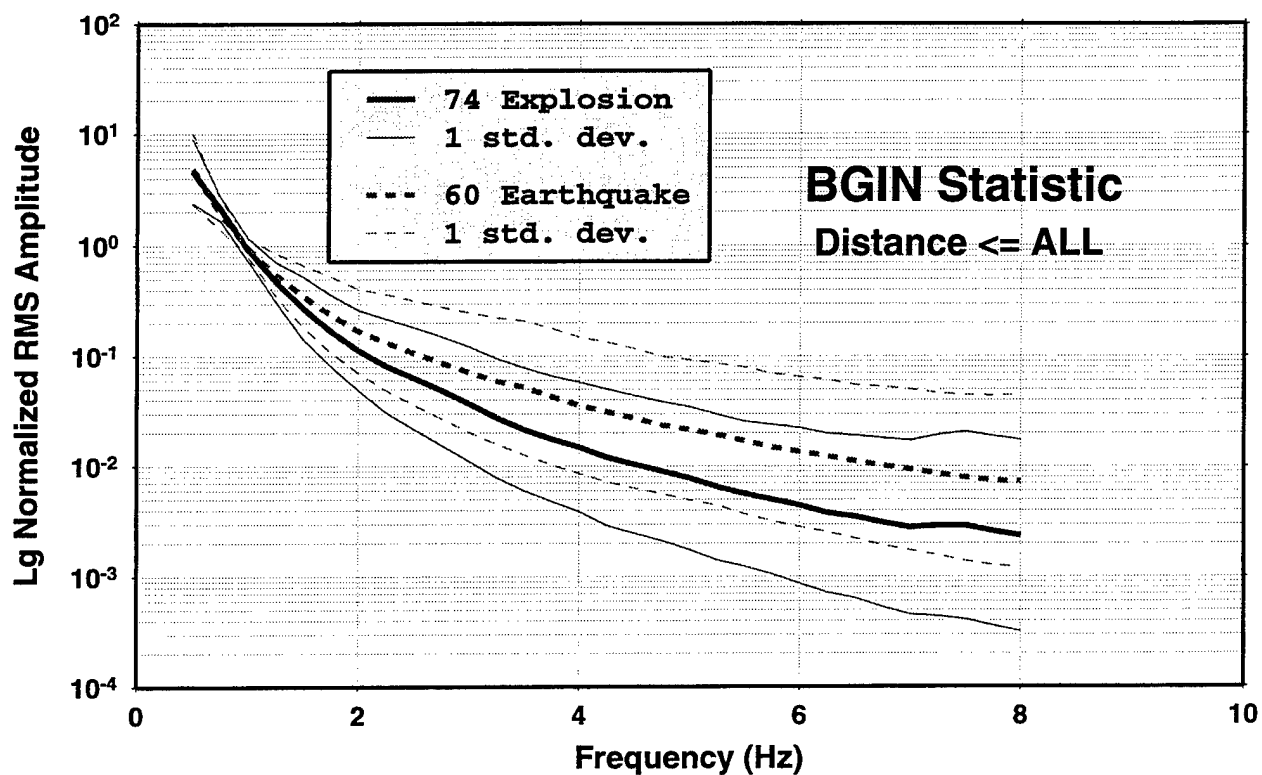
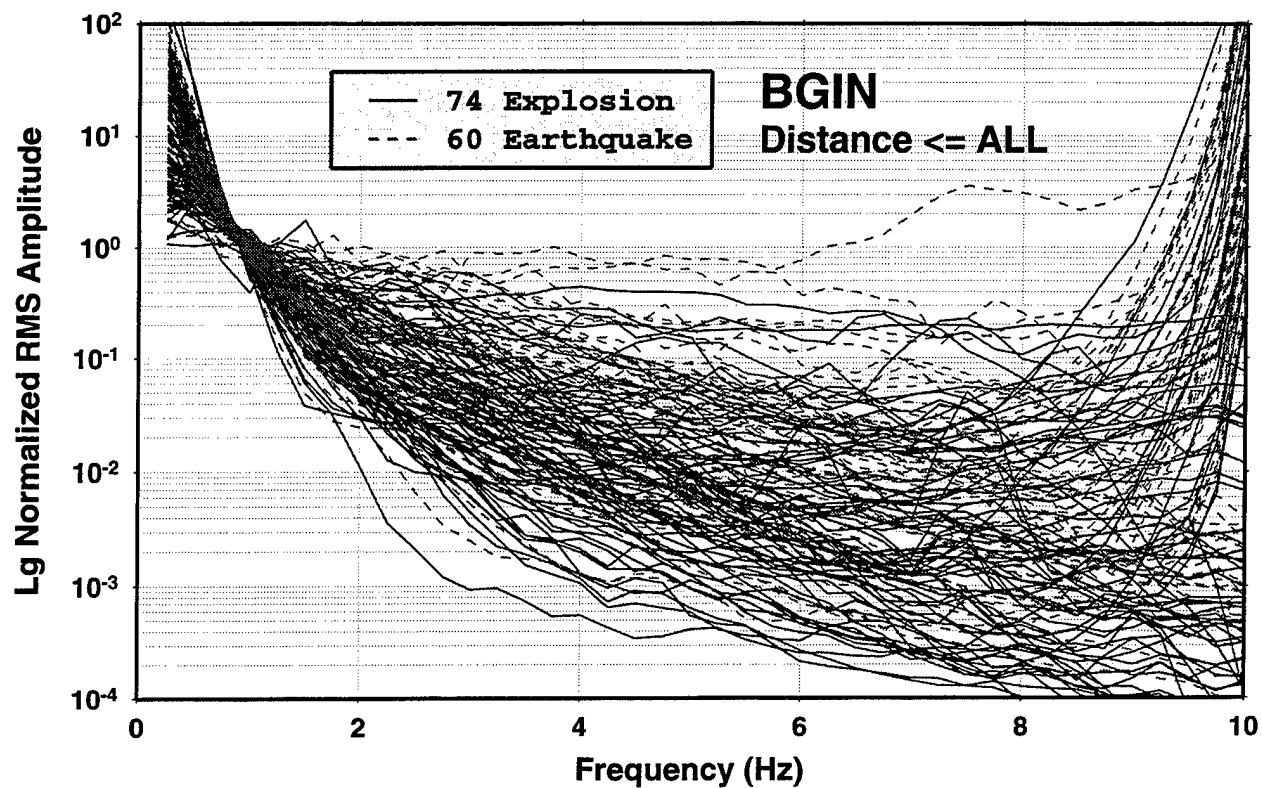


Figure 20.  $L_g$  spectral ratios from Figure 19 after corrections for instrument responses applied to 74 explosion signals (solid lines) and 60 earthquake signals (dashed lines).

same separation of the means and about the same standard deviations as in Figure 19. This appears to be consistent with our previous observation that the instrument corrections have only a small effect on the spectral ratio measurements, and we would not expect the effect to be different between the two source types. Figure 21 shows the  $L_g$  spectral ratios after corrections for the instrument responses and for the model-predicted attenuation factors. The corrected individual spectral ratio measurements in the top plot appear to be totally mixed. The mean curves in the bottom plot still show a difference with the earthquakes still showing relatively more high-frequency energy on average than the explosions, but the standard deviation for the corrected explosion ratios is very large and the scatter completely envelopes the corresponding earthquake ratios.

The results in Figure 21 suggest little reason for optimism about the transportability of the  $L_g$  spectral ratio discriminant. However, we can use this large database to help understand situations where the discriminant might work. In particular, we noted above that  $L_g$  signals at many of the farther regional stations are contaminated by noise at high frequencies and that the large corrections predicted by the attenuation model can artificially inflate  $L_g$  spectral ratios and lead to inaccurate measurements. Ideally, we would like to eliminate such noise-contaminated observations from our analyses. To assess how this might affect discriminant performance, we have considered two different subsets of the data sample. In the first subset we consider the attenuation- and instrument-corrected  $L_g$  spectral ratios observed at stations at distances of  $5^\circ$  or less. These are plotted in Figure 22 for 35 explosion measurements and 18 earthquake measurements within this  $5^\circ$  distance range. Although it may not be clear from the top plot of all the data, the bottom plot of the means and standard deviations for the two source types does show that the mean of the corrected earthquake  $L_g$  spectral ratios lies above the mean for the explosion spectral ratios. Furthermore, for the frequency band from approximately 3 Hz to above 6 Hz, we find the greatest separation with the earthquake mean spectral ratio above the mean-plus-one-standard-deviation for the explosions. In Figure 23 we show a similar plot for observations at stations at distances less than  $10^\circ$ , including 41 explosion measurements and 31 earthquake measurements. In this case the earthquake and explosion averages show somewhat greater separation, but

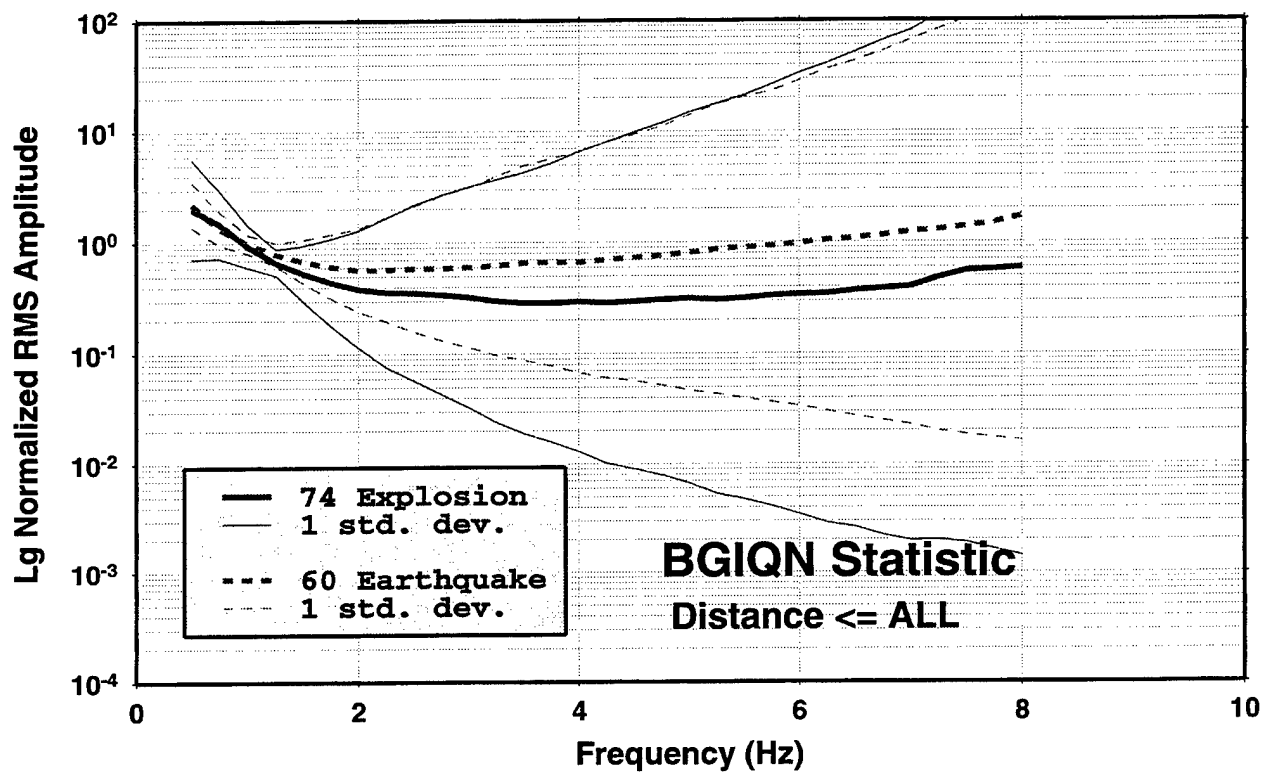
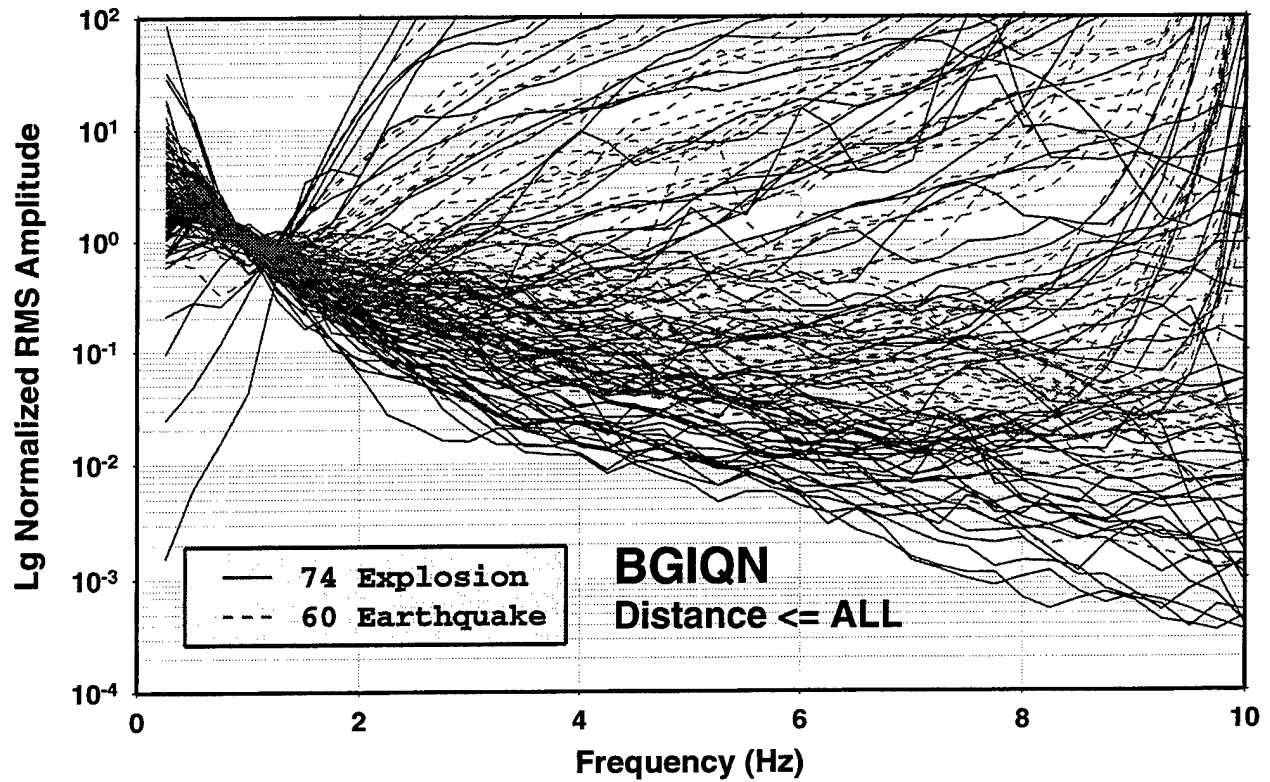


Figure 21.  $L_g$  spectral ratios from Figure 20 after corrections for path attenuation applied to 74 explosion signals (solid lines) and 60 earthquake signals (dashed lines).

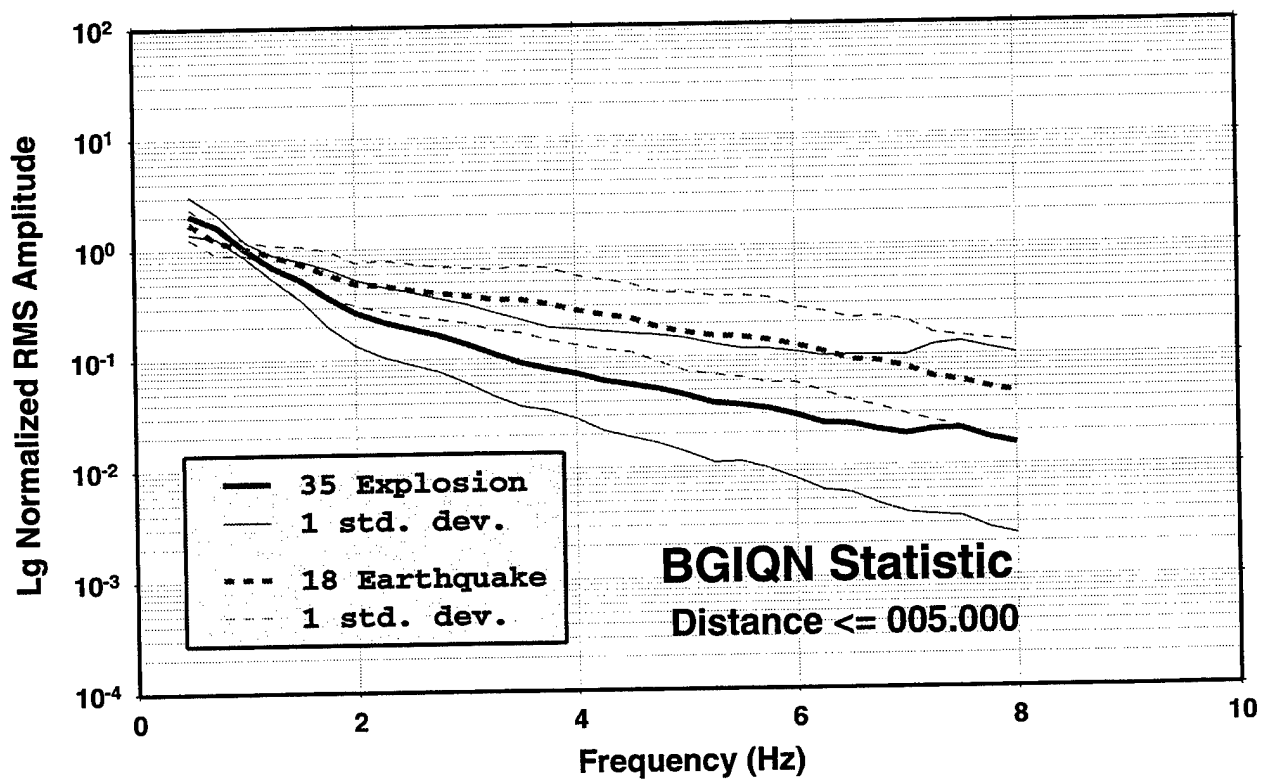
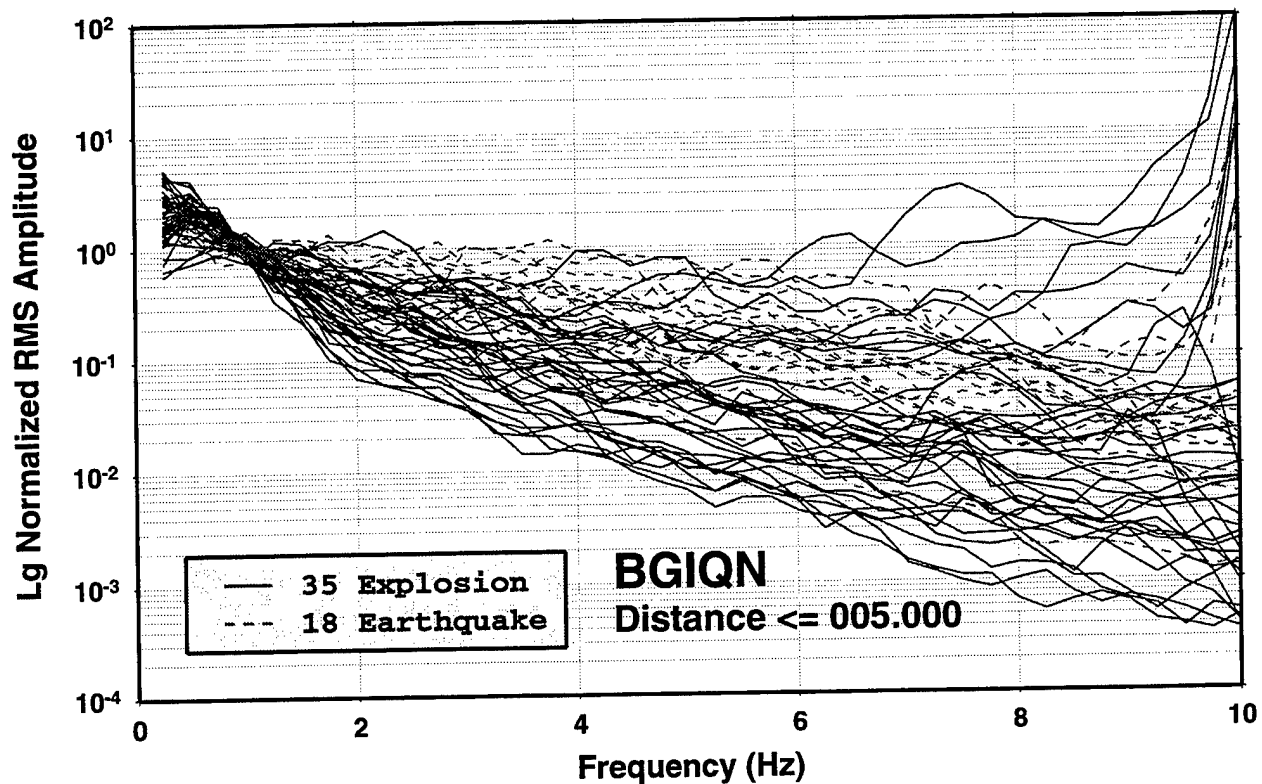


Figure 22.  $L_g$  spectral ratios after instrument and attenuation corrections for 35 explosion signals (solid lines) and 18 earthquake signals (dashed lines) at station distances less than 5 degrees.

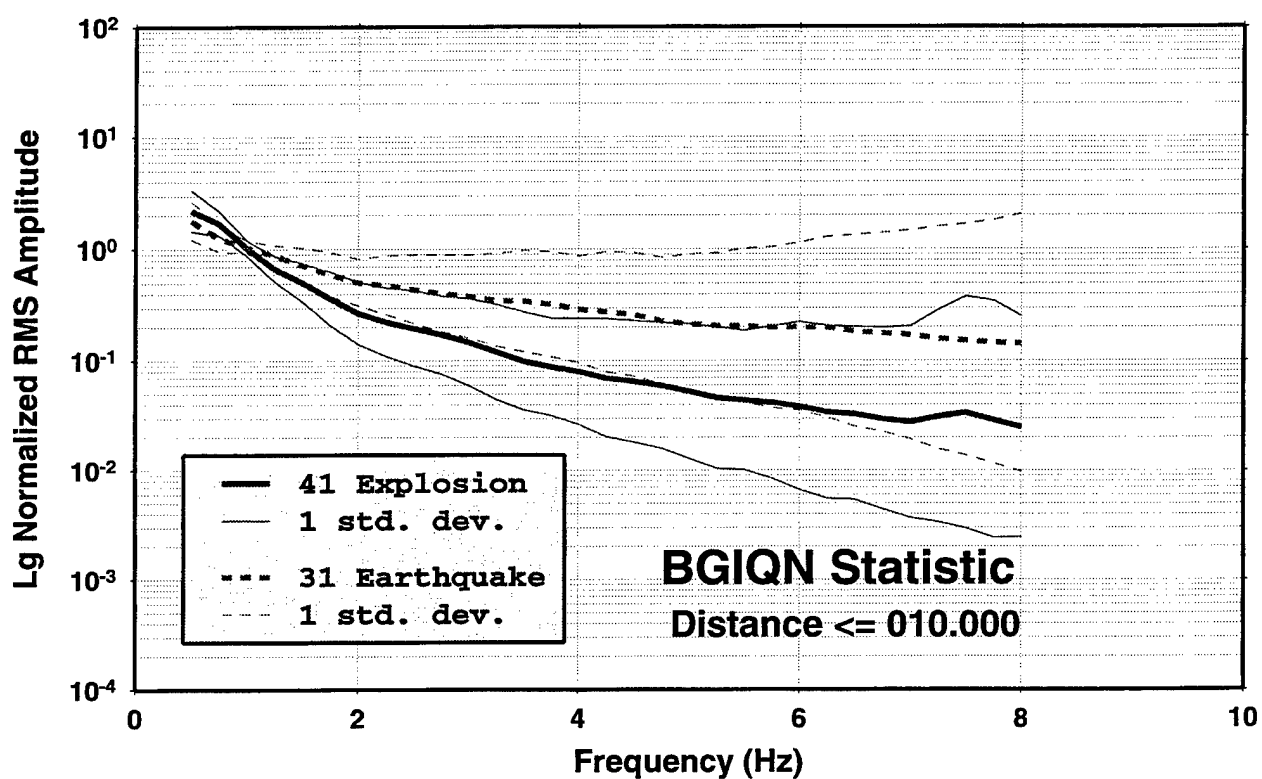
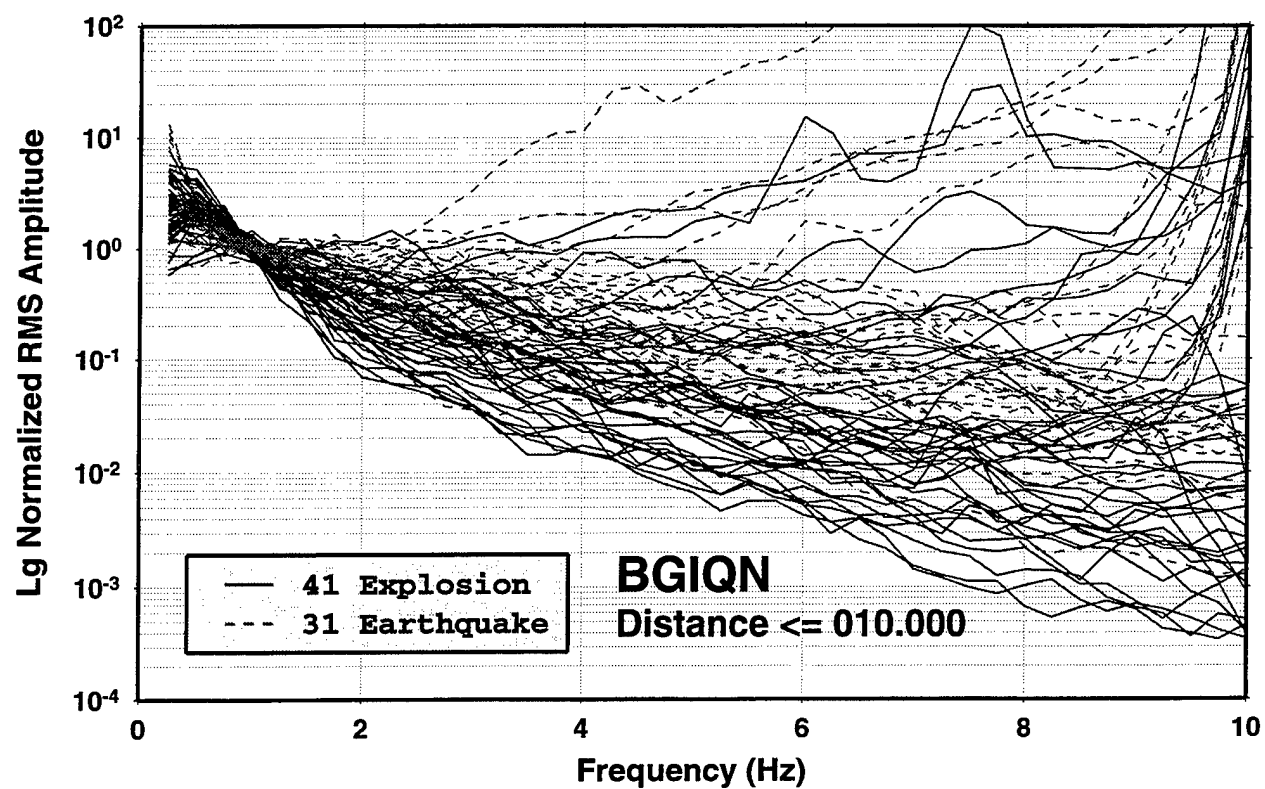


Figure 23.  $L_g$  spectral ratios after instrument and attenuation corrections for 41 explosion signals (solid lines) and 31 earthquake signals (dashed lines) at station distances less than 10 degrees.

the standard deviations are also somewhat larger. The best separation between the observations is still over the frequency band from just above 2 Hz to about 6 Hz. So, these results suggest that the  $L_g$  spectral ratio discriminant might be effective for observations at stations less than  $10^\circ$ ; and closer regional station measurements would probably work even better.

In Figure 24 we attempted to partition the corrected  $L_g$  spectral ratio measurements in a different way. Instead of excluding those stations beyond some fixed distance range, we decided to exclude observations which appeared to be outliers from the measurements. We have initially made the outlier decision process rather arbitrary by eliminating measurements from stations where the  $L_g$  spectral ratios were greater than two at 8 Hz. Although the choice of the outlier cutoff is somewhat arbitrary, it is consistent with the idea of eliminating noise-contaminated spectral ratio measurements which have been artificially inflated by the attenuation corrections; and it also seems to agree with the general trend established by the distance-limited observations in Figures 22 and 23 (i.e. outliers are assumed to be those measurements which are outside the bounds of the behavior seen for the spectral ratio observations at the nearer regional stations). Figure 24 shows the corrected  $L_g$  spectral ratio measurements with the outliers removed. The results at the top are shown for 52 explosion measurements and 35 earthquake measurements, and the corresponding means and standard deviations are plotted at the bottom. The means and standard deviations appear to be about the same as those for the smaller sample of observations at the stations for distances less than  $5^\circ$  seen in Figure 22. The best separation of the explosion and earthquake samples appears to be over the band from about 3 Hz to 6 Hz.

As one final additional attempt at partitioning the data, we separated the corrected  $L_g$  spectral ratio measurements for observations in the U.S. from those in Eurasia. These are shown in Figure 25. The U.S. (i.e. western hemisphere) sample includes 22 explosion measurements and 48 earthquake measurements, while the Eurasian (i.e. eastern hemisphere) sample includes 22 explosion measurements and 48 earthquake measurements. We see that the U.S. sample includes numerous explosion observations which are consistently below the earthquake observations, although there are clearly



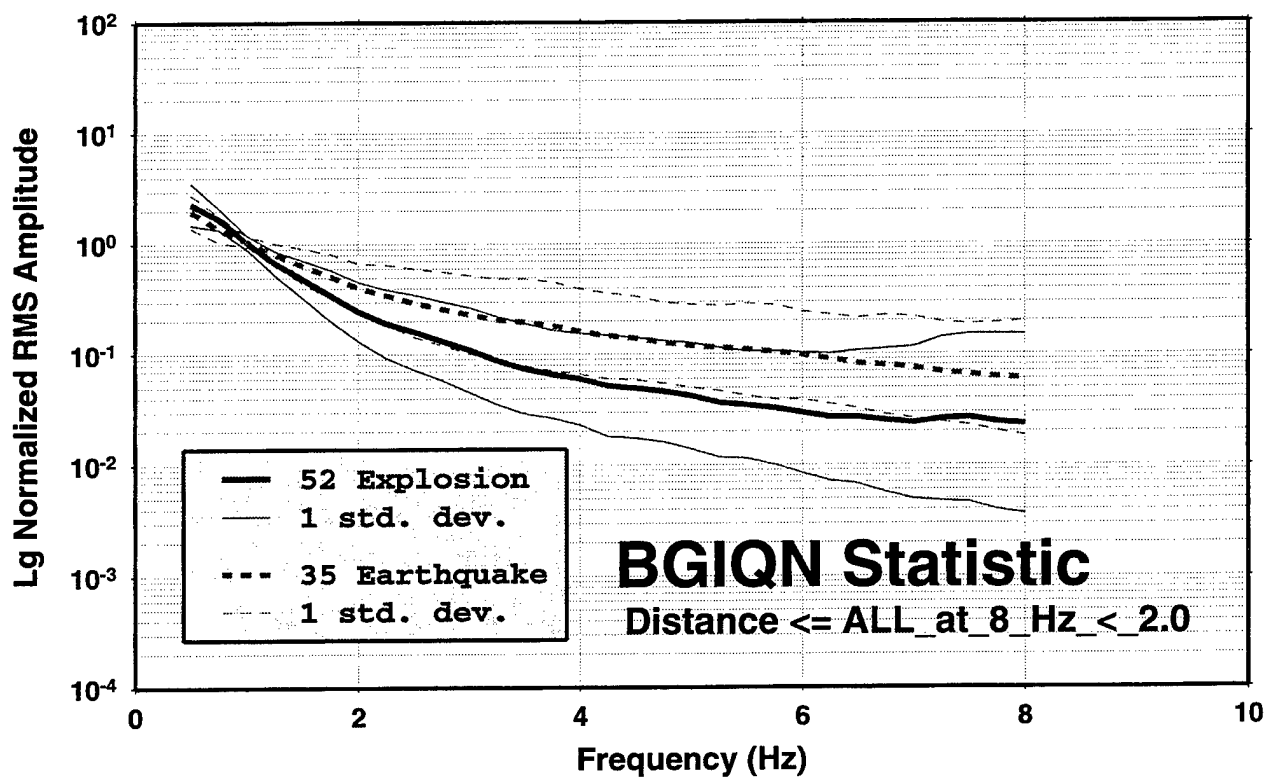
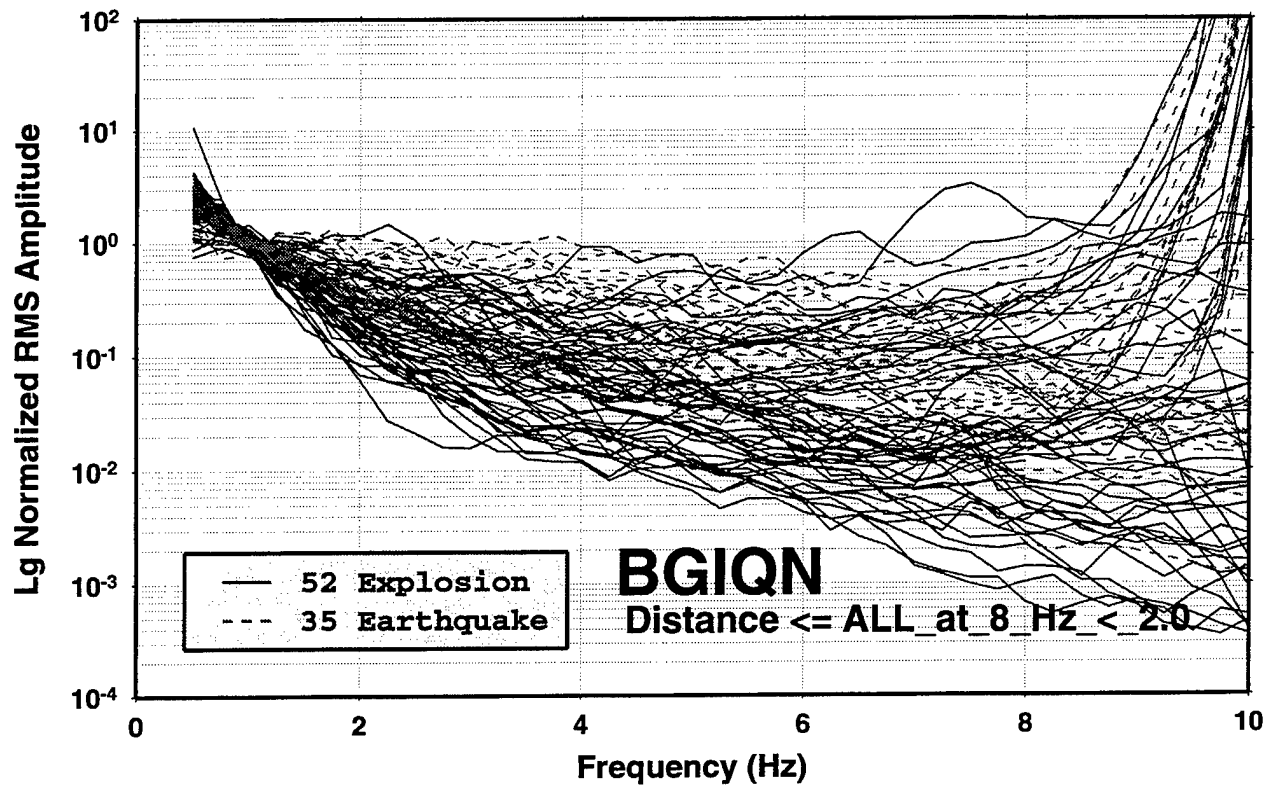


Figure 24.  $L_g$  spectral ratios after instrument and attenuation corrections for 52 explosion signals (solid lines) and 35 earthquake signals (dashed lines) for all distances with outliers removed.

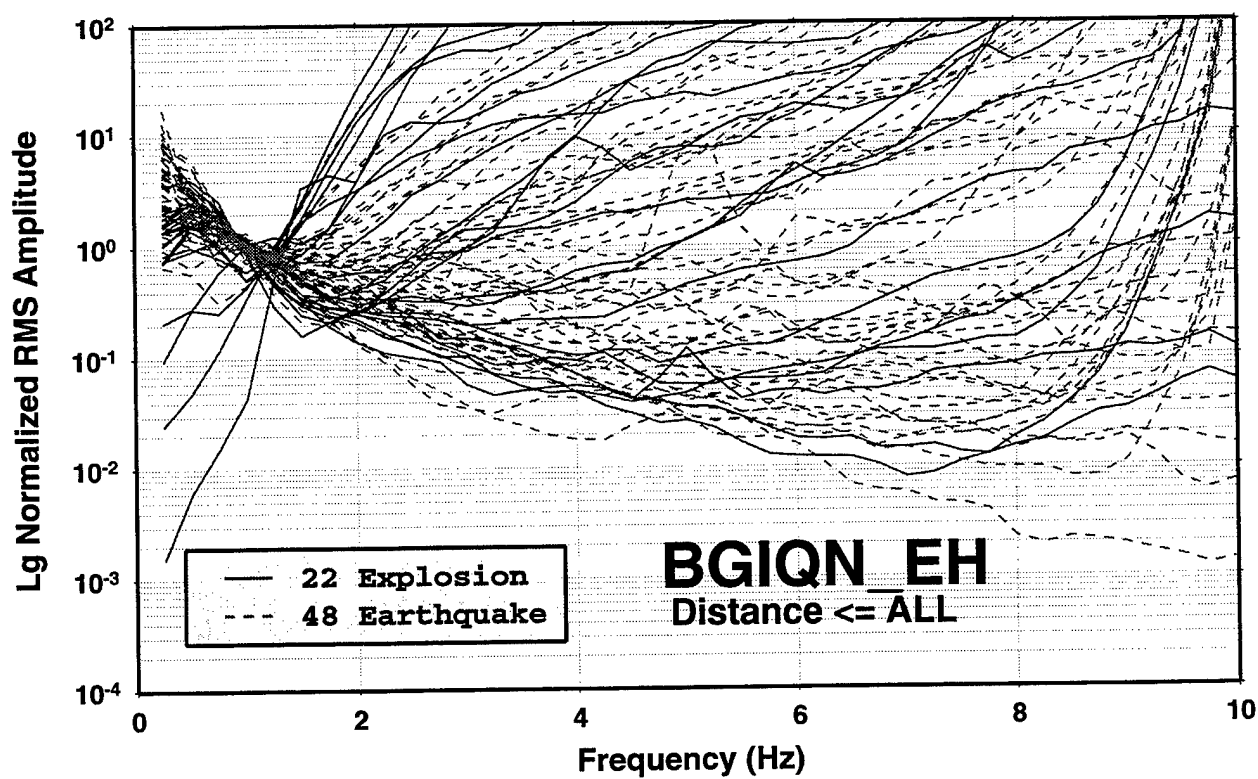
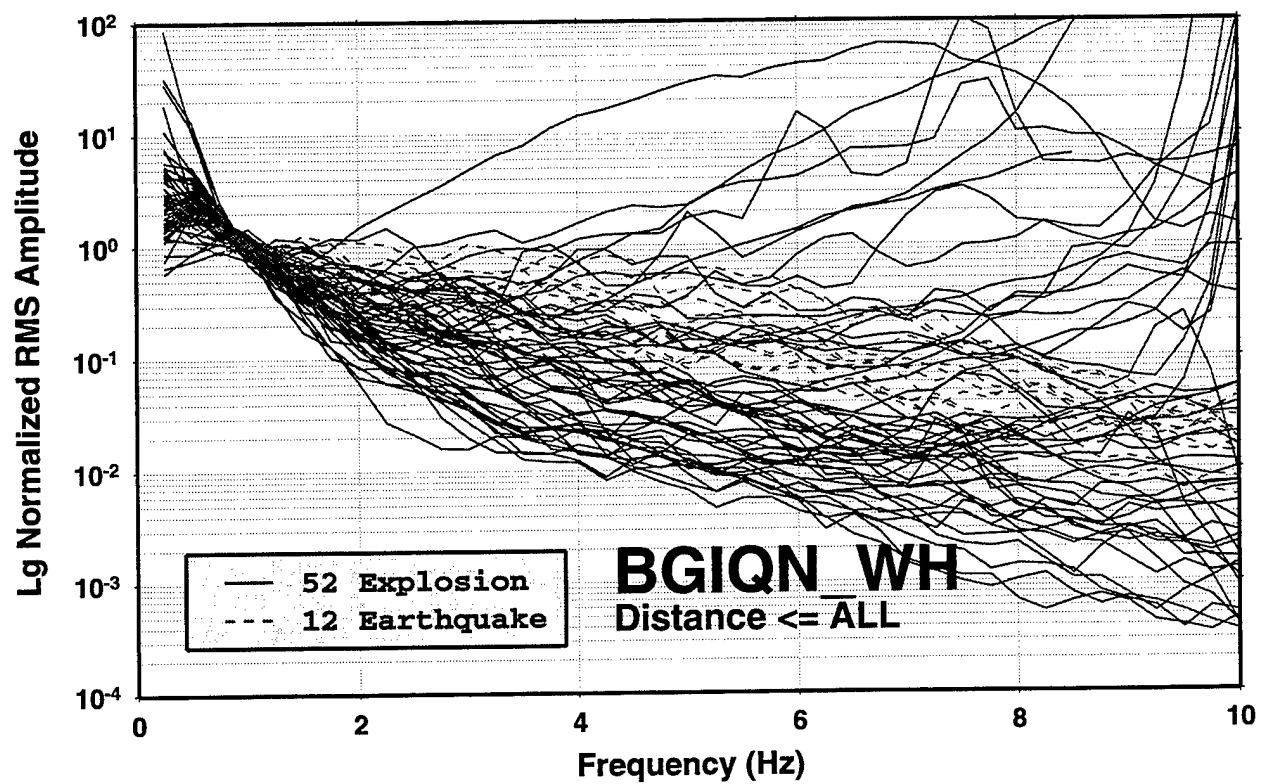


Figure 25. Comparison of  $L_g$  spectral ratios after instrument and attenuation corrections for explosion and earthquake signals in the western hemisphere (top) and eastern hemisphere (bottom) for events at all regional distances.

some outliers in the explosion data sample. The observations from the Eurasian sample appear to be more mixed with possible examples of noise contamination in many of the measurements. If we look at the same data samples for only the observations at less than  $10^\circ$  (cf. Figure 26), the behavior becomes somewhat more clear. For the U.S. sample, this partition removes a few of the explosion outliers; but somewhat surprisingly several of the corrected  $L_g$  spectral ratio measurements for explosions still appear to be large and into the earthquake population. One possibility is that the anomalous measurements are from the small NPE explosion and that some of those observations were noise-contaminated. For the Eurasian sample in Figure 26, the corrected  $L_g$  spectral ratios at the nearer stations appear to be more consistent with the average experience for the total sample, as the distance partition eliminates many of the distant explosion measurements which were clearly contaminated by noise at high frequencies. Unfortunately, we are left with a very restricted sample; but there are additional regional data for nearer stations which could be used to further assess the  $L_g$  spectral ratio behavior for more Eurasian explosions.

#### 4.3 Discrimination Analyses of Selected Events

In this section we describe discrimination analyses based on the attenuation- and instrument-corrected  $L_g$  spectral ratios for each of five selected events. The five events used in the analyses were all in Eurasia and include several specific areas of interest for CTBT monitoring (e.g. North Korea, Pakistan, and the Middle East). For each of these events we determined the  $L_g$  spectral ratios at the available regional seismic stations and applied the corrections for instrument response and model-predicted attenuation. We then compared the corrected  $L_g$  spectral ratios for the specific event to the trends of the overall data samples for explosion and earthquake sources with the outliers removed (cf. Figure 24 above).

**Eastern Kazakhstan Event of 1996/03/26** - For the eastern Kazakhstan event of 1996/03/26 we analyzed the  $L_g$  signals from five regional stations at epicentral distances between  $1.2^\circ$  and  $9.6^\circ$ . The event had a magnitude of 3.8 and was located at  $50.08^\circ\text{N}$   $76.97^\circ\text{E}$ , as described in Table 1 above. Good  $L_g$  signals were recorded at all five

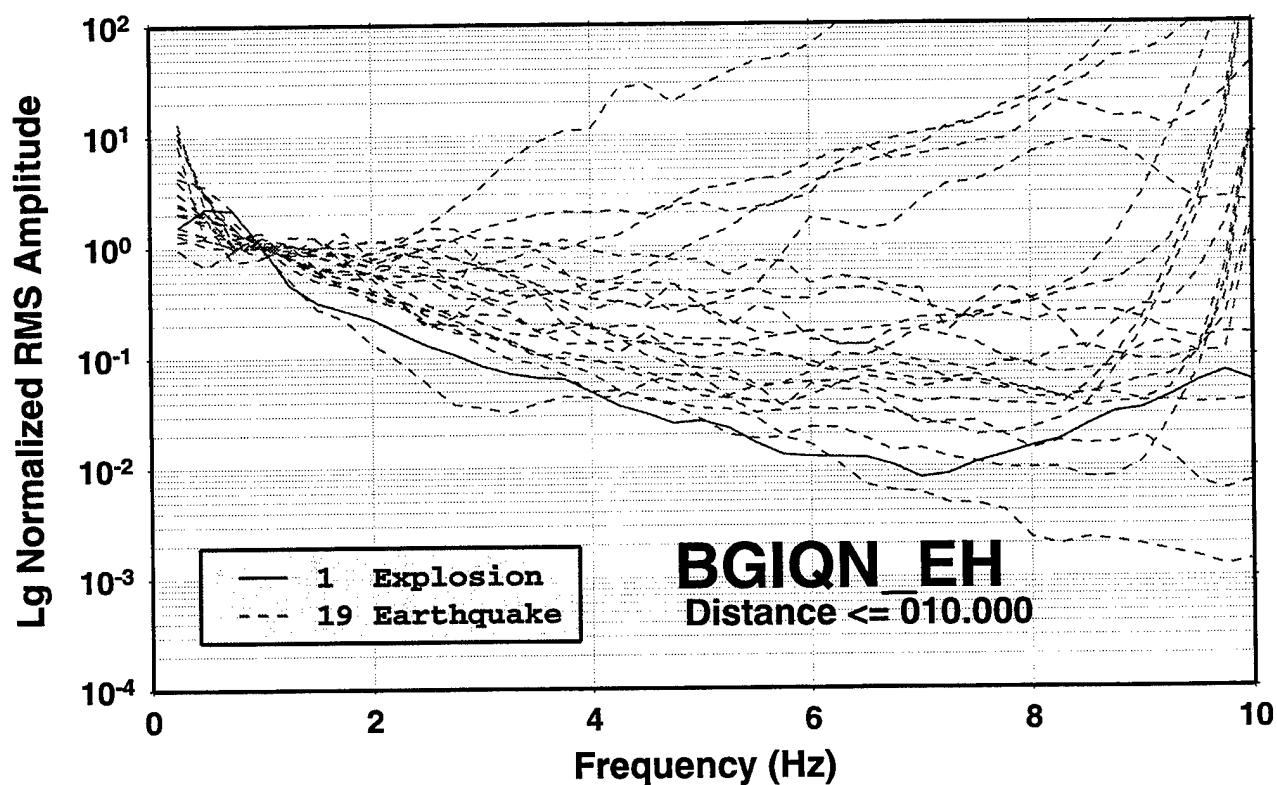
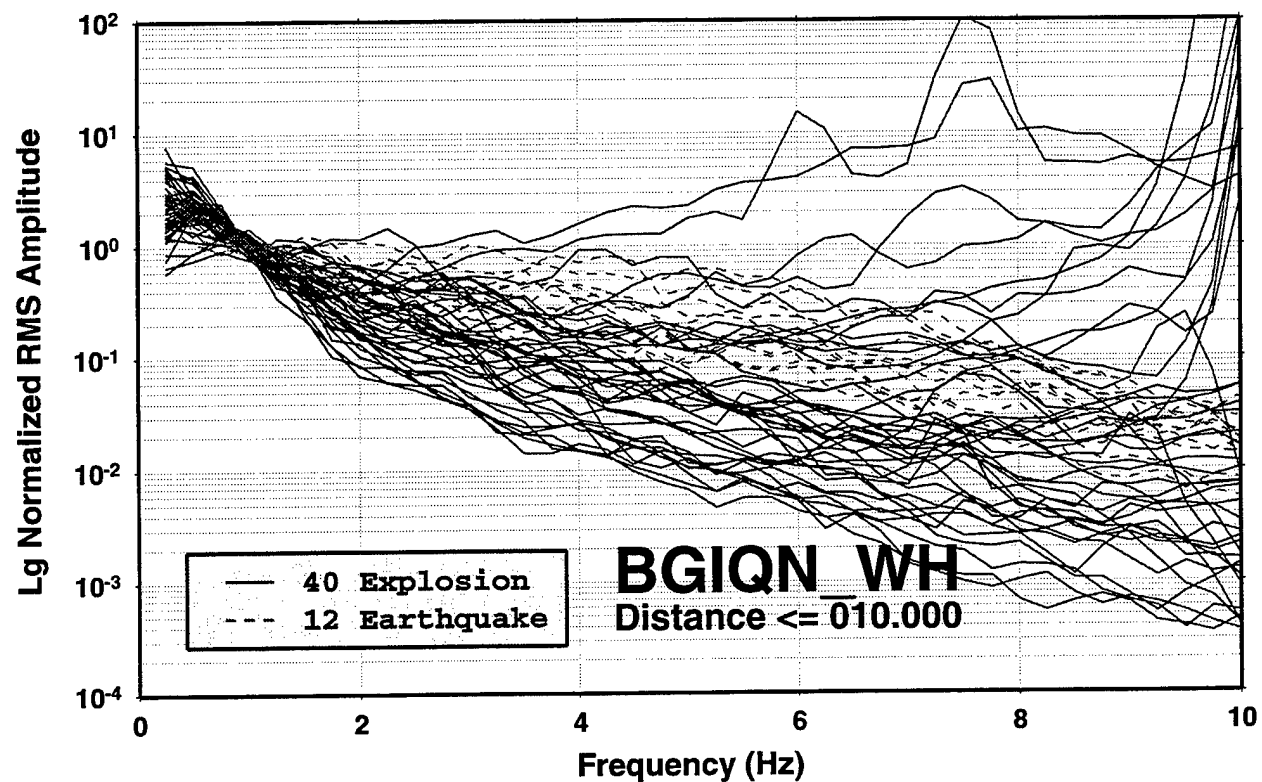


Figure 26. Comparison of  $L_g$  spectral ratios after instrument and attenuation corrections for explosion and earthquake signals in the western hemisphere (top) and eastern hemisphere (bottom) for events recorded at distances less than 10 degrees.

stations; the Gaussian band-pass filtering procedure was used to compute the spectral ratio estimates for these  $L_g$  signals, as described above. Figure 27 (top) shows the  $L_g$  spectral ratios at each of the five stations after correcting for instrument response and the predicted attenuation factor for each station path. The  $L_g$  spectral ratios from the five stations show a scatter range falling within about a factor of 10 over the frequency band from 3 Hz to 8 Hz. The station measurements could be brought into closer correspondence if the Q model were revised slightly to include lower Q to the west and south of the epicenter and/or higher Q to the north and east. In the bottom plot we show the average corrected  $L_g$  spectral ratio from the five station measurements as a function of frequency compared to the overall explosion and earthquake samples. The average  $L_g$  spectral ratios for the 1996/03/26 eastern Kazakhstan event lie in the range between the mean and the mean-plus-one-standard-deviation of the earthquake sample. The average ratios for the event lie above the mean-plus-one-standard-deviation for the explosion sample. So, the discrimination analysis would indicate that the 1996/03/26 eastern Kazakhstan event was most likely an earthquake; and we could assign the appropriate probabilities to this identification based on the statistics corresponding to the measurement distributions.

**Jordan-Syria Border Event of 1997/03/26** - For the Jordan-Syria border event of 1997/03/26 we analyzed the  $L_g$  signals at three stations with epicentral distances between  $2.0^\circ$  and  $9.7^\circ$ . The event had a magnitude of 4.6 and was located at  $33.75^\circ\text{N}$   $35.46^\circ\text{E}$ . We show at the top of Figure 28 the corrected  $L_g$  spectral ratios for the three stations. The behavior of the  $L_g$  spectral ratio at station GNI appears to be noise-contaminated above about 3 Hz; and review of the original filtered traces indicates that this is true. The spectral ratios at stations JER and EIL could be brought into closer correspondence by revising the Q model to have lower Q in the area between JER and EIL. The average corrected  $L_g$  spectral ratios for the three station measurements in the bottom plot of Figure 28 lie between the mean and the mean-plus-one-standard-deviation for the explosion sample, but they also fall into the interval between the mean and the mean-minus-one-standard-deviation for the earthquake sample. So, the discrimination analysis for this event is ambiguous. If we throw out the observations from station GNI, the

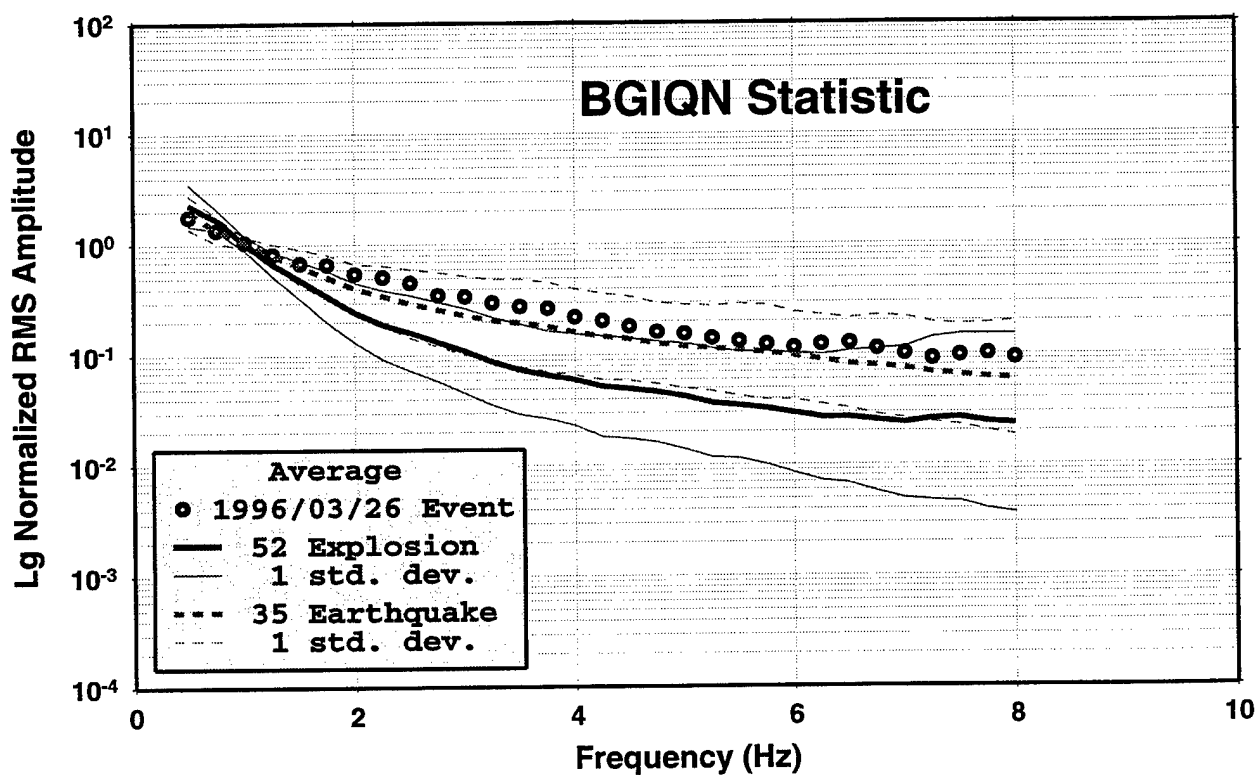
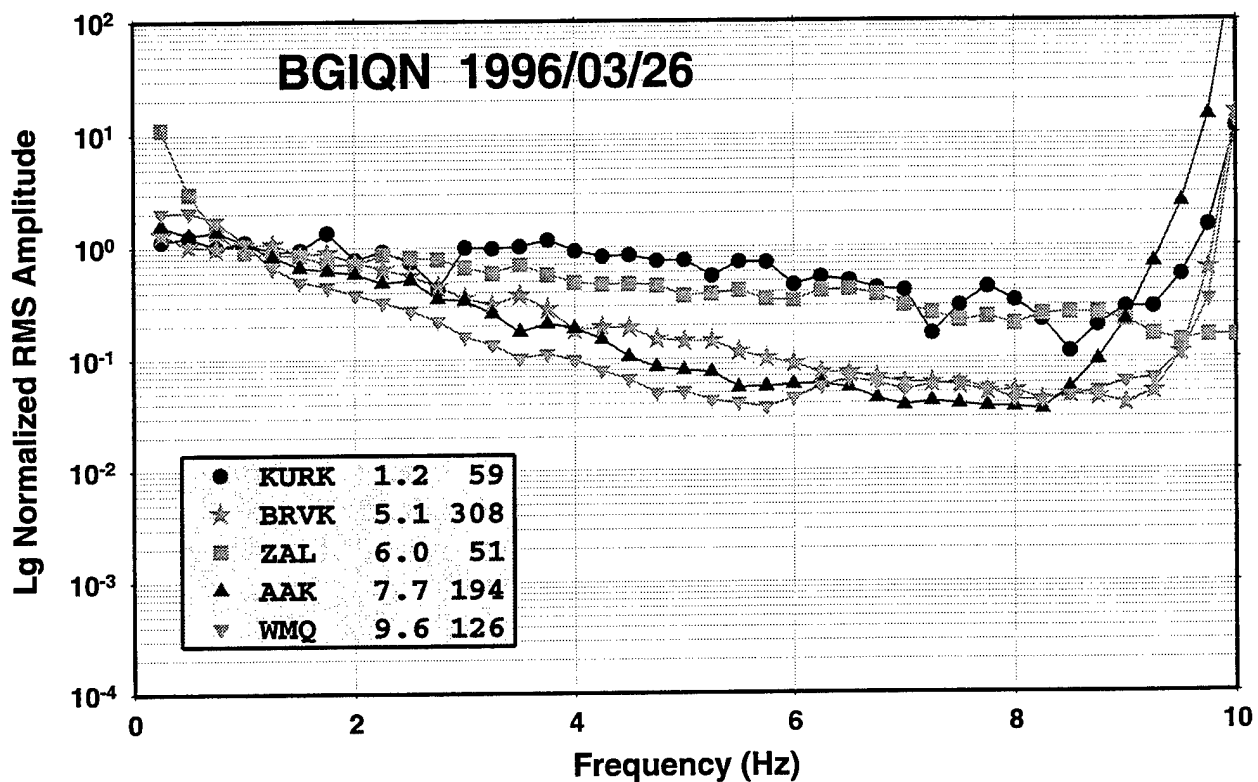


Figure 27.  $L_g$  spectral ratios after corrections at five stations (top) and discrimination analysis based on average  $L_g$  spectral ratios (bottom) for East Kazakhstan event of 1996/03/26.

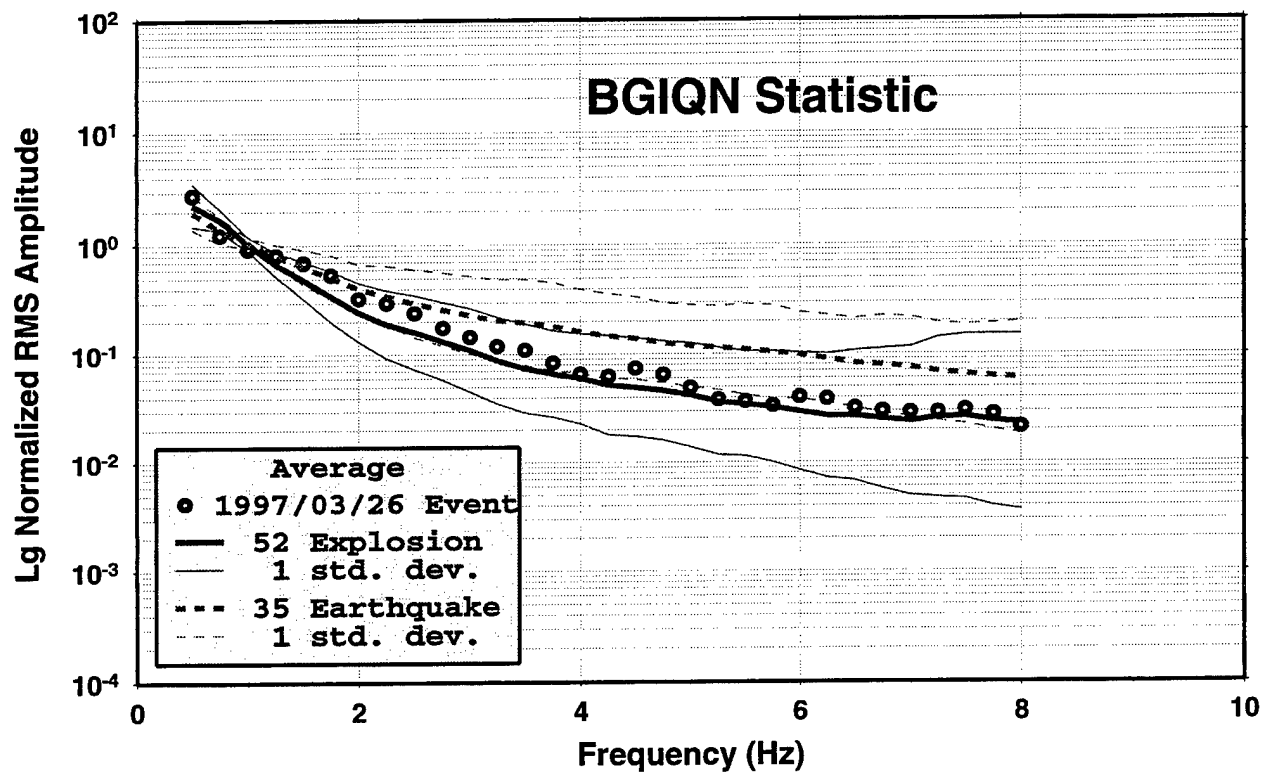
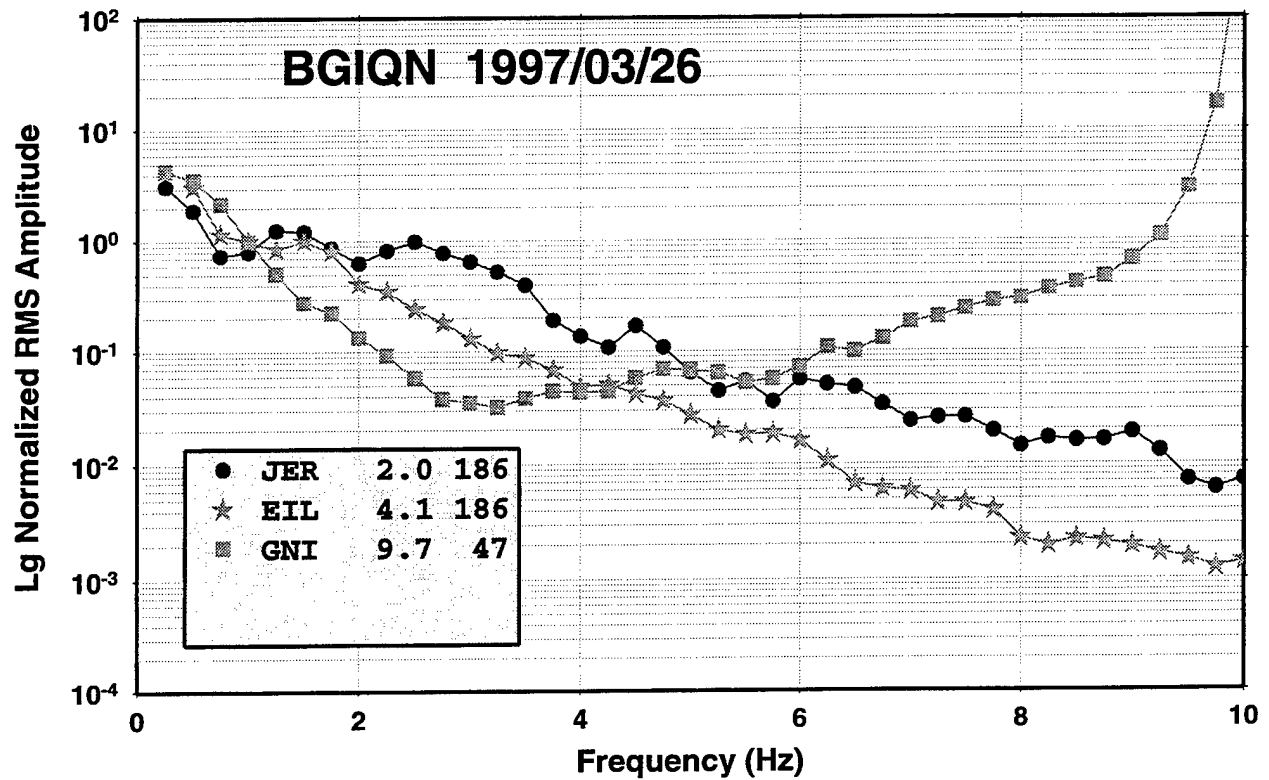


Figure 28.  $L_g$  spectral ratios after corrections at three stations (top) and discrimination analysis based on average  $L_g$  spectral ratios (bottom) for Jordan-Syria event of 1997/03/26.

spectral ratios would go higher (i.e. more earthquake-like) over the band 2 - 4 Hz but would go lower (i.e. more explosion-like) over the band above 4 Hz. So, the  $L_g$  spectral ratio discriminant is indeterminate in identifying the 1997/03/26 Jordan-Syria border event.

**North Korea Event of 1996/09/14** - For the 1996/09/14 event in North Korea, we analyzed the  $L_g$  signals at three stations in the range  $6.7^\circ$  to  $7.6^\circ$ . The event had a magnitude of 3.94 and was located at  $38.58^\circ\text{N}$   $125.82^\circ\text{E}$ . The corrected  $L_g$  spectral ratios for the three stations are shown at the top of Figure 29. Although the ratios are fairly consistent between stations, the increasing trend in the  $L_g$  spectral ratios at higher frequencies is not consistent with experience in other areas. The observed spectral ratios could be made more consistent with experience elsewhere by modifying the attenuation model for the region to have larger  $Q$ , with increased  $Q_0$  and/or increased  $\eta$ . The bottom plot in Figure 29 shows the average corrected  $L_g$  spectral ratios for the three stations. The ratios lie above the mean-plus-one-standard-deviation for the earthquake sample and probably above the mean-plus-two-standard-deviations for the explosion sample. The comparisons would indicate that this event was most likely an earthquake, subject to the caveat that revisions to the  $Q$  model would likely lower the  $L_g$  spectral ratios for the event.

**Pakistan Event of 1996/12/22** - For the 1996/12/22 event in Pakistan, we analyzed the  $L_g$  signals for only a single station at a distance of  $3.6^\circ$ . This event had a magnitude of 4.28 and was located at  $31.21^\circ\text{N}$   $70.09^\circ\text{E}$ . The corrected  $L_g$  spectral ratio as a function of frequency for the station is shown at the top of Figure 30, and at the bottom we compare the measurements for this event with the experience for the earthquakes and explosions. The comparisons indicate that the  $L_g$  spectral ratio measurements for the Pakistan event just about coincide with the average experience for the earthquake sample. The ratios are just about at the mean-plus-one-standard-deviation for the explosion sample. The comparisons suggest that the event was probably an earthquake.

**Balapan, Eastern Kazakhstan Event of 1988/09/14** - For the 1988/09/14 event at the Balapan test site in eastern Kazakhstan, we analyzed the  $L_g$  signals from three stations at distances between  $8.6^\circ$  and  $13.8^\circ$ . The event had a magnitude of 6.1 and was located at



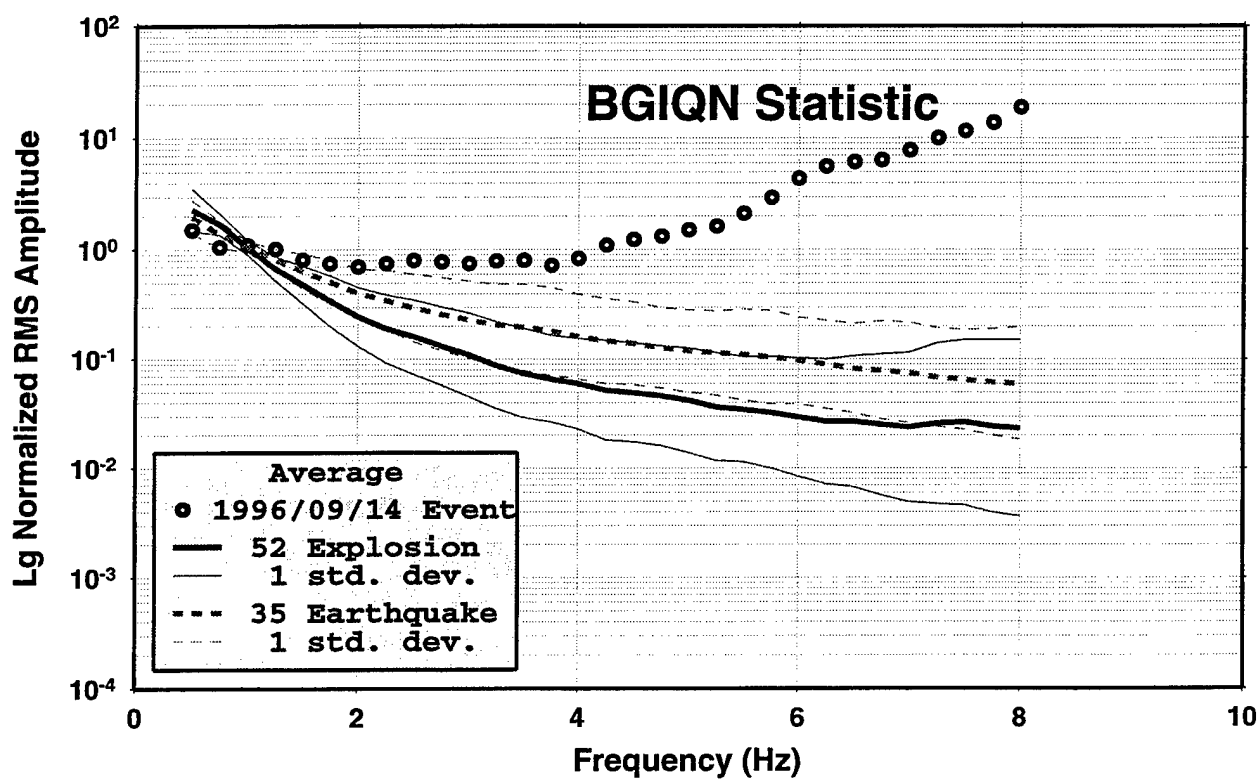
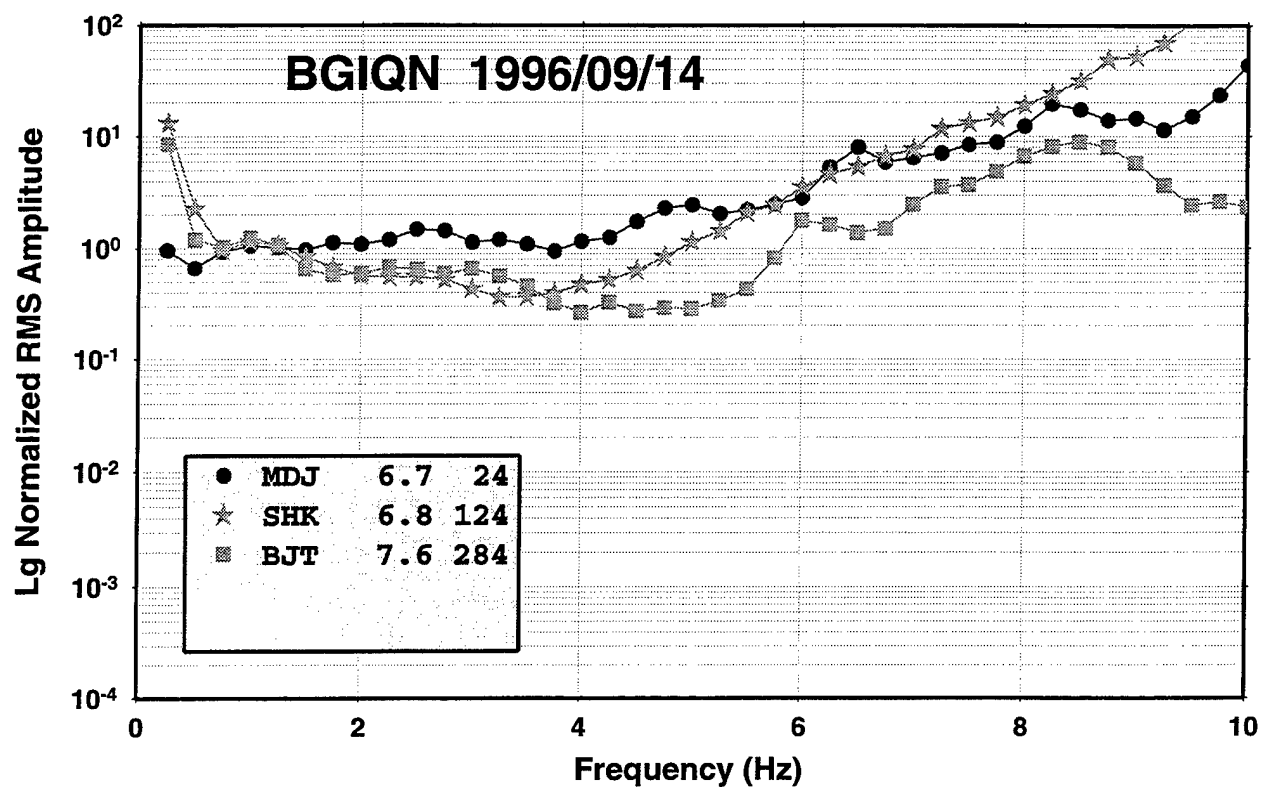


Figure 29. L<sub>g</sub> spectral ratios after corrections at three stations (top) and discrimination analysis based on average L<sub>g</sub> spectral ratios (bottom) for North Korea event of 1996/09/14.

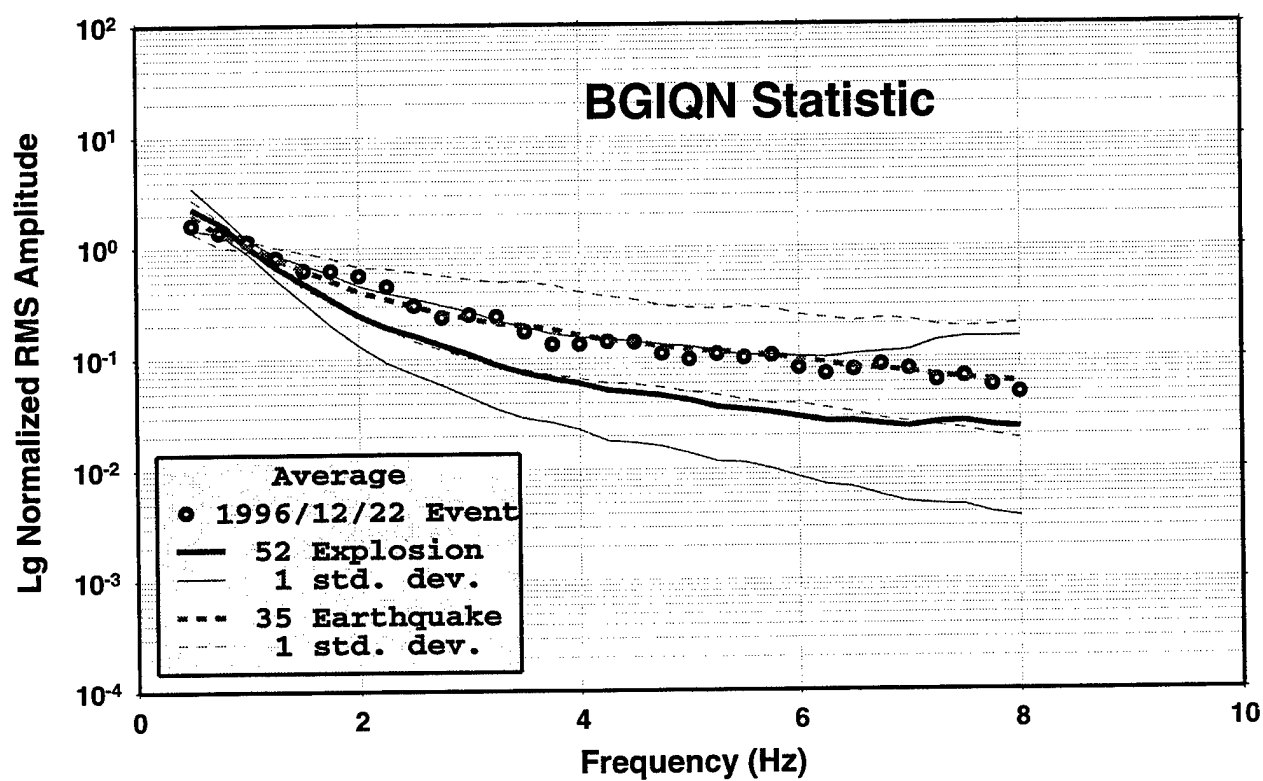
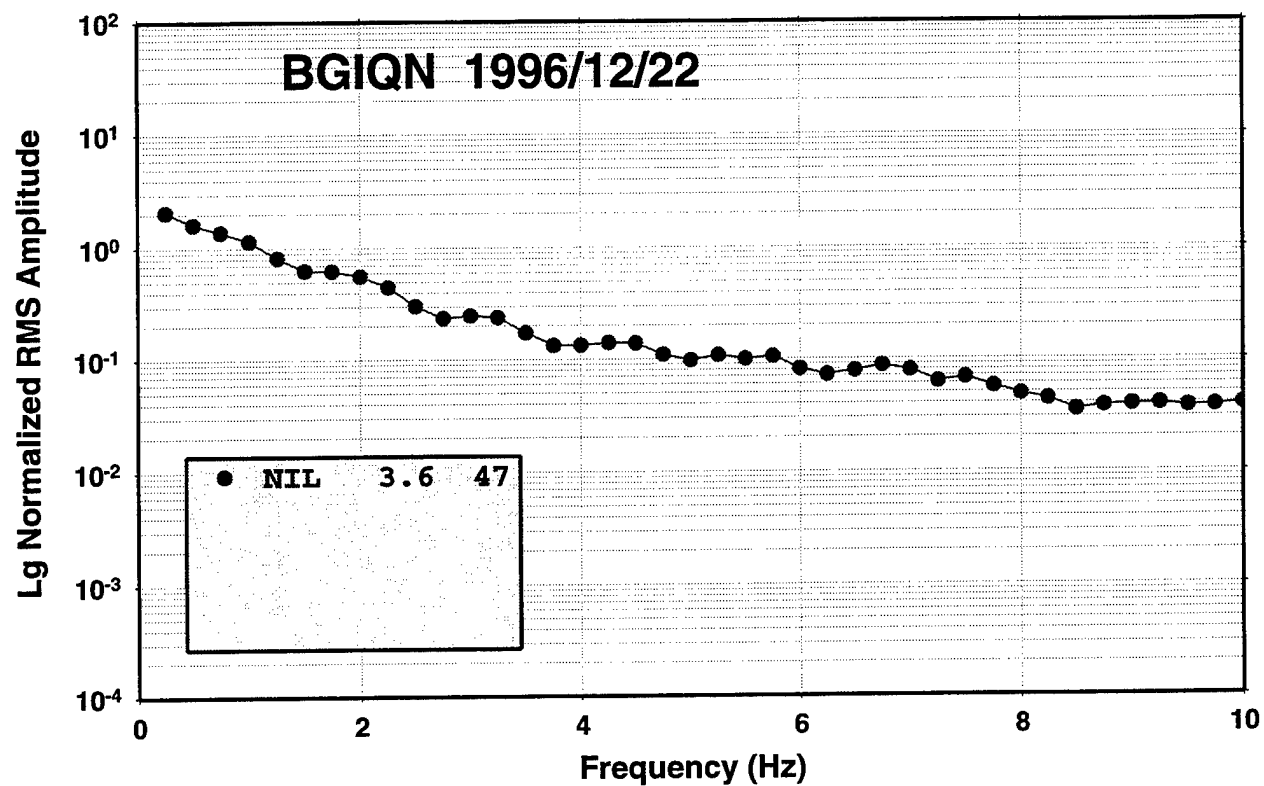


Figure 30.  $L_g$  spectral ratios after corrections at single station (top) and discrimination analysis based on average  $L_g$  spectral ratios (bottom) for Pakistan event of 1996/12/22.

49.86°N 78.82°E. The corrected  $L_g$  spectral ratios for the three stations are shown at the top of Figure 31. The corrected  $L_g$  spectral ratios for the three stations match very closely out to beyond 4 Hz, which suggests that the attenuation model for these source-station paths is fairly good. At about 5 Hz and above, the  $L_g$  spectra diverge with the measurements for GAR and ARU increasing, while the measurements at WMQ continue to decrease before beginning a steady increase above 7 Hz. These increases suggest noise contamination which is affecting the farther stations at somewhat lower frequencies. The average  $L_g$  spectral ratio, shown in the bottom plot of Figure 31, indicates that the event was probably an explosion, as the average falls between the mean and the mean-minus-one-standard-deviation of the earthquake sample and below the mean-minus-one-standard-deviation of the earthquake sample over the reliable frequency range of the data. So, the discrimination analysis with the corrected  $L_g$  spectral ratio for the 1988/09/14 Balapan event appears to be accurate in identifying the event, which we know to have been the JVE test, as an explosion.

Overall, the experience from these discrimination analyses with the attenuation- and instrument-corrected  $L_g$  spectral ratios is somewhat mixed. It is somewhat unsatisfactory that the distinction between the measurements for explosions and earthquakes is not more clear. The fact that the distribution for the earthquake observations in the interval from the mean to the mean-minus-one-standard-deviation overlays the distribution for the explosion observations for the interval from the mean to the mean-plus-one-standard-deviation limits the reliance which can be placed on the identification of events. Furthermore, it seems clear that the attenuation model can be improved and is probably incorrect for some regions. Such corrections and refinements could help to increase the reliability of the discriminant measure. Given these kinds of problems, it is probably remarkable that the application of the discrimination procedure to the selected events worked at all. The analysis procedure appears to be successful in identifying four of the five events, and one event is ambiguous. It seems particularly noteworthy that the  $L_g$  spectral ratio discrimination procedure described here is successful in identifying a nuclear explosion and an earthquake from the same general area. In particular, this procedure seems to be accurate in indicating that the 1988/09/14

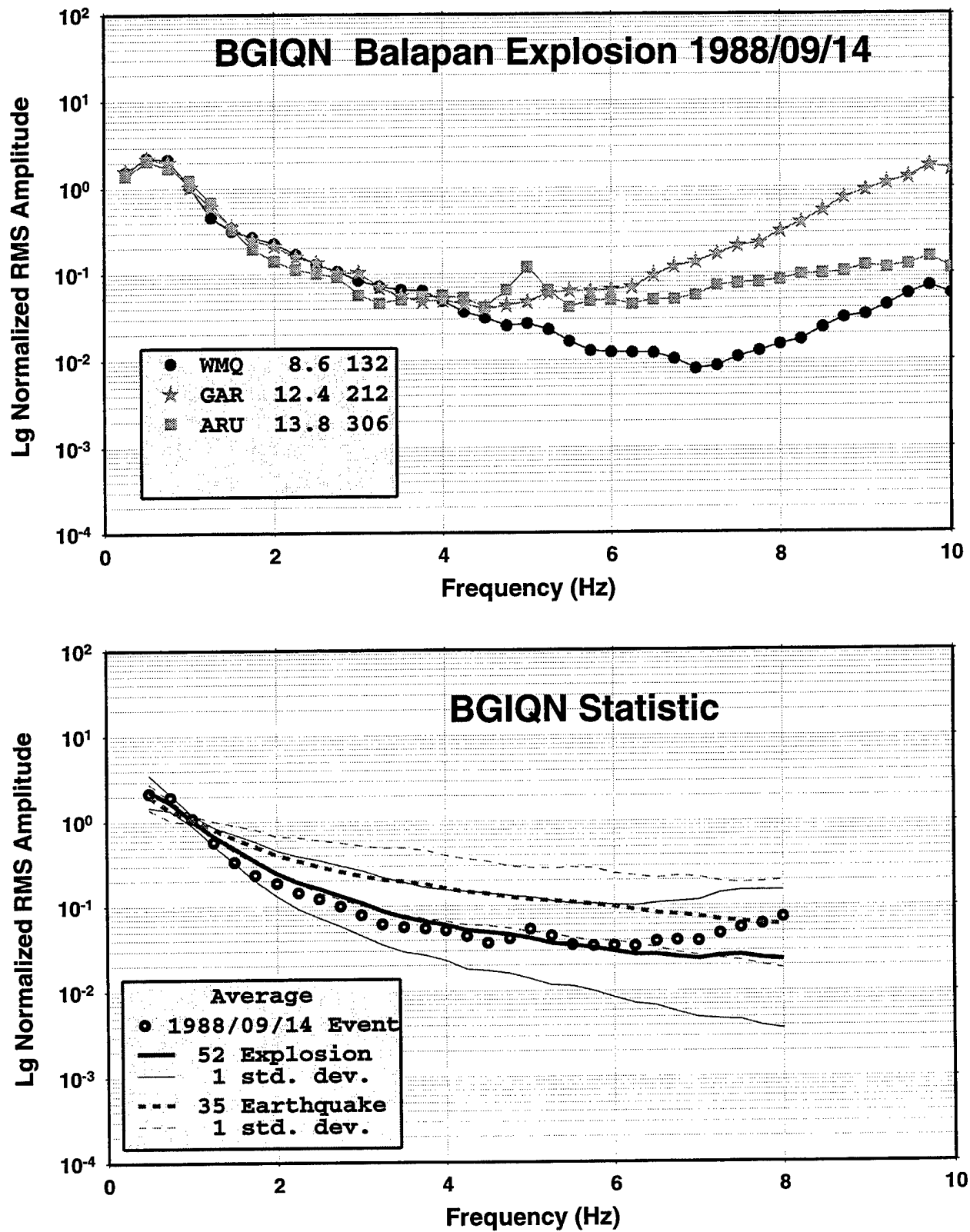


Figure 31.  $L_g$  spectral ratios after corrections at three stations (top) and discrimination analysis based on average  $L_g$  spectral ratios (bottom) for Balapan, East Kazakhstan explosion of 1988/09/14.

JVE in eastern Kazakhstan was an explosion and that the 1996/03/26 event in eastern Kazakhstan was probably an earthquake.

## 5. Conclusions and Recommendations

### 5.1 Summary of Main Findings

Regional seismic observations are critical to monitoring the CTBT at low magnitude levels. Regional signals are needed to refine event locations and identify source type. However, regional discrimination techniques generally remain untested and unproved for many potential source regions throughout the world. To demonstrate the transportability of regional discrimination techniques into untested areas, we need to determine how regional discriminant measures are affected by the propagation characteristics and adjust the procedures to account for propagation differences between the calibrated and the untested regions. In the studies reported here, we investigated the effects of propagation as well as recording instrument response on  $L_g$  spectral ratios, which have been considered a potentially valuable regional discrimination technique. To analyze these effects, we applied a regionalized model based on prior knowledge of  $L_g$  attenuation to correct  $L_g$  spectral measurements and to determine spectral ratio discriminants which should be independent of the region in which the measurement is made and of the station response.

Initial elements in this phase of the research project focused 1) on establishing spectral estimation techniques for use in determining regional phase spectral ratios, 2) on defining an attenuation model for use in determining corrections to the observed regional phase spectral ratios, and 3) on identifying a sample of regional seismic records from events of various source types and in various source regions which could be used to test the procedures. We compared several spectral analysis procedures applied to regional phase signals. We found that a band-pass filtering procedure which used narrow-band Gaussian filters with center frequencies spaced at uniform small increments provided spectral estimates for regional signals which closely matched spectral estimates produced by Fourier analyses of the same signals. Although this filtering procedure was somewhat more time-consuming than Fourier analysis, we believe that it provides some operational advantages for routine processing in that prior knowledge of event location and record windowing is not critical to application of the filtering procedures.

To determine appropriate propagation path corrections for the regional phase spectral ratios, we used prior knowledge of crustal  $Q$  and its frequency dependence. We applied this procedure mainly to  $L_g$  signals, although in principle similar procedures should be effective for other guided regional phases. The propagation correction factors were determined by tracing the regional phase path through the gridded model corresponding to the effective  $Q$  and its frequency dependence. This 2-D model summed the contributions to the effective attenuation from each cell in the grid along the path between the source and station. For this model we used the  $Q_0$  and  $\eta$  (frequency dependence) values for the grid cells derived previously by Mitchell and his colleagues for the U.S., Eurasia, and Africa. We tested the corrections derived from this model on several data samples and found that they usually produced reductions in the scatter of the  $L_g$  spectral ratios between stations for common events. However, the reduction of the scatter was not complete; so some refinements and corrections to the attenuation models (particularly in some regions) would probably help to reduce the uncertainty of the corrected  $L_g$  spectral ratio observations for different source types.

The spectral estimation technique, instrument corrections, and model-predicted attenuation corrections have been implemented in a systematic procedure for determining  $L_g$  spectral ratios. This procedure can be routinely applied to seismic waveform data from other stations and sources. Furthermore, the procedures can be easily revised as new information on the attenuation model or other path corrections become available.

With regard to the effectiveness of the  $L_g$  spectral ratios as discriminant measures, application of the  $L_g$  attenuation corrections did not clearly separate the explosion observations from the earthquake observations presented in this report. The data presented were contaminated by noise in many cases (particularly at distant stations and higher frequencies) which made the interpretation of the data difficult. It is clear, however, that, even if the measurements corrupted by noise were removed, there would still be significant overlap in the two source-type populations over much of the frequency band. Three factors that might contribute to the overlap are 1) inadequacy of the  $Q$  model, 2) station site biases, and 3) source site effects due to factors like focal depth, topography, and geologic structure. Several of these factors need to be investigated in

greater detail before we can come to definite conclusions on the adequacy of this discriminant.

On the positive side, testing of the  $L_g$  spectral ratio discriminant performance on several specific events from certain areas of potential interest for CTBT monitoring appeared to show some promise. We found that, for several selected events (viz. from eastern Kazakhstan, North Korea, and Pakistan), the corrected  $L_g$  spectral ratios fit into the appropriate distribution corresponding to that source type, based on comparison to the larger data sample. We found it noteworthy that the corrected  $L_g$  spectral ratio observations seemed to accurately distinguish a nuclear explosion and an earthquake from the same general area of eastern Kazakhstan. One apparent earthquake from the Jordan-Syria region was more ambiguous and fell into the area between the means for the two source types where the populations overlap. Clearly, if the  $L_g$  spectral ratio discriminant is to be effective, work is needed to reduce the scatter and increase the separation between the measurement populations for different source types.

## 5.2 Recommendations

Perhaps one of the biggest problems with regional phase spectral ratio measurements is noise contamination in the frequency bands needed to form the ratios. It seems clear that, given a rather sparse network of seismic stations for use in CTBT monitoring, regional phase signals for small events will often be contaminated by noise. The best stations for use in forming the regional discriminant measures are likely to be the one or two stations nearest to the event. The best regional discrimination procedures are likely to be those which do not require too broad spectral estimates of the signals for their implementation, because higher-frequency observations are more likely to be adversely affected by the noise. Studies are needed to assess how broad a frequency band is required to determine reliable regional phase spectral ratio discriminant measures and what are the useful frequency bands of the regional signals at individual stations of the CTBT monitoring network from various source locations and event magnitudes.

Some of the major contributions to the remaining scatter in the corrected  $L_g$  spectral ratio measurements probably come from errors in the attenuation model used to



adjust the observations. This needs to be explored more completely. Dependence of the scatter on factors like distance, frequency, and azimuth need to be studied further. The models clearly have errors and greater uncertainty in some regions, and these need to be improved.

Station site effects may also be a factor in the variability of the observations for individual events. For stations with adequate data, the significance of such effects could be tested. First, the hypothesis that a systematic station bias exists should be tested; then methods of determining and applying station bias corrections could be devised. Besides station site effects, source differences might also contribute to some of the scatter in the observations. Factors like source depth, topography, and geologic structure contribute to variations in regional phase spectra. It may be possible to use larger databases of well-understood events to further investigate how these factors affect the regional phase spectral ratio measurements from sources in different areas.

## 6. References

- Bennett, T. J., and J. R. Murphy (1986). "Analysis of Seismic Discrimination Capabilities Using Regional Data from Western United States Events," *Bull. Seism. Soc. Am.*, 76, pp. 1069 -1086.
- Bennett, T. J., B. W. Barker, K. L. McLaughlin, and J. R. Murphy (1989). "Regional Discrimination of Quarry Blasts, Earthquakes and Underground Nuclear Explosions," GL-TR-89-0114, ADA223148.
- Bennett, T. J., A. K. Campanella, J. F. Scheimer, and J. R. Murphy (1992). "Demonstration of Regional Discrimination of Eurasian Seismic Events Using Observations at Soviet IRIS and CDSN Stations," PL-TR-92-2090, ADA253275.
- Bennett, T. J., B. W. Barker, M. E. Marshall, and J. R. Murphy (1995). "Detection and Identification of Small Regional Seismic Events," PL-TR-95-2125, ADA305536.
- Bennett, T. J., M. E. Marshall, B. W. Barker, and J. R. Murphy (1996). "Investigations of Regional Phase Spectral Ratios: Transportability and Measurement Algorithms," PL-TR-96-2283, ADA323127.
- Blandford, R. (1981). "Seismic Discrimination Problems at Regional Distances," in *Identification of Seismic Source - Earthquake or Underground Explosion*, D. Reidel Publishing Co., pp. 695-740.
- Mitchell, B. J. (1997). Personal Communication.
- Mitchell, B. J., Y. Pan, and J. K. Xie (1996). "The Variation of  $L_g$  Coda Q Across Eurasia and Its Relation to Continental Evolution," PL-TR-96-2154, ADA317387.
- Murphy, J. R., and T. J. Bennett (1982). "A Discrimination Analysis of Short-Period Regional Seismic Data Recorded at Tonto Forest Observatory," *Bull. Seism. Soc. Am.*, 72, pp. 1351 - 1366.
- Murphy, J. R., D. D. Sultanov, B. W. Barker, I. O. Kitov, and M. E. Marshall (1996). "Regional Seismic Detection Analyses of Selected Soviet Peaceful Nuclear Explosions," SSS-DFR-96-15503.
- Pomeroy, P. W., W. J. Best, and T. V. McEvelly (1982). "Test Ban Treaty Verification with Regional Data - A Review," *Bull. Seism. Soc. Am.*, 72, pp. S89 - S129.

- Ryall, Alan (1970). "Seismic Identification at Short Distances," in Copies of Papers Presented at Woods Hole Conference on Seismic Discrimination, 2, DARPA, Arlington, VA.
- Taylor, S. R., N. W. Sherman, and M. D. Denny(1988). "Spectral Discrimination Between NTS Explosions and Western United States Earthquakes at Regional Distances," Bull. Seism. Soc. Am., 78, pp. 1563 - 1579.
- Taylor, S. R., M. D. Denny, E. S. Vergino, and R. E. Glaser (1989). "Regional Discrimination Between NTS Explosions and Western U. S. Earthquakes," Bull. Seism. Soc. Am., 78, pp. 1142 - 1176.
- Xie, J. K., and B. J. Mitchell (1990). "A Back-Projection Method for Imaging Large-Scale Lateral Variations of Lg Coda Q with Application to Continental Africa," Geophys. Jour. Int., 100, pp. 161 - 181.

THOMAS AHRENS  
SEISMOLOGICAL LABORATORY 252-21  
CALIFORNIA INSTITUTE OF  
TECHNOLOGY  
PASADENA, CA 91125

AIR FORCE RESEARCH LABORATORY  
ATTN: VSOE  
29 RANDOLPH ROAD  
HANSCOM AFB, MA 01731-3010  
(2 COPIES)

AIR FORCE RESEARCH LABORATORY  
ATTN: RESEARCH LIBRARY/TL  
5 WRIGHT STREET  
HANSCOM AFB, MA 01731-3004

AIR FORCE RESEARCH LABORATORY  
ATTN: AFRL/SUL  
3550 ABERDEEN AVE SE  
KIRTLAND AFB, NM 87117-5776  
(2 COPIES)

RALPH ALEWINE  
NTPO  
1901 N. MOORE STREET, SUITE 609  
ARLINGTON, VA 22209

MUAWIA BARAZANGI  
INSTOC  
3126 SNEE HALL  
CORNELL UNIVERSITY  
ITHACA, NY 14853

T.G. BARKER  
MAXWELL TECHNOLOGIES  
8888 BALBOA AVE.  
SAN DIEGO, CA 92123-1506

DOUGLAS BAUMGARDT  
ENSCO INC.  
5400 PORT ROYAL ROAD  
SPRINGFIELD, VA 22151

THERON J. BENNETT  
MAXWELL TECHNOLOGIES  
11800 SUNRISE VALLEY DRIVE, STE 1212  
RESTON, VA 22091

WILLIAM BENSON  
NAS/COS  
ROOM HA372  
2001 WISCONSIN AVE. NW  
WASHINGTON DC 20007

JONATHAN BERGER  
UNIVERSITY OF CA, SAN DIEGO  
SCRIPPS INST. OF OCEANOGRAPHY  
IGPP, 0225  
9500 GILMAN DRIVE  
LA JOLLA, CA 92093-0225

ROBERT BLANDFORD  
AFTAC  
1300 N. 17TH STREET  
SUITE 1450  
ARLINGTON, VA 22209-2308

LESLIE A. CASEY  
DEPT. OF ENERGY/NN-20  
1000 INDEPENDENCE AVE. SW  
WASHINGTON DC 20585-0420

CENTER FOR MONITORING RESEARCH  
ATTN: LIBRARIAN  
1300 N. 17th STREET, SUITE 1450  
ARLINGTON, VA 22209

ANTON DAINTY  
HQ DSWA/PMA  
6801 TELEGRAPH ROAD  
ALEXANDRIA, VA 22310-3398

CATHERINE DE GROOT-HEDLIN  
UNIV. OF CALIFORNIA, SAN DIEGO  
INST. OF GEOP. & PLANETARY PHYSICS  
8604 LA JOLLA SHORES DRIVE  
SAN DIEGO, CA 92093

DTIC  
8725 JOHN J. KINGMAN ROAD  
FT BELVOIR, VA 22060-6218 (2 COPIES)

DIANE DOSER  
DEPT OF GEOLOGICAL SCIENCES  
THE UNIVERSITY OF TEXAS AT EL PASO  
EL PASO, TX 79968

MARK D. FISK  
MISSION RESEARCH CORPORATION  
735 STATE STREET  
P.O. DRAWER 719  
SANTA BARBARA, CA 93102-0719

LORI GRANT  
MULTIMAX, INC.  
311C FOREST AVE. SUITE 3  
PACIFIC GROVE, CA 93950

HENRY GRAY  
SMU STATISTICS DEPARTMENT  
P.O. BOX 750302  
DALLAS, TX 75275-0302

I. N. GUPTA  
MULTIMAX, INC.  
1441 MCCORMICK DRIVE  
LARGO, MD 20774

DAVID HARKRIDER  
BOSTON COLLEGE  
INSTITUTE FOR SPACE RESEARCH  
140 COMMONWEALTH AVENUE  
CHESTNUT HILL, MA 02167

THOMAS HEARN  
NEW MEXICO STATE UNIVERSITY  
DEPARTMENT OF PHYSICS  
LAS CRUCES, NM 88003

MICHAEL HEDLIN  
UNIV. OF CALIFORNIA, SAN DIEGO  
SCRIPPS INST. OF OCEANOGRAPHY  
IGPP, 0225  
9500 GILMAN DRIVE  
LA JOLLA, CA 92093-0225

DONALD HELMBERGER  
CALIFORNIA INST. OF TECHNOLOGY  
DIV. OF GEOL. & PLANETARY SCIENCES  
SEISMOLOGICAL LABORATORY  
PASADENA, CA 91125

EUGENE HERRIN  
SOUTHERN METHODIST UNIVERSITY  
DEPARTMENT OF GEOLOGICAL  
SCIENCES  
DALLAS, TX 75275-0395

ROBERT HERRMANN  
ST. LOUIS UNIVERSITY  
DEPT OF EARTH & ATMOS. SCIENCES  
3507 LACLEDE AVENUE  
ST. LOUIS, MO 63103

VINDELL HSU  
HQ/AFTAC/TTR  
1030 S. HIGHWAY A1A  
PATRICK AFB, FL 32925-3002

RONG-SONG JIH  
HQ DSWA/PMA  
6801 TELEGRAPH ROAD  
ALEXANDRIA, VA 22310-3398

THOMAS JORDAN  
MASS. INST. OF TECHNOLOGY  
BLDG 54-918  
77 MASSACHUSETTS AVENUE  
CAMBRIDGE, MA 02139

LAWRENCE LIVERMORE NAT'L LAB  
ATTN: TECHNICAL STAFF (PLS ROUTE)  
PO BOX 808, MS L-175  
LIVERMORE, CA 94551

LAWRENCE LIVERMORE NAT'L LAB  
ATTN: TECHNICAL STAFF (PLS ROUTE)  
PO BOX 808, MS L-208  
LIVERMORE, CA 94551

LAWRENCE LIVERMORE NAT'L LAB  
ATTN: TECHNICAL STAFF (PLS ROUTE)  
PO BOX 808, MS L-202  
LIVERMORE, CA 94551

LAWRENCE LIVERMORE NAT'L LAB  
ATTN: TECHNICAL STAFF (PLS ROUTE)  
PO BOX 808, MS L-195  
LIVERMORE, CA 94551

LAWRENCE LIVERMORE NAT'L LAB  
ATTN: TECHNICAL STAFF (PLS ROUTE)  
PO BOX 808, MS L-205  
LIVERMORE, CA 94551

LAWRENCE LIVERMORE NAT'L LAB  
ATTN: TECHNICAL STAFF (PLS ROUTE)  
PO BOX 808, MS L-200  
LIVERMORE, CA 94551

LAWRENCE LIVERMORE NAT'L LAB  
ATTN: TECHNICAL STAFF (PLS ROUTE)  
PO BOX 808, MS L-221  
LIVERMORE, CA 94551

THORNE LAY  
UNIV. OF CALIFORNIA, SANTA CRUZ  
EARTH SCIENCES DEPARTMENT  
EARTH & MARINE SCIENCE BUILDING  
SANTA CRUZ, CA 95064

ANATOLI L. LEVSHIN  
DEPARTMENT OF PHYSICS  
UNIVERSITY OF COLORADO  
CAMPUS BOX 390  
BOULDER, CO 80309-0309

JAMES LEWKOWICZ  
WESTON GEOPHYSICAL CORP.  
325 WEST MAIN STREET  
NORTHBORO, MA 01532

LOS ALAMOS NATIONAL LABORATORY  
ATTN: TECHNICAL STAFF (PLS ROUTE)  
PO BOX 1663, MS F659  
LOS ALAMOS, NM 87545

LOS ALAMOS NATIONAL LABORATORY  
ATTN: TECHNICAL STAFF (PLS ROUTE)  
PO BOX 1663, MS F665  
LOS ALAMOS, NM 87545

LOS ALAMOS NATIONAL LABORATORY  
ATTN: TECHNICAL STAFF (PLS ROUTE)  
PO BOX 1663, MS D460  
LOS ALAMOS, NM 87545

LOS ALAMOS NATIONAL LABORATORY  
ATTN: TECHNICAL STAFF (PLS ROUTE)  
PO BOX 1663, MS C335  
LOS ALAMOS, NM 87545

GARY MCCARTOR  
SOUTHERN METHODIST UNIVERSITY  
DEPARTMENT OF PHYSICS  
DALLAS, TX 75275-0395

KEITH MCLAUGHLIN  
CENTER FOR MONITORING RESEARCH  
(SAIC)  
1300 N. 17TH STREET, SUITE 1450  
ARLINGTON, VA 22209

BRIAN MITCHELL  
DEPT OF EARTH & ATMOSPHERIC  
SCIENCES  
ST. LOUIS UNIVERSITY  
3507 LACLEDE AVENUE  
ST. LOUIS, MO 63103

RICHARD MORROW  
USACDA/IVI  
320 21ST STREET, N.W.  
WASHINGTON DC 20451

JOHN MURPHY  
MAXWELL TECHNOLOGIES  
11800 SUNRISE VALLEY DRIVE, STE 1212  
RESTON, VA 22091

JAMES NI  
NEW MEXICO STATE UNIVERSITY  
DEPARTMENT OF PHYSICS  
LAS CRUCES, NM 88003

ROBERT NORTH  
CENTER FOR MONITORING RESEARCH  
1300 N. 17th STREET, SUITE 1450  
ARLINGTON, VA 22209

OFFICE OF THE SECRETARY OF  
DEFENSE  
DDR&E  
WASHINGTON DC 20330

JOHN ORCUTT  
INST. OF GEOPH. & PLANETARY PHYSICS  
UNIV. OF CALIFORNIA, SAN DIEGO  
LA JOLLA, CA 92093

PACIFIC NORTHWEST NAT'L LAB  
ATTN: TECHNICAL STAFF (PLS ROUTE)  
PO BOX 999, MS K6-48  
RICHLAND, WA 99352

PACIFIC NORTHWEST NAT'L LAB  
ATTN: TECHNICAL STAFF (PLS ROUTE)  
PO BOX 999, MS K6-40  
RICHLAND, WA 99352

PACIFIC NORTHWEST NAT'L LAB  
ATTN: TECHNICAL STAFF (PLS ROUTE)  
PO BOX 999, MS K6-84  
RICHLAND, WA 99352

PACIFIC NORTHWEST NAT'L LAB  
ATTN: TECHNICAL STAFF (PLS ROUTE)  
PO BOX 999, MS K5-12  
RICHLAND, WA 99352

FRANK PILOTTE  
HQ AFTAC/TT  
1030 S. HIGHWAY A1A  
PATRICK AFB, FL 32925-3002

KEITH PRIESTLEY  
DEPARTMENT OF EARTH SCIENCES  
UNIVERSITY OF CAMBRIDGE  
MADINGLEY RISE, MADINGLEY ROAD  
CAMBRIDGE, CB3 0EZ UK

JAY PULLI  
BBN SYSTEMS AND TECHNOLOGIES, INC.  
1300 NORTH 17TH STREET  
ROSSLYN, VA 22209

DELAINE REITER  
AFRL/VSOE (SENCOM)  
29 RANDOLPH ROAD  
HANSCOM AFB, MA 01731-3010

PAUL RICHARDS  
COLUMBIA UNIVERSITY  
LAMONT-DOHERTY EARTH OBSERV.  
PALISADES, NY 10964

MICHAEL RITZWOLLER  
DEPARTMENT OF PHYSICS  
UNIVERSITY OF COLORADO  
CAMPUS BOX 390  
BOULDER, CO 80309-0309

DAVID RUSSELL  
HQ AFTAC/TTR  
1030 SOUTH HIGHWAY A1A  
PATRICK AFB, FL 32925-3002

CHANDAN SAIKIA  
WOODWARD-CLYDE FED. SERVICES  
566 EL DORADO ST., SUITE 100  
PASADENA, CA 91101-2560

SANDIA NATIONAL LABORATORY  
ATTN: TECHNICAL STAFF (PLS ROUTE)  
DEPT. 5704  
MS 0979, PO BOX 5800  
ALBUQUERQUE, NM 87185-0979

SANDIA NATIONAL LABORATORY  
ATTN: TECHNICAL STAFF (PLS ROUTE)  
DEPT. 9311  
MS 1159, PO BOX 5800  
ALBUQUERQUE, NM 87185-1159

SANDIA NATIONAL LABORATORY  
ATTN: TECHNICAL STAFF (PLS ROUTE)  
DEPT. 5704  
MS 0655, PO BOX 5800  
ALBUQUERQUE, NM 87185-0655

SANDIA NATIONAL LABORATORY  
ATTN: TECHNICAL STAFF (PLS ROUTE)  
DEPT. 5736  
MS 0655, PO BOX 5800  
ALBUQUERQUE, NM 87185-0655

THOMAS SERENO, JR.  
SAIC  
10260 CAMPUS POINT DRIVE  
SAN DIEGO, CA 92121

AVI SHAPIRA  
SEISMOLOGY DIVISION  
THE INST. FOR PETROLEUM RESEARCH  
AND GEOPHYSICS  
P.O.B. 2286  
NOLON 58122 ISRAEL

ROBERT SHUMWAY  
410 MRAK HALL  
DIVISION OF STATISTICS  
UNIVERSITY OF CALIFORNIA  
DAVIS, CA 95616-8671

DAVID SIMPSON  
IRIS  
1200 NEW YORK AVE., NW  
SUITE 800  
WASHINGTON DC 20005

JEFFRY STEVENS  
MAXWELL TECHNOLOGIES  
8888 BALBOA AVE.  
SAN DIEGO, CA 92123-1506

BRIAN SULLIVAN  
BOSTON COLLEGE  
INSITUTE FOR SPACE RESEARCH  
140 COMMONWEALTH AVENUE  
CHESTNUT HILL, MA 02167

TACTEC  
BATTELLE MEMORIAL INSTITUTE  
505 KING AVENUE  
COLUMBUS, OH 43201 (FINAL REPORT)

NAFI TOKSOZ  
EARTH RESOURCES LABORATORY, M.I.T.  
42 CARLTON STREET, E34-440  
CAMBRIDGE, MA 02142

LAWRENCE TURNBULL  
ACIS  
DCI/ACIS  
WASHINGTON DC 20505

GREG VAN DER VINK  
IRIS  
1200 NEW YORK AVE., NW  
SUITE 800  
WASHINGTON DC 20005

FRANK VERNON  
UNIV. OF CALIFORNIA, SAN DIEGO  
SCRIPPS INST. OF OCEANOGRAPHY  
IGPP, 0225  
9500 GILMAN DRIVE  
LA JOLLA, CA 92093-0225

TERRY WALLACE  
UNIVERSITY OF ARIZONA  
DEPARTMENT OF GEOSCIENCES  
BUILDING #77  
TUCSON, AZ 85721

JILL WARREN  
LOS ALAMOS NATIONAL LABORATORY  
GROUP NIS-8  
P.O. BOX 1663  
LOS ALAMOS, NM 87545 (5 COPIES)

DANIEL WEILL  
NSF  
EAR-785  
4201 WILSON BLVD., ROOM 785  
ARLINGTON, VA 22230

RU SHAN WU  
UNIV. OF CALIFORNIA SANTA CRUZ  
EARTH SCIENCES DEPT.  
1156 HIGH STREET  
SANTA CRUZ, CA 95064

JIANG XIE  
COLUMBIA UNIVERSITY  
LAMONT DOHERTY EARTH OBSERV.  
ROUTE 9W  
PALISADES, NY 10964

JAMES E. ZOLLWEG  
BOISE STATE UNIVERSITY  
GEOSCIENCES DEPT.  
1910 UNIVERSITY DRIVE  
BOISE, ID 83725